Title
Evaluating System ATMIS Technologies Via Rapid Estimation Of Network Flows: Final Report

Authors
Moore, II, James E.
Kim, Geunyoung
Cho, Seongdil
et al.

Publication Date
1997

EVALUATING SYSTEM ATMIS TECHNOLOGIES VIA RAPID ESTIMATION OF NETWORK FLOWS: FINAL REPORT

by

James E. Moore II, Associate Professor
School of Urban Planning and Development, and
the Department of Civil Engineering

Geunyoung Kim, Ph.D. Candidate
School of Urban Planning and Development

Seongkil Cho, Ph.D. Student
School of Urban Planning and Development

Hsi-Hwa Hu, Ph.D. Student
School of Urban Planning and Development

and

Rong Xu, Research Associate
Department of Economics
University of New York, Buffalo

VKC-351, MC-0042
University of Southern California
Los Angeles, CA 90089-0042

August 18, 1997

Abstract

Earthquakes damage freeway bridges and structures, resulting in significant impacts on transportation system performance and regional economy. The California Department of Transportation (Caltrans) has developed bridge seismic retrofit programs that include seismic risk analysis (SRA) procedures for structural re-enforcement projects. Caltrans' SRA procedure establishes retrofit priorities for vulnerable highway bridges.

Existing SRA procedures use average daily traffic (ADT) volumes to determine the importance of a bridge. This is not adequate. The importance of network links should be evaluated in terms of the system cost of failure. Incorporation of an efficient transportation modeling technology in the SRA procedures is essential.

The objectives of this research are: (1) to develop an efficient transportation network analysis (TNA) procedure for many different traffic flow analyses under numerous scenario earthquakes, and (2) to evaluate the applicability of the procedure to a large-scale transportation network. An important feature of the TNA procedure is the use of an associative memory (AM) approach as a cost-effective means in network flow modeling. The AM approach is a heuristic method derived from the artificial intelligence field.

A simple synthetic transportation network with seven zones and twenty-four links is developed to evaluate the applicability of the TNA procedure to simulated traffic flows. An aggregated representation of the Los Angeles highway network is defined as an empirical example. Five empirical link-failure system states are identified based on the opening of the Glen Anderson Freeway (I-105), the discrete, simultaneous closure of several links caused by the 1994

Northridge earthquake, and the gradual repair of network links. Empirical transportation system data sets including link capacities, free-flow link travel times, link volumes, and an origin-destination trip matrix are developed to simulate network flows with respect to additional synthetic link-failure system states.

The TNA procedure is applied to transportation network analyses (TNA) for the aggregated Los Angeles highway network. We combine synthetic, user equilibrium transportation flows with empirical data associated with the five empirical link-failure system states.

Results from traffic flow analyses demonstrate the applicability of the TNA procedure to the network flow modeling problem. Associative memory models provide better estimates of network flows compared to the conventional network equilibrium model in the case of five empirical link-failure system states. The performance of associative memory models improves if empirical and synthetic system states are combined. Results from travel demand studies indicate that a large number of peak-hour weekday trips change trip origins and/or destinations with respect to the opening or closure of network links.

Associative memory, decision-making, earthquakes, freeways, origin-destination trip matrix, retrofit programs, seismic risk analysis, simulation, system state, traffic flows, travel time

Executive Summary

This report summarizes progress on research funded under PATH MOU 120/212. Parts of this report were based on the doctoral dissertation of Geunyoung Kim. The work as originally proposed focused on using associative memory techniques for rapid estimation of network flows under conditions defined by the implementation of various ATMIS strategies. The period between approval of the research and allocation of the award included the Northridge Earthquake. Following the earthquake, the Principal Investigator, PATH, and the Office of New Technologies of Caltrans agreed to reorient the work toward modeling to support freeway structure retrofit decisions and the evaluation and improvement of retrofit strategies and decision rules.

This extension is consistent with the original thrust of the research, in that the core question remains how can flows in large scale transportation networks be subjected to rapid estimation. However, instead of attaching these estimates to a hypothetical set of ATMIS strategies, the estimates can be attached to empirical change in the capacity of the Los Angeles freeway network.

Current Caltrans retrofit criteria account for the characteristics of the structure, the average daily traffic (ADT) count the structure accommodates, and the geotechnical characteristics of the site. No attempt is made to account for the systemic effects associated with the loss of the facility, or for the combinatorial effects associated with the loss of other facilities in the network. This is a daunting prospect, because it implies prediction of network flows on a large scale.

These changes in the research project are easily accommodated by the associative memory approach: In either case, rapid estimation of network flows is a primary objective. However the current research requires more empiricism than would otherwise be possible. One output will be a summary data set of observed and seasonally adjusted freeways flows for Los Angeles' Caltrans District 7 that spans a range of unique events, including

(1) the opening of the Glen Anderson Freeway (I-105),

(2) the discontinuous, simultaneous removal of several links in the network following the Northridge event, and

(3) incremental, staggered return of these facilities to service.

In addition, a system of compact freeway traffic analysis zones have been built up out of 1990 census tracts based on the arrangement of Caltrans District 7 freeway links and traffic count stations.

Table of Contents

List of Tables

List of Figures

1. Introduction

Rapid estimation and prediction of traffic flows is one of the most important problems faced by transportation planners. Efficient and effective network flow models are of use in the short term as transportation agencies make incremental adjustments in guide way controls. Efficient and effective models are important in the intermediate term as agencies work to optimize their scare resources. Lastly, in the long term, the value of models lies in the means of defining and evaluating public and private transportation investment options.

Our research focuses on the relevance of rapid flow prediction models to the bridge retrofit criteria used by the California Department of Transportation (Caltrans). Caltrans has developed seismic risk analysis (SRA) procedures for prioritizing and retrofitting vulnerable bridges of California highway systems. Caltrans' SRA procedures apply average daily traffic (ADT) volumes to determine the importance of a bridge.

However, ADT volumes would be effective only when transportation networks are not significantly changed. Traffic flows of all transportation links would alter if there is a change in the transportation network. Thus, an appropriate SRA procedure not only should predict potential earthquake damage of system components such as buildings or bridges, but also should predict system-wide traffic impacts of earthquakes on overall transportation systems. The importance of system-wide traffic flow analyses with respect to bridge failures is addressed by Gilbert (1993):

> "A highway system is a complex network of vulnerable links. Bridge structures are by far the most critical links because of their vulnerability to damage when subjected to earthquake loads .... It is increasingly important to evaluate seismic reliability of the lifeline from a network systems point of view. Each critical element, or bridge, must be considered as part of a global system."

This research has three primary objectives. The first objective is to provide reliable estimates of network flows with respect to changes in transportation networks, and to incorporate these changes to the decision-making procedures used by Caltrans in making bridge retrofit decisions. This requires the development of an efficient transportation network analysis (TNA) procedure applicable to traffic flow analyses due to link failures of transportation systems.

The second objective is to evaluate the applicability of the TNA procedure to a large-scale transportation network. The evaluation of the TNA procedure requires numerical traffic flow simulations. A simple synthetic transportation network is developed and used to evaluate the TNA procedure. Network flows are simulated using a static user equilibrium model and synthetic transportation system data sets. Simple associative memory, recurrent associative memory, and multicriteria associative memory models are applied to estimate simulated network flows.

The TNA procedure is also applied to a large-scale representation of the Los Angeles highway network. Five empirical link-failure system states are identified based on the opening of the Glen Anderson Freeway (I-105) and the closure of freeway links caused

by the 1994 Northridge earthquake. Additional synthetic network flows are simulated based on synthetic coupled-link failure earthquake scenarios. Associative memory models are applied to estimate empirical traffic volumes. The effectiveness of the TNA procedure is evaluated in terms of the difference between empirical traffic volumes and estimated traffic flows.

The third objective is to identify travel demand changes due to the opening or closure of network links in the aggregated Los Angeles highway network. Travel demand of a transportation network may vary significantly after the occurrence of earthquakes. Earthquakes damage freeway/roadway bridges, resulting in the closure of network links. Drivers alter their routes or trip starting times after experiencing delays in commuting in the short run. In the long run, drivers change their travel behaviors by reducing their trips for excessive activities, or by altering their trip origins and/or destinations. Our procedure provides a way of predicting origin-destination trip changes with respect to the opening or closure of network links.

This research describes an efficient transportation network analysis (TNA) procedure that provides the system-wide changes of network flows under numerous scenario earthquakes. An important feature of the TNA procedure is the use of an associative memory (AM) approach as a cost-effective means in network flow modeling. The AM approach is a heuristic method derived from the artificial intelligence field. It provides

good approximate solutions to constrained optimization problems such as the transportation network flow problem.

The transportation network analysis procedure also includes methodologies for initializing or improving network input data. Conventional network flow models, link volume adjustment methods, and/or origin-destination trip estimation models are used as components of the TNA procedure. This research demonstrates two versions of the TNA procedure according to the quality of transportation system data: the general TNA procedure and the simplified TNA procedure. Overall features of the two TNA procedures will be described in section 4-1.

2. Research Design

Establishing or refining a priority rating for structural reinforcement of existing bridges requires analysis of the likelihood of a bridge's collapse or damage from earthquakes, and the consequences of these outcomes. Developing an appropriate procedure requires identification and study of various factors such as each bridge's design criteria, ground conditions, structural conditions, locations of faults, and impacts on traffic flows. Caltrans' multi-attribute decision procedure uses such data to provide an event likelihood calculation. The details of the procedure are described in Section 3-1-4.

Our revised procedure replaces the average daily traffic volumes attributes with changes in the system's total travel times due to various changes to the transportation network. Consider retrofitting one link of the Santa Monica Freeway. The change in the

total system travel times resulting from the link failure is computed by the following steps:

(1) identify equilibrium flows and travel times of each link under perfect transportation system;

(2) compute the total system travel times by multiplying equilibrium flows with travel times in each link, and by summing up each link's total travel times;

(3) remove each link from the transportation system, and compute the total system travel times;

(4) identify the total system travel time change due to the failure of each link in transportation network;

(5) remove several links from the transportation system, and compute the total system travel times;

(6) identify each link's portion from the total system travel time change caused by the failure of several links; and

(7) sum up the system travel time changes of one link due to the failure of one or more links under different link failures including the selected link.

Our research presents a transportation network analysis (TNA) procedure that provides quick and reliable estimates of traffic flows with respect to different link failure system states given numerous scenario earthquakes. This transportation network analysis procedure involves associative memory (AM) models as heuristic means suitable for use in predicting system-wide changes of network flows. If a set of observed link volumes for different post-earthquake system states is available from metropolitan planning

organizations (MPOs), AM models are applied to estimate network flows based on the association between network configurations and link volumes of post-earthquake system states.

Observed traffic volumes for post-earthquake system states may not be available from MPOs. A transportation network is developed in this case. Transportation system data sets including free-flow link travel times, link capacity data, and an origin-destination trip matrix are developed using data sources available from MPOs. Synthetic link-failure system states are selected based on different scenario earthquakes. A static user equilibrium model is employed to simulate synthetic traffic flows. Network configurations and simulated traffic flows are used as input data sets to train associative memory models. The best associative memory matrix is applied to estimate simulated traffic flows for additional link-failure system states.

The major advantage of the AM approach over the current standard ones is its simplicity both conceptually and computationally. Rapid flow estimates provided by the AM approach are used to predict changes of total system travel times due to link failures caused by earthquakes. This research evaluates the applicability of the TNA procedure to network flow prediction. Two example transportation networks are developed to evaluate the performance of the TNA procedure: a simple synthetic network and an aggregated Los Angeles highway network.

The simple synthetic network is used to evaluate the feasibility of the TNA procedure before applying the procedure to a large-scale transportation network. The synthetic network has seven traffic analysis zones and twenty-four directed links connecting each zone with its adjacent zones. The aggregated representation of the Los Angeles highway network includes 105 traffic analysis zones and 292 links. It is used to evaluate the applicability of the TNA procedure to empirical traffic flow analyses with respect to link failures due to the 1994 Northridge earthquake.

3. Literature Review

3-1. California Department of Transportation Current Bridge Retrofit Criteria

Caltrans' bridge seismic retrofitting program has been in existence for nearly 25 years, dating back to 1971. The programs' current decision-making criteria regarding risk identification and prioritization of bridges in California is the result of considerable research and several major improvements.

3-1-1. Historical Background

The 1933 magnitude 6.2 Long Beach earthquake induced substantial improvements in seismic design practices and enforcement of the seismic building code provisions. The California State Legislature passed the Riley Act and the Field Act to develop seismic building practices in California. During the 1940s, Caltrans began developing its own seismic design criteria and programs to cope with the risk of earthquake damages to California's transportation facilities. The first bridge seismic code requirements were introduced in 1940. The first seismic design criteria for new bridges were brought up in 1943, and revised in 1965.

The 1971 San Fernando earthquake produced clear evidence that existing bridges were vulnerable to damages from the earthquakes. Caltrans revised its seismic criteria after the

San Fernando earthquake. Caltrans also launched a retrofit program to correct the seismic deficiencies of existing bridges.

3-1-2. The Level One Risk Analysis Procedure

Caltrans' first risk analysis procedure for bridge retrofit is the Level One Risk Analysis procedure developed in 1971. This procedure is distinguished from conventional risk analysis procedures by use of expert judgments in addition to large scale statistical data. The procedure consists of five steps.

(1) Identify major faults with high event probabilities.

(2) Develop attenuation pattern models for all the faults identified in Step (1).

(3) Define a critical (minimum) ground acceleration level at which severe damage to the bridge would occur.

(4) Identify all the bridges within high risk zones, which are defined according to the attenuation models developed in Step (2) and the critical acceleration boundary specified in Step (3).

(5) Prioritize the threatened bridges according to their "risk values." These values are calculated as follows. First, assign priority weighs (0.0 to 1.0) to each of the following characteristics:

- ground acceleration,
- average daily traffic (ADT),
- column design, i.e., single or multiple column beams,
- confinement details of column,
- route type, i.e., major or minor,
- length of bridge,
- skew of bridge, and
- availability of detour.

The procedure scores each bridge for each of the above characteristics. The risk value for each bridge equals the sum of its weighted scores across all these characteristics.

Caltrans raised the priority of its retrofit program in 1987 due to the magnitude 5.9 Whittier Narrows earthquake. This earthquake occurred during the morning peak hour. The earthquake produced significant damage to the transportation system, including the near collapse of a 5-column bent supporting the crossing of the I-605 freeway over the I-5 freeway.

In 1989, the magnitude 7.1 Loma Prieta earthquake caused the collapse of numerous buildings and transportation structures, amounting to almost $6 billion in damages. The earthquake damage increased concerns about bridge safety and intensified interest in State-wide retrofit programs. Caltrans proposed an accelerated schedule for retrofitting its 392 single column bent bridges. Caltrans put the remaining State-owned bridges on the retrofit agenda. Caltrans also modified the Level One Risk Analysis procedure by incorporating technical improvements in earthquake engineering. The priority weights assigned to each of the original characteristics were adjusted. New characteristics were added to the list. The additional characteristics are

- soil type,
- hinges, including type and number,
- exposure, i.e., the combination of length and ADT,
- height,
- abutment type, and

- type of facility crossed.

3-1-3. The Vulnerability Assessment and Prioritization Procedure

Caltrans' Vulnerability Assessment and Prioritization Procedure responded to an executive order by Governor Dekmejian in 1990. The order called for a priority listing of transportation structures to be scheduled for seismic retrofit. In the Report to the Governor on Seismic Safety (Caltrans, 1990), Caltrans describes its basic steps for the Vulnerability Assessment and Prioritization Procedure as follows.

(1) Identify all structure requiring retrofitting to ensure they are safe from collapse or major damages during earthquakes.

(2) Identify "complex" or "vital transportation link" structures using special criteria, and analyze and retrofit them to reduce the risk of major damages and to ensure their function can be maintained after an earthquake.

(3) Prioritize all structures requiring retrofitting.

Caltrans reviewed all available general structure plans for about 24,000 state and local bridges. Types of bridges initially removed from consideration are:

- timber bridges,
- culverts,
- single span bridges,
- short monolithic structures,
- structures designed after 1980, and
- recently designed single-column retrofit structures.

Other general factors considered by Caltrans in assessing transportation structures are:

- fault crossings,
- airspace,
- pedestrian bridges, and
- special knowledge acquired by Caltrans engineers regarding structural problems.

After the initial screening, Caltrans assessed the seismic vulnerability of each bridge using the 12 weighting factors shown in Table 1. Caltrans established a seismic priority factor between zero (low) and one (high). The bridges were ordered with the highest priority.

The bridge prioritization procedure employs a simplified scheme for seismic risk assessment. This procedure is computationally simple. However, the overall rank may produce inconsistent evaluations of relative risk. The procedure adds the weighted factors affecting the probability of failure to those affecting the consequences of failure (Gilbert, 1993).

Table 1: Seismic Vulnerability Weighting Factors

Weight, %	Factor
13	Year Designed
12	Peak Rock Acceleration
12	Soil at Site
11	Number of Hinges
10	Columns Per Bent
8	Traffic Exposure
7	Height
7	Skew
6	Facility Crossed
5	Route Type

5	Length of Detour
4	Abutment Type

100	Total

3-1-4. Caltrans Multi-Attribute Decision Procedure

Caltrans experienced from its vulnerability assessment and prioritization procedure that risk is properly evaluated by multiplying the probability of failure with the consequences of failure. Thus, Caltrans revised the previous prioritization scheme in 1992, and developed a multi-attribute decision procedure. Like the previous prioritization procedure, this procedure assigns a priority rating to each bridge to determine which bridge is more vulnerable to seismic activity based on current conditions. The major improvement of the new procedure is the framework of two-level approach that separates the seismic hazard from the impact and structural vulnerability criteria. This allows a bridge with low seismic hazard to receive a lower overall risk rating than a similar structure with higher seismic hazards. This outcome has not been achieved with previous prioritization schemes because the early methods rely on a point-score summation. The formula for the prioritization rating R is

$$R = \left(\prod_{i=1}^{2} \left(w_i(c_i) \sum_{j=1}^{n_i} x_{ij}(a_{ij}) \cdot g_{ij}(a_{ij}) \right) \right) \cdot \left(\sum_{i=3}^{4} \left(w_i(c_i) \sum_{j=1}^{n_i} x_{ij}(a_{ij}) \cdot g_{ij}(a_{ij}) \right) \right), \quad (1)$$

where

c_i = *four criteria used in rating,*
a_{ij} = *a set of attributes associated with the* i*th criteria,*
n_i = *the number of attributes associated with the* i*th criteria,*
$w_i(c_i)$ = *weights assigned to each criteria,*
$x_{ij}(a_{ij})$ = *weights assigned to each attribute, and*
$g_{ij}(a_{ij})$ = *global utility functions created for each attributes*.

The details of the criteria, attributes, and global utility functions are shown in Table 2.

Table 2: Criteria, Attribute, and Utility Function Details

Criterion	Criterion Weights	Attribute	Attribute Weights	Global Utility Function
c_1 = seismic activity	$w(c_1) = 1.0$	a_{11} = seismic activity	$x_{11}(a_{11}) = 100\%$	0.25 = low; 0,50 = moderate; 0.75 = active; 1.0 = high
c_2 = hazard	$w(c_2) = 1.0$	a_{21} = soil conditions	$x_{21}(a_{21}) = 33\%$	1 = high risk zone; 0 = else
		a_{22} = peak rock acceleration	$x_{22}(a_{22}) = 38\%$	linear, normalized to 0.7g
		a_{23} = seismic duration	$x_{23}(a_{23}) = 29\%$	0.5 = short; 0.75 = intermediate; 1 = long
c_3 = impact	$w(c_3) = 0.6$	a_{31} = average daily traffic on structure	$x_{31}(a_{31}) = 28\%$	parabola for a max. ADT of 20000
		a_{32} = average daily traffic under/over structure	$x_{32}(a_{32}) = 12\%$	See ADT above
		a_{33} = Detour Length	$x_{33}(a_{33}) = 14\%$	linear, normalized to 100 miles
		a_{34} = Leased Air Space (Residential, Office)	$x_{34}(a_{34}) = 15\%$	1 - present; 0 = else.
		a_{35} = Leased Air Space (Parking, Storage)	$x_{35}(a_{35}) = 7\%$	1 - present; 0 = else.
		a_{36} = Route Type on Bridge	$x_{36}(a_{36}) = 7\%$	1.0 = interstate; 0.8 = US, ST rte, or stream; 0.7 = RR; 0.5 = fed funded Co rte or city str; 0.2 = nonfed funded Co rte of city str; 0.0 = fed land, ST land, other
		a_{37} = Critical Utility	$x_{37}(a_{37}) = 10\%$	1 - present; 0 = else.
		a_{38} = Facility Crossed	$x_{38}(a_{38}) = 7\%$	See Rte Type on Bridge
c_4 = vulnerability	$w(c_4) = 0.4$	a_{41} = year designed (constructed)	$x_{41}(a_{41}) = 25\%$	0.5 = yr<1946; 1.0 = 1946≤yr≤1971; 0.25 = 1972≤yr≤1979; 0.0 =yr>1979.
		a_{42} = hinges (drop type failure)	$x_{42}(a_{42}) = 16.5\%$	0.0 = no hinge; 0.5 = 1 hinge; 1.0 = 2 or more hinges
		a_{43} = outriggers, shared column	$x_{43}(a_{43}) = 22\%$	1 - present; 0 = else.
		a_{44} = bent redundancy	$x_{44}(a_{44}) = 16.5\%$	0.0 = no col.; 0.25 = pier walls; 0.5 = multi col bents; 1.0 = single col bent
		a_{45} = skew	$x_{45}(a_{45}) = 12\%$	linear, normalized to 90
		a_{46} = abutment type	$x_{46}(a_{46}) = 8\%$	0 = monolithic; 1 = non monolithic

3-1-5. Comments

Caltrans' existing retrofit criteria have proven useful. All of the 122 Southern California bridges were retrofitted before the occurrence of the 1994 Northridge earthquake. All survived from the magnitude 6.8 earthquake. The Northridge earthquake damaged eleven freeway bridges. Out of eleven bridges, ten were scheduled for retrofitting. The reason for the exception was an undetected active fault, not the prioritization procedure.

However, there is still room for improvement on the procedure. Caltrans' current retrofit criteria depend primarily on the Average Daily Traffic (ADT) volume to determine the importance of a bridge. This is not adequate. For example, one of the public policy questions arising after the Northridge earthquake is the appropriate retrofit priority rating for the Santa Monica Freeway. Given the heavy traffic the freeway carries, structural engineering experts suggest that the rating should be high. But numerous alternative surface streets are available, which reduces the relative importance of retrofitting the Santa Monica freeway.

Average Daily Traffic (ADT) volume is an important indicator only when there is no significant change in the transportation network. If network configurations such as link capacities are changed, it is better to use system-wide changes of network flows as the prioritization indicator rather than the current ADT volumes. In other words, a much more meaningful approach for determining the importance of a bridge (or any freeway

link) is a system-wide traffic flow analysis. A way of evaluating the system-wide changes of network flows in a transportation network is to compute total system travel times based on simulated or observed network flows. The change of total system travel times between the presence and absence of a bridge can be used in representing the importance of bridges in a transportation network.

3-2. Models and Algorithms for Predicting Network Flows

3-2-1. Background

Network flow problems are essentially route choice or traffic assignment problems. The question is how to determine the way in which people, vehicle, and goods use the transportation network. The notion of equilibrium plays a central role (Florian, 1984) in all the attempts to construct mathematical models to network flow.

The idea of traffic equilibrium appears as early as 1920 in the work of Pigou, who considers a two-node, two-link (two path) transportation network. The principle is further developed by Knight (1924). From the economic perspective, traffic equilibrium is a special case of market equilibrium. The demand side of the market corresponds to the users of the network. The supply side of the market is represented by the network itself, with market prices corresponding to travel costs (Nagurney, 1993).

The economic concept of traffic equilibrium is essentially the same as that of short run market equilibrium for any good or services. However, the presence of certain special characteristics associated with network configuration and congestion processes makes the traffic equilibrium problem very special and particularly complex. The importance of the problem with considering those difficulties has stimulated intensive research in the area.

Wardrop (1952) developed two principles that formulate the notion of traffic equilibrium. He introduced user behavior postulates associated with these two principles. His first principle states that "At equilibrium no user can reduce his journey time by unilaterally changing routes." Another standard way of stating this principle is "The journey times on all routes actually used are equal and less than those which would be experienced by a single vehicle on any unused route." An underlying assumption for this principle is that each user chooses the route that he perceives to be the best. For this reason, traffic flows satisfying Wardrop's first principle are usually referred to as the user equilibrium flows.

By contrast, Wardrop's second principle states that, "At equilibrium the average journey time is minimum." This implies that each user behaves cooperatively in choosing his own route to ensure the most efficient use of the whole system. Traffic flows satisfying Wardrop's second principle are generally known as the system equilibrium.

As Wardrop himself reports, his first principle is a practical one that is most likely to happen in reality. His second principle describes an ideal equilibrium situation in which the total travel cost of the whole network is minimized, such as would occur under a set of optimal congestion tolls.

In large, uncongested networks in which the link travel costs are constant, there is no difference between the user and system equilibrium flows. The difference becomes significant when the network is congested on all or part of its links. In general, user equilibrium flows differ from system equilibrium flows in a congested network.

Beckman et al. (1956) are the first to rigorously formulate and analyze the equilibrium conditions mathematically. They establish the equivalence between these conditions and the Kuhn-Tucker conditions of an appropriately constructed optimization problem. Their seminal work shows that the traffic equilibrium flows can be obtained as solutions to mathematical programming problems.

3-2-2. Formulations of Network Equilibrium Models

Standard network flow models are steady state models. Although the details of the models vary widely from one problem setting to another, the basic form remains essentially the same.

Consider a transportation network with N nodes and A links. The flow on each directed link $a \in A$ is v_a. Each link is associated with a transportation cost function

$C_a(\boldsymbol{v})$, where $\boldsymbol{v}$ is the vector of link flows over the entire network. This cost function is usually assumed to be monotone, continuous, and differentiable. It measures the delay for travel on each link. It is also referred to as the link performance function or volume delay function.

For certain origin-destination (O-D) pairs $i \in I \subseteq N \times N$, there is a given positive flow demand $d_i(\boldsymbol{u})$, where $\boldsymbol{u}$ is the vector of travel costs for all the O-D pairs in the network. Define K_i to be the set of paths connecting each O-D pair i, and h_k to be the flows on paths $k \in K_i$. Then $C_k(\boldsymbol{v})$, the total travel cost for each path k, is the sum of the link travel costs on that path, i.e.,

$$C_k(v) = \sum_a \delta_{ak} \cdot C_a(v), \qquad k \in K_i, \qquad i \in I, \tag{2}$$

where

$$\delta_{ak} = \begin{cases} 1, & \text{if link } a \text{ belongs to path } k, \\ 0, & \text{otherwise.} \end{cases} \tag{3}$$

Let $u_i(\boldsymbol{v})$ be the cost of the least cost path for any O-D pair i, namely,

$$u_i = \min_{k \in K_i} C_k, \qquad i \in I. \tag{4}$$

Then, the user equilibrium condition can be formulated as

$$C_k - u_i \begin{cases} = 0, & \text{if } h_k > 0, \\ \geq 0, & \text{if } h_k = 0, \end{cases} \qquad k \in K_i, \qquad i \in I, \tag{5}$$

subject to the path flow conservation and nonnegativity conditions

$$\begin{cases} \sum_{k \in K_i} h_k = d_i, \\ h_k \geq 0, \quad k \in K_i, \end{cases} \qquad i \in I, \tag{6}$$

or the link flow conservation and nonnegativity conditions

$$\begin{cases} v_a = \sum_{i \in I} \sum_{k \in K_i} \delta_{ak} \cdot h_k, \\ v_a \geq 0, \end{cases} \qquad a \in A. \tag{7}$$

It is easily seen that condition (5) may also be stated in the complementary form

$$C_k \geq u_i \quad and \quad (C_k - u_i)\, h_k = 0, \qquad k \in K_i, \qquad i \in I. \tag{8}$$

The user equilibrium condition may be formulated in several mathematical forms. The most general and useful one is the variational inequality form, which is

$$(C_k - u_i)(h_k^* - h_k) \geq 0, \qquad k \in K_i, \qquad i \in I, \tag{9}$$

where h_k^* is any feasible set of path flows. The variation inequality formulation provides a way to address multi-nodal models with elastic demands, for which no equivalent optimization formulation of the equilibrium conditions are available.

If cycle flows do not occur and the demand functions have an upper bound, the existence of a solution to the network equilibrium model is ensured by the continuity of the user cost and demand functions and by the fact that the feasible set (5) or (6) is compact (Florian, 1985). When the link performance functions are strictly monotone and the demand functions and their inverses are strictly antitone, link flows and O-D costs of network are unique (though, in general, path flows are not). Dafermos and Nagurney (1983) demonstrate that small changes in the travel demands and in the link performance functions result in only small changes in the traffic flows, demonstrating that the network equilibria are stable.

Most applied network equilibrium models assume that each link performance function depends only on the flow on that link. Each demand function depends only on the travel cost between the corresponding O-D pair. That is, $C_a(\boldsymbol{v}) = C_a(v_a)$ and $d_i(\boldsymbol{u}) = d_i(u_i)$. Due to such conditions it is possible to construct convex optimization problems for which first-order optimality condition is the equilibrium condition. A user optimization problem of this sort has the form of

$$\min_{v_a} \quad \sum_{a \in A} \int_0^{v_a} C_a(x)\, dx, \tag{10}$$

subject to (6) and (7). The corresponding system optimization problem is

$$\min_{v_a} \quad \sum_{a \in A} v_a \cdot C_a(v_a), \tag{11}$$

subject to (6) and (7).

Formulations described above are static equilibrium models. Considerable research has also been done on formulating stochastic and dynamic network problems. The derivation of a stochastic equilibrium model requires probability distribution assumptions concerning the travel demand process and/or route selection process. Stochastic user equilibrium (SUE) models are more realistic than the static UE models. They assume

that travelers are not perfectly informed when they choose routes (Ran and Boyce, 1994). Most SUE models are based on the logit models in which route choice is modeled as a discrete choice problem. SUE models appear in Dial (1971), Daganzo and Sheffi (1977), Davis and Nihan (1993), Davis (1994), and Soumis and Nagurney (1993). The entropy-maximizing models introduced by Wilson (1970a, 1970b) and Wilson and Senior (1974) provide an alternative interpretation for SUE models.

The crucial consideration in forming dynamic network models is how to formulate the time-dependent link performance functions and the temporal O-D demand relationships. Merchant and Nemhauser (1978) constructed the first dynamic system optimal (DSO) traffic assignment models. Carey (1986) showed that a dynamic traffic assignment model formulated as a nonlinear and non convex optimization model. Carey's dynamic traffic assignment model satisfies a "constraint qualification." This further ensures the validity of Kuhn-Tucker based analysis of the model. Dynamic user optimal (DUO) problems for a simple transportation network were studied by Matsu (1987) using optimal control theory. A generalized DUO model over a multiple O-D network was presented by Wie et al. (1990). Friesz et al. (1989) analyzed some of the fundamental properties of DUO and DSO models.

3-2-3. Algorithms

The variational inequality formulation opened the way for understanding and solving complicated network equilibrium problems. However, most of the practical models are still based on the initial work of Beckman et al. (Florian, 1985). These models are frequently solved through a number of efficient algorithms designed for optimization problems.

The most commonly used algorithm for solving convex cost minimization problems with linear constraints are the feasible direction method of Frank and Wolfe (1956) and some of its variants. Take the fixed demand problem given by (10), (6), and (7) as an example. Starting from an initial feasible link flow solution $v_a^{(0)}$, the Frank-Wolfe algorithm obtains a feasible direction by linearizing the objective function, solving a linear programming subproblem, and then finding an improved solution on the line segment between the current solution and the solution of the subproblem. The linearized subproblem at iteration j is

$$\min_{f_k} \quad _{i\llcorner I\ k\llcorner K_i a\llcorner A} C_a(v_a^{(j)})?\delta_{ak}?f_k, \tag{12}$$

subject to

$$\sum_{k\in K_i} f_k = d_i, \qquad i \in I, \tag{13}$$

and

$$f_k \geq 0, \qquad k \in K_i, \qquad i \in I. \tag{14}$$

The objective (11) is also equivalent to

$$\min_{f_k} \quad \sum_{i \in I} \sum_{k \in K_i} C_k^{(j)} \cdot f_k. \tag{15}$$

The solution to this linearized problem, $f_k^{(j)}$, is obtained trivially by computing shortest paths for each O-D pair i and allocating the demand d_i to that path. The solution to the problem (11)-(13) is then give by

$$f_a^{(j)} = \sum_{i \in I} \sum_{k \in K_i} \delta_{ak} \cdot f_k^{(j)}, \tag{16}$$

and the direction of decent is simply $f_a^{(j)} - v_a^{(j)}$. The algorithm then proceeds by solving the problem

$$\min_{0 \le \lambda \le 1} \sum_{a \in A} \int_0^{v_a^{(j)} + \lambda \left(f_a^{(j)} - v_a^{(j)} \right)} C_a(x)\, dx, \tag{17}$$

for the optimal step length $\lambda^{(j)}$. Alternatively, $\lambda^{(j)}$ can be found as a solution to the equation

$$\sum_{a \in A} C_a\left(v_a^{(j)} + \lambda \left(f_a^{(j)} - v_a^{(j)} \right) \right) \cdot \left(f_a^{(j)} - v_a^{(j)} \right) = 0, \tag{18}$$

The process stops either when the direction of descent is zero or when the decrement of the objective function is less than a predetermined termination criteria.

The Frank-Wolfe algorithm has several advantages. It is easy to understand and simple to implement. The core storage requirements are small. However, the algorithm is only efficient in the first few iterations. Its overall performance is not fully satisfactory. It has notoriously slow convergence and exhibits oscillation near equilibrium. The main reason for this behavior is that the search generated by the linear subproblem solution tends to become perpendicular to the steepest descent direction as the number of iterations increases (Larsson and Patriksson, 1992).

Algorithms proposed to solve variational inequalities formulations of the network equilibrium models can be divided into three main categories (Fresz, 1985): (a) linearization methods, (b) diagonalization methods, and (c) simplicial decomposition methods. Pang and Chen (1982) give a detailed discussion and general treatment of

convergence properties of linearization algorithms. Diagonalization methods are analyzed by Dafermos (1982), Florian and Los (1982), and Pang and Chen (1982). Simplicial decomposition methods are discussed in Larsson and Patriksson (1992). Patriksson (1993) shows that a number of algorithms frequently applied to network equilibrium problems may be described in a unified manner as instance of a partial linearization algorithm. These frequently used algorithms include the standard Frank-Wolfe algorithm, Newton type methods, projection methods, and Jacobi/Gauss-Seidal methods.

3-2-4. Comparing the Standard Approach with Stochastic and Dynamic Extensions

Modeling traffic flows in transportation networks remains an area of intense investigation. The deterministic, static formulation of network flows subject to endogenous link travel costs remains the standard formulation in the field. Extensions intended to treat randomness in user decisions, represent queues at bottlenecks, and account for transient demand are of considerable theoretical importance. Progress has been made in all of these dimensions. However, real time estimation of urban network flows by any means analytically, numerically, or simulation remains unachieved. The standard formulation is being improved incrementally to make user flow models more realistic, but there are neither standard representations of stochastic user equilibrium nor

of dynamic user equilibrium. Real time modeling of flows on urban transportation networks will most likely be achieved via improvements in traffic flow simulation models. The literature describing simulation as a stochastic process and numerical models of network flows has only recently begun to converge.

3-3. Estimating Origin-Destination (O-D) Trip Matrices from Traffic Volumes

This section explains the methods of obtaining an updated O-D trip matrix that will be used as the input data for the static user equilibrium model described in section 3-2.

3-3-1. Background

The demand for travel within a given area is estimated by dividing the area into a set of Origin-Destination (O-D) zones. The travel demand between each O-D pair in the network is assumed to be known in the formulation of network equilibrium models. These demands form a two-dimensional O-D matrix that accounts for the total number V_{ji} of trips between all designated origin and destination zones served by the highway/ roadway system being considered.

The traditional method for estimating the O-D matrix is Origin-Destination surveys. However, such surveys are generally very expensive in terms of manpower, time, and expense. By comparison, traffic counts are relatively inexpensive to obtain, and are routinely collected automatically for multiple purposes. Consequently, there is considerable interest in developing procedures for estimating O-D matrices from traffic counts. The literature includes several O-D trip estimation methods.

Approaches to estimating or updating O-D trip tables from traffic counts are primarily divided into two groups: parameter calibration methods and matrix estimation methods. Parameter calibration methods are based on gravity type models. Prior to the 1970s, traffic volume data was used primarily for the study of traffic control and road construction. Robillard (1973) suggests a method for determining origin-destination trip tables based on observed link volumes. Under Robillard's approach, the cost of travel between every origin-destination-pair is used to estimate the O-D matrix based on a gravity model. A regression problem is solved to determine total trips originating from and terminating in each zone, and then a generalized gravity model is used to determine the trip table. Robillard (1975), Low (1972), Smith and McFarlane (1978), and Symons et al. (1976) estimate O-D matrices from by a gravity model in which parameters can be calibrated based on traffic counts. This approach reduces to a linear or nonlinear least squares problem in which the sum of squared deviations between the link flows predicted form the gravity model and the traffic counts obtained for each link is minimized.

Matrix estimation methods fall into three categories:

(1) equilibrium assignment (EA) approaches,

(2) entropy maximizing (EM)/information minimizing (IM) approaches, and

(3) statistical estimation approaches.

In the case of matrix estimation methods, the equilibrium assignment methods developed in North America are based on optimization approaches intended to satisfy Wardrop's user equilibrium principle. Under this equilibrium assignment approach, the link performance function is assumed to be known, and an initial (target) O-D matrix must be provided (frequently by exercising trip distribution models). The objective is to determine the minimum correction in the target O-D matrix that will satisfy equilibrium assignment conditions and replicate the observed traffic counts. Willumsen (1981), Nguyen (1977, 1978), and Turnquist and Gur (1979) demonstrate such an approach.

In contrast, the entropy maximizing/ information minimizing approaches may not employ a prior trip table if it is not available. These methods use the objective of either maximizing the entropy of the trip matrix or minimizing the information contained in the link flows to estimate the most likely trip matrix consistent with the observed traffic counts. Examples of various applications of this approach can be found in Hall et al. (1980), Beagan and Bromage (1987), and Lam and Lo (1991).

In general, link volumes alone do not provide enough information to construct a unique trip table. This underspecification problem follows from the use of a small number of observed links relative to a large number of unknown origin-destination interchanges. The problem can only be overcome by using additional information. In equilibrium approaches, an initial trip table is used. In EM or IM approaches, the path (or link) choice proportions and the maximum entropy principle define the required increment in information. The statistical estimation approaches estimate future trips based on prior information by using Bayesian inference or least squares estimation techniques. These approaches have not been as widely applied as the equilibrium assignment or entropy maximizing/information minimizing approaches. Consequently, the statistical estimation approaches are not investigated here.

3-3-2. Equilibrium Assignment (EA) Approaches

The equilibrium assignment approach estimates an O-D matrix that both satisfies equilibrium assignment conditions and is consistent with the observed link flows. The approach requires knowledge of the actual travel costs for all links and an initial (target) O-D trip table. The suggested solution algorithm is initialized by the target trip table, then corrects the table so that it approximates as closely as possible with the observed

flows. Because this model accounts for congestion in the network and uses traffic counts, it is well suited to estimating an O-D trip matrix in a congested urban area.

This approach was first developed by S. Nguyen (Turnquist and Gur, 1979). Based on the initial trip table that satisfies Wardrop's first principle, Nguyen specifies a nonlinear optimization problem to which the trip table replicates observed flows when the trip table is assigned under user equilibrium. Thus this approach identifies an O-D trip matrix. Nguyen's optimization problem is similar to equilibrium assignment under elastic demand.

Turnquist and Gur (1979) state the problem of finding an O-D matrix that, when assigned, replicates observed link volumes as follows,

$$\min F = \sum_a \left[\int_0^{f_a} t_a(x)dx \right] - \sum_j u_j T_j \qquad (19)$$

subject to

$$T_j - \sum_k h_j{}^k = 0 \qquad \text{for each O-D pair j} \qquad (20)$$

$$\sum_j \sum_k d_{ja}{}^k h_j^k = f_a \qquad \text{for each link a, and} \qquad (21)$$

$$f_a, T_j, h_j^k \geq 0 \qquad (22)$$

where

F = *objective function of the optimization problem*
f_a = *observed flows on link a,*

$t_a(x)$ = *impedance function for link a,*
u_j = *observed O-D impedance for trip interchange j,*
T_j = *trips for interchange j,*
h_j^k = *number of trips from interchange j using path k, and*
d_{ja}^k = *1, if link a is in path k for interchange j*
0, otherwise.

An interchange is a flow between a specific O-D pair. This model begins with an initial O-D trip matrix. The initial O-D trip matrix is assigned to the given transportation network, and generates the simulated traffic flows. The model updates the initial O-D trip matrix until the difference between the simulated total travel times and the total travel times from the observed link volumes is minimized.

This optimization model applies the Frank-Wolfe algorithm. The solution is obtained by an iterative procedure, and requires the following basic steps (algorithm):

Step 1. Let $i = 1$.

Step 2. Specify an initial trip table $T^{i=1}$ and a volume-delay function for each link.

Step 3. Based on the observed link impedance, find u_j, the observed O-D impedance for trip interchange *j*.

Step 4. Assign $T^{i=1}$ to the unloaded network by using free flow impedance v_j to obtain a set of link volumes $f^{i=1}$.

Step 5. Determine link impedance at the current volume f^i and again build minimum impedance trees.

Step 6. Given T_j^i, u_j, v_j, and w_j^i, find a correction trip table V_j^i based on the differences of the path impedance:

$$V_j^i = T_j^i \times \left[1 + 2 \times \left\{\left(u_j - w_j^i\right)/\left(w_j^i - v_j\right)\right\}\right] \quad if\ u_j > w_j^i \tag{23}$$

$$= if\ \ u_j > w^i_j \tag{24}$$

Step 7. Assign V_j^i to the tree built in step 5 to obtain correction link volumes s^i.

Step 8. Find a weight r^i such that $0 \le r^i \le 1$ and the solution $[(f^{i+1}, T^{i+1}) = r^i(s^i, V^i) + (1\text{-}r^i) * (f^i, T^i)]$ minimizes the objective function F.

Step 9. Check the convergence criterion. If it is met, stop; otherwise, set $T_j^i = V_j^i$ and $i=i+1$, and go to step 5.

where,

i = *iteration counter,*
v_j = *free flow O-D impedance for trip interchange j,*
w_j^i = *O-D impedance for trip interchange j at iteration i,*
f^i = *a set of link volumes at iteration i,*
s^i = *a set of correction link volumes at iteration i,*
V_j^i = *correction trips trip interchange j at iteration i.*

This equilibrium assignment approach requires the following data,

- observed link volumes (for all links),
- link impedance,
- link performance function, and
- initial trip table.

The approach is summarized in Figure 1.

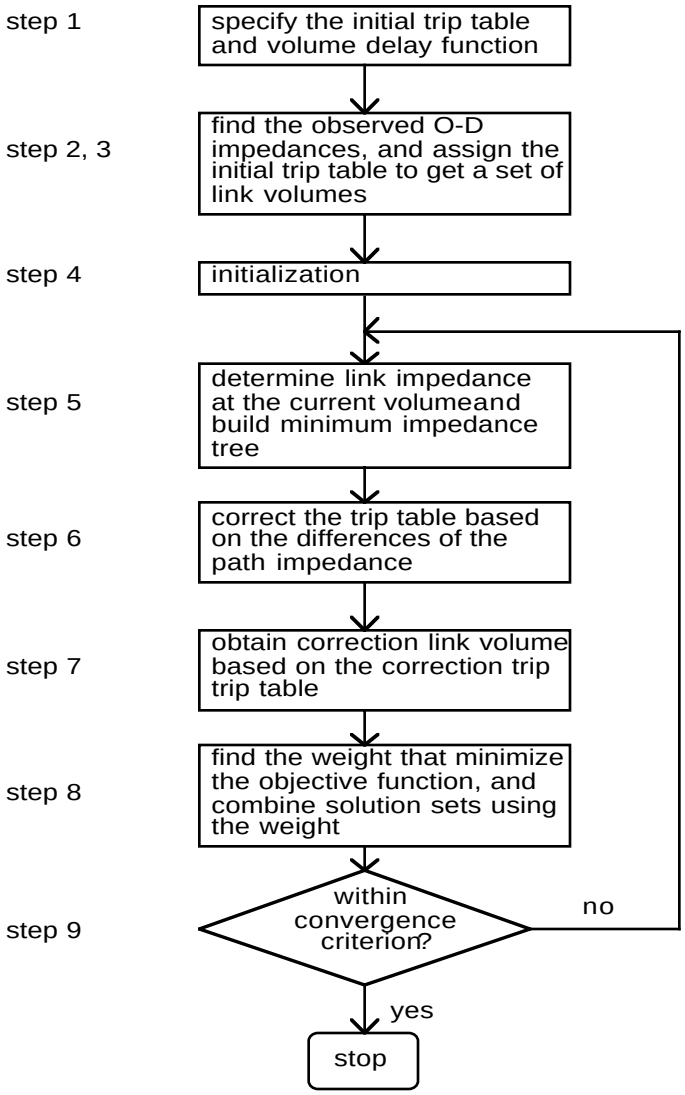

Figure 1: Equilibrium Assignment Approach Flow Chart.

3-3-3. Entropy Maximizing (EM) or Information Minimizing (IM) Approaches

This type of model estimates the most probable O-D matrix based on traffic counts under proportional assignment conditions. The estimate is consistent with the constraints with an entropy maximization problem. This model requires neither the traffic counts on

all links in the network nor an initial O-D matrix. But there are modified EM or IM models in which an available initial trip table can be used to increase accuracy. This approach is inaccurate if travel behavior is not well represented by the gravity model or similar formulations.

Willumsen (1981) provides the mathematical formulation and algorithm for the original EM model. The formulations and solution algorithms of modified EM and IM models are similar to those of the original, except for the addition of prior (initial) trip interchange terms. According to the Willumsen's entropy model, Stirling's approximation can be used to express the entropy of a network as

$$S = -\sum_{ij} \ln T_{ij}! = -\sum_{ij} (T_{ij} \ln T_{ij} - T_{ij}). \tag{25}$$

The Entropy Maximization formulation is

$$\max \quad S(T_{ij}) = -\sum_{ij} (T_{ij} \ln T_{ij} - T_{ij}) \tag{26}$$

subject to

$$\sum_{ij} T_{ij} P_{ij}^{a} = V_a \tag{27}$$

$$T_{ij} \geq 0 \tag{28}$$

where

P_{ij}^{a} = *proportion of trips from origin i to destination j which use link a,*
T_{ij} = *trips from origin i to destination j, and*
V_a = *observed volume of link a.*

The Lagrangian L may be maximized to obtain the set of T_{ij}'s that maximizes $S(T_{ij})$ subject to constraints (27).

$$L = S(T_{ij}) + \sum_a \lambda_a (V_a - \sum_{ij} T_{ij} P_{ij}^a) \tag{29}$$

and where terms λ_a are Lagrangian multipliers. The terms T_{ij}s, which constitute the most probable distribution of trips, are solutions to the following set of first order conditions.

$$\frac{\partial L}{\partial T_{ij}} = -\ln T_{ij} + \sum_a (-\lambda_a P_{ij}^a) = 0. \tag{30}$$

$$\therefore T_{ij} = \exp\{\sum_a (-\lambda_a P_{ij}^a)\} = \prod_a X_a^{P_{ij}^a} \tag{31}$$

where

$$X_a = \exp(-\lambda_a). \tag{32}$$

The entropy maximization approaches require following data,

- observed link volumes (at least in part),
- path or link use proportions (P_{ij}^{a}), and
- an initial trip table (for modified EM model and IM model).

3-3-4. Comparing EA Models with EM/IM Models

The strengths and weaknesses of each approach are summarized as follows. EA models are applicable to congested network (strength), but need an initial trip table (are sensitive to the initial trip table), and require volume counts for all links (weaknesses). EM/IM models have flexible data requirements (partial link counts will do, and initial trip table is not necessarily required), seek the most probable O-D pattern based on the information available (strengths), but do not provide an adequate treatment of congestion (do not use link performance characteristics), and assume proportional assignment i.e., require terms P_{ij}^{a} (weaknesses).

3-4. Artificial Intelligence (AI) Approaches to Modeling

Associative memories are part of artificial intelligence approaches that make computers learn and remember in ways similar to human memory processes. The

associative memory approach is a newly-developed, heuristic approach. Associative memories address the pair association problem between stimulus and response matrices.

The associative memory approach requires a procedure computing associative memory matrices (training step) and evaluating the performance of the computed memory matrices (test step). Associative memories are computed by using a pair set of training input data so that the application of a set of stimulus inputs produces the desired (or at least consistent) set of response inputs. The computed memory matrices are later used to estimate response outputs for a set of new stimulus inputs that have not been used to create the associative memory matrices. The performance of different associative memory matrices is evaluated in the test step by comparing the estimated outputs with test response outputs.

Researchers at the University of Southern California have experimented with the associative memory approach to various regional modeling problems. The group has had success applying various versions of associative memory matrices to difficult parameter identification problems (Kalaba, Lichtenstein, Simchony, and Tesfatsion 1990; Kalaba and Tesfatsion 1991; Kalaba and Udwadia 1991; Moore II, Kalaba, Kim, and Park 1993; Moore II, Kim, Seo, and Kalaba 1994; Kalaba, Moore, Xu, and Chen 1994; and Moore II, Kalaba, Kim, Seo, and Kim 1994), including constrained optimization problems (Kalaba, Kim, and Moore II 1991, 1992; Moore II, Kim, Seo, Wu, and Kalaba 1991).

This research employs the associative memory approach to estimate changes in network flows (response vectors) with respect to given network configurations (stimulus vectors) of post-earthquake system states due to different scenario earthquakes. This research employs three associative memory models. They are: (1) Simple Associative Memories (SAM), (2) Recurrent Associative Memories (RAM), and (3) Multicriteria Associative Memories (MAM). Details of the three associative memory models are described in the following sections.

3-4-1. Simple Associative Memories (SAM)

As Figure 2 indicates, associative memories address the pair association problem. Does there exist an associative memory $\boldsymbol{M}$ (Kohonen 1989) that will map a finite set of arbitrarily selected stimulus vectors to the corresponding set of system response vectors? The stimulus- response notion is crucial: For each of K training cases, let the stimulus vector $\boldsymbol{s}_k$ of dimension $p \times 1$, and the system response vector $\boldsymbol{r}_k$ of dimension $q \times 1$, be specified.

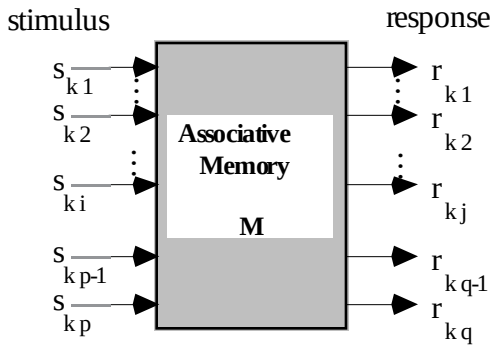

Figure 2: An Ideal Associative Memory

The objective is to determine an associative memory matrix $\boldsymbol{M}^*$ of dimension $q \times p$, so that $\boldsymbol{M}^* \boldsymbol{s}_k$ will equal $\boldsymbol{r}_k$ as nearly as possible for *k = 1, 2, . . . , K*. Following Kohonen (1989), we take this to mean that if we form the stimulus matrix $\boldsymbol{S}$ of dimension $p \times K$, whose k^{th} column is $\boldsymbol{s}_k$, and the response matrix $\boldsymbol{R}$ of dimension $q \times K$, whose k^{th} column is $\boldsymbol{r}_k$, then the matrix $\boldsymbol{M}^*$ is to be determined by minimizing the L_2 norm of the difference matrix $\boldsymbol{R} - \boldsymbol{M}\boldsymbol{S}$,

$$\boldsymbol{M}^* = \arg\min_{\boldsymbol{M}} \| \boldsymbol{R} - \boldsymbol{M}\boldsymbol{S} \|^2 . \tag{33}$$

The hope is, then, that even if $\boldsymbol{s}$ is not in the training set, $\boldsymbol{M}^* \boldsymbol{s}$ will provide a good approximation to the system's response to stimulus $\boldsymbol{s}$. Clearly, minimizing the L_2 norm minimizes mean square error. Noting that

$$\|\boldsymbol{M}\| = \left(Trace(\boldsymbol{M}^T \boldsymbol{M})\right)^{1/2}, \tag{34}$$

it follows that

$$\begin{aligned} \|\boldsymbol{R} - \boldsymbol{MS}\|^2 &= Trace\left((\boldsymbol{R} - \boldsymbol{MS})^T (\boldsymbol{R} - \boldsymbol{MS})\right) \\ &= Trace\left(\boldsymbol{R}^T \boldsymbol{R} - \boldsymbol{R}^T \boldsymbol{MS} - \boldsymbol{S}^T \boldsymbol{M}^T \boldsymbol{R} + \boldsymbol{S}^T \boldsymbol{M}^T \boldsymbol{MR}\right), \end{aligned} \tag{35}$$

Minimizing Equation (33) over $\boldsymbol{M}$,

$$\partial \|\boldsymbol{R} - \boldsymbol{MS}\|^2 / \partial \boldsymbol{M} = Trace\left(2\boldsymbol{M} * \boldsymbol{SS}^T - 2\boldsymbol{RS}^T\right) = 0, \tag{36}$$

and, assuming $\boldsymbol{SS}^T$ to be nonsingular, it follows that

$$\boldsymbol{M}* = \boldsymbol{RS}^T (\boldsymbol{SS}^T)^{-1}. \tag{37}$$

More generally, the solution to this problem is

$$\boldsymbol{M}* = \boldsymbol{RS}^+, \tag{38}$$

where $\boldsymbol{S}^+$, dimension $K \times p$, is the Moore-Penrose generalized inverse of the rectangular matrix $\boldsymbol{S}$. $\boldsymbol{S}^+$ can be calculated even if $\boldsymbol{S}$ is not of full rank. Codes for calculating this generalized inverse are available in standard software packages such as Mathematica, Matlab, and SAS.

3-4-2. Recurrent Associative Memories (RAM)

For constrained optimization (Kalaba, Kim and Moore II 1991; Kalaba, Kim, Moore II, Seo and Wu 1991; Kalaba, Kim, and Moore II, 1992) and certain types of deterministic parameter identification problems (Moore II, Kim, Seo, and Kalaba 1992), a recurrent extension of the associative memory approach has been shown to provide much improved estimates of response vectors. A recurrent associative memory matrix $\boldsymbol{M}^{**}$ is estimated by extending each original training stimulus vector $\boldsymbol{s}_k$ with $f(\boldsymbol{r}_k^*)$, a nonlinear damping transformation of the simple associative memory estimate corresponding to training response vector $\boldsymbol{r}_k$. Given $\boldsymbol{M}^*$, a simple associative memory matrix of dimension $q \times p$, and $\boldsymbol{R}^*$, an estimated training response matrix of dimension $q \times K$, the recurrent extension updates the training stimulus matrix to be

$$\boldsymbol{S}_r = \left| \frac{\boldsymbol{S}}{f(\boldsymbol{R}^*)} \right| \tag{39}$$

dimension $(p+q)\times K$. The recurrent associative memory matrix is computed thus

$$\boldsymbol{M}^{**} = \boldsymbol{R}\boldsymbol{S}_r^{+} = \boldsymbol{R}\left|\frac{\boldsymbol{S}}{f(\boldsymbol{R}^{*})}\right|^{+}. \tag{40}$$

The procedure is summarized in Figure 3. Note that the procedure subsumes the calculation of a simple associative memory.

3-4-3. Multicriteria Associative Memories (MAM)

Unfortunately, associative memories are known to be particularly sensitive to noise (Kalaba, Lichtenstein, Simchnoy, and Tesfatsion 1990, Kalaba and Tesfatsion 1991). Noise can produce scaling problems in the matrices $\boldsymbol{M}^{*}$ and $\boldsymbol{M}^{**}$. The numerical problems posed by relatively large matrix elements can be addressed in a number of ways. For example, expression (33) can be modified by attaching a penalty to the size of the elements in the associative memory matrix (Kalaba and Tesfatsion 1992, Kalaba and Udwadia 1991). Computing such a multicriteria associative memory matrix $\hat{\boldsymbol{M}}$ involves a trade-off. The objective is to find a matrix that replicates the training data as closely as possible, but minimizes the magnitudes of the elements necessary to achieve the best approximation. If α is defined to be a coefficient describing the relative importance of the first criteria, i.e., the importance of fitting the training data, expression (33) becomes

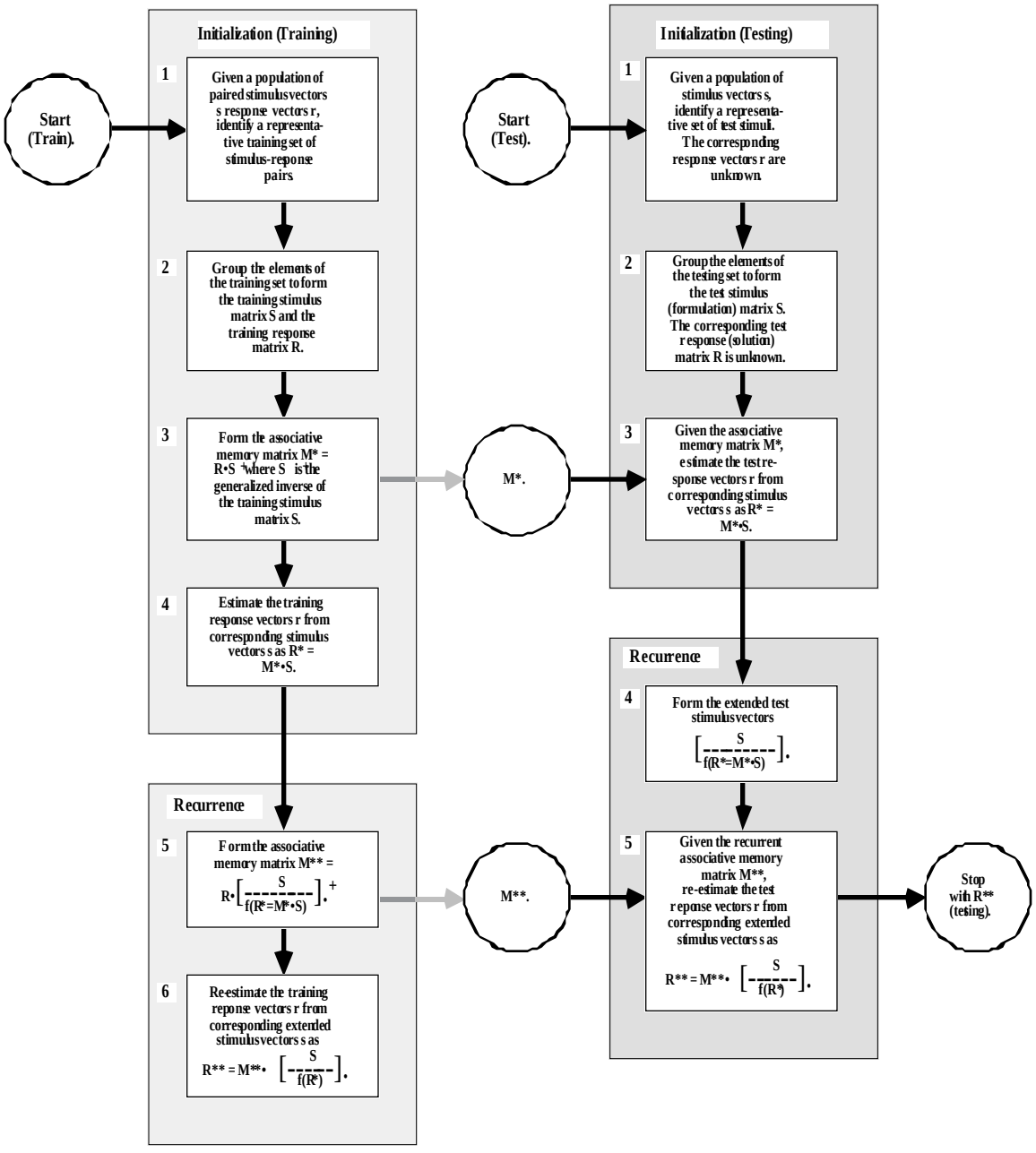

Figure 3: Computing a Recurrent Associative Memory: A nonlinear transformation of $\boldsymbol{R}^*$ is appended to the stimulus matrix $\boldsymbol{S}$. The associative memory is recomputed.

$$\hat{\boldsymbol{M}} = \arg\min_{\boldsymbol{M}} \left(\alpha \| \boldsymbol{R} - \boldsymbol{M}\boldsymbol{S} \|^2 + (1-\alpha) \| \boldsymbol{M} \|^2 \right). \tag{41}$$

Expanding,

$$\begin{aligned} & a\|R - MS\|^2 + (1-a)\|M\|^2 \\ & \quad = Trace\left(\boldsymbol{a}(\boldsymbol{R} - \boldsymbol{M}\boldsymbol{S})^{\boldsymbol{T}} (\boldsymbol{R} - \boldsymbol{M}\boldsymbol{S}) + (\boldsymbol{1}-\boldsymbol{a}) \boldsymbol{M}^{\boldsymbol{T}} \boldsymbol{M} \right). \end{aligned} \tag{42}$$

Minimizing Equation (40) over $\boldsymbol{M}$,

$$\begin{aligned} & \partial \left(a\|\boldsymbol{R} - \boldsymbol{M}\boldsymbol{S}\|^2 + (1-a)\|\boldsymbol{M}\|^2 \right) \Big/ \partial \boldsymbol{M} \\ & \quad = Trace\left(2a \hat{\boldsymbol{M}} \boldsymbol{S}\boldsymbol{S}^T - 2a \boldsymbol{R}\boldsymbol{S}^T + 2(1-a)\hat{\boldsymbol{M}} \right) = 0. \end{aligned} \tag{43}$$

It follows that

$$\hat{\boldsymbol{M}} = \alpha \boldsymbol{R}\boldsymbol{S}^T [\alpha \boldsymbol{S}\boldsymbol{S}^T + (1-\alpha)\boldsymbol{I}]^{-1}. \tag{44}$$

In the special case of a simple associative memory

$$\alpha = 1, \tag{45}$$

and equation (45) reduces to equation (37).

In general, the optimal value of α is unknown. However, Kalaba and Tesfatsion report low sensitivity to values on the interval [0.1, 0.9]. Our previous research shows that the estimation performance of the multicriteria associative memory matrices are not sensitive to the value of α in predicting network flows. The general procedure of finding the best α value is to incrementally increase the value of α from 0.1 to 0.9. The MAM approach often provides better estimates of test data sets compared to the SAM and RAM approaches.

3-4-4. General Issues in Application of Associative Memories

The associative memory approach is applied to the cases in which there seems to be a strong association between stimulus and response vectors. Whether the association is described by a linear or complex nonlinear function, the association between vector pairs constituting stimulus and response vectors is essential to the associative memory approach.

How to select an appropriate number of training cases is often unclear. Past computation experience indicates associative memories capture the information in

training cases quickly, but generalize less well then more complex connectionist techniques such as neural networks. If empirical data is used for training, it will include outcomes related to both structural relationships and system noise. The objective is to identify and predict structure, not noise. Noise, by definition, cannot be predicted. Neural networks, like other statistical techniques, can be accidentally trained to replicate noise. This degrades the use of a trained network as a predictive tool. One way to avoid this outcomes is to train connectionist heuristics against a set of validation response vectors defined by the same pair association rules as the training vectors but kept separate from the training vectors. Training stops when the outputs of the connectionist model offer no improvement against the validation set. The rationale is that the noise in the validation set is different from the noise in the training set. Thus overfitting to training noise can be avoided.

Multicriteria associative memories appear to be less subject to overtraining than neural networks. They are intended to be, but the same validation concept can be used to decide how much empirical information should be used to define the training set. The question of how large the training set should be is a question of what information the associative memory needs to identify the structural relationships driving the outcomes in the system. The equation is more difficult to answer if the training set entirely synthetic. The synthetic data used for training is almost free. There is no risk of overfitting to noise. We have been deliberately conservative. The training sets used in this case are relatively

small, and have been incrementally enlarged to see how quickly the estimation performance of the associative memories is improved.

Over the past few years, research at the University of Southern California (USC) has focused on the application of associative memory models to various constrained optimization problems. Our past research experience has revealed that associative memory models cost-effectively provide approximate solutions to constrained optimization problems. The estimation performance of the three associative memory models described here (SAM, RAM, and MAM) varies according to the nature of the constrained optimization problems to which they are applied. This research applies all three associative memory models to find the most accurate associative memory matrix to predict network flows.

4. Using Associative Memories to Model a Synthetic Network

This chapter describes the overall features of a transportation network analysis (TNA) procedure and its application to a simple synthetic network. Metropolitan Planning Organizations (MPOs) possess different levels in terms of quantity and quality of transportation system data that can be used for system-wide traffic flow analyses. Section 4-1 briefly describes how the models introduced in chapter 3 are used as the various components of the TNA procedure. Two versions of the TNA procedure are developed based on the quality of transportation system data available from MPOs: the general TNA procedure and the simplified TNA procedure.

Section 4-2 develops a simple synthetic network as an application example for simulating network flows using the static user equilibrium model. Network assumptions are described for numerical traffic flow analyses given synthetic link-failure system states. Transportation system data sets including link capacities, free-flow link travel times, and an origin-destination trip matrix are generated.

Section 4-3 simulates traffic flows with respect to synthetic link-failure system states given two scenario earthquakes: single-link failures and double-link failures. Simulated link-failure system states are randomly selected. The static user equilibrium model is applied to simulate network flows with respect to the link-failure system states given the three synthetic transportation system data sets.

Section 4-4 applies associative memory models to estimate simulated network flows. Different pairs of link failure configurations and simulated network flows are used to evaluate the performance of associative memory models. The remaining link failure configurations and their simulated network flows are used as training input data for computing different associative memory matrices. A comparison is made between simulated network flows provided by the static user equilibrium model and flow estimates provided by the associative memory models. Results from the application of the TNA procedure are discussed.

4-1. The Transportation Network Analysis Procedure

The development of efficient transportation network analysis (TNA) procedure is essential in traffic flow analyses for a large number of system states due to different scenario earthquakes. This section describes two versions of the TNA procedure: the general TNA procedure and the simplified TNA procedure. The difference between the two TNA procedures is based on the availability and quality of transportation system data from MPOs.

4-1-1. The General Transportation Network Analysis Procedure

The general TNA procedure is developed based on the assumption that both observed post-earthquake link volumes and an accurate O-D trip matrix are not available. This

procedure consists of five modules: (1) initialization of the procedure including data acquisition and modification, (2) identification of total and sample system states based on scenario earthquakes, (3) simulation of network equilibrium flows based on the sample link-failure system states, (4) application of artificial intelligence techniques for estimating network flows of the remaining link-failure system states, and (5) aggregation and interpretation of results. The overall framework of the general TNA procedure is shown in Figure 4.

The initialization module is a pre-processor to the general TNA procedure. This module develops reliable transportation system data sets containing free-flow link travel times, link capacities, and an origin-destination (O-D) trip matrix. A transportation network is defined based on the study area, the study purpose, the actual transportation network, and the availability of transportation system data. Free-flow link travel times and link capacities are either obtained from MPOs, or computed using network-related source data and simple formula.[1] Baseline link volumes are determined by extracting seasonal and/or trend variations from observed link volumes using a link volume adjustment method. An O-D trip estimation method is applied to estimate an O-D trip matrix from the baseline link volumes.

The identification module is another pre-processor to the general TNA procedure. This module determines an adequate number of link-failure system states. This module begins with the selection of scenario earthquakes. The total number of link-failure

system states are computed for each scenario. Sample link-failure system states are randomly selected from the total system states. Network configurations for the sample system states are identified. They are used as input data in the simulation module. Network configurations of the remaining system states are also identified. They are used as input data in the artificial intelligence module.

[1] These formula will be described in Chapter 6.

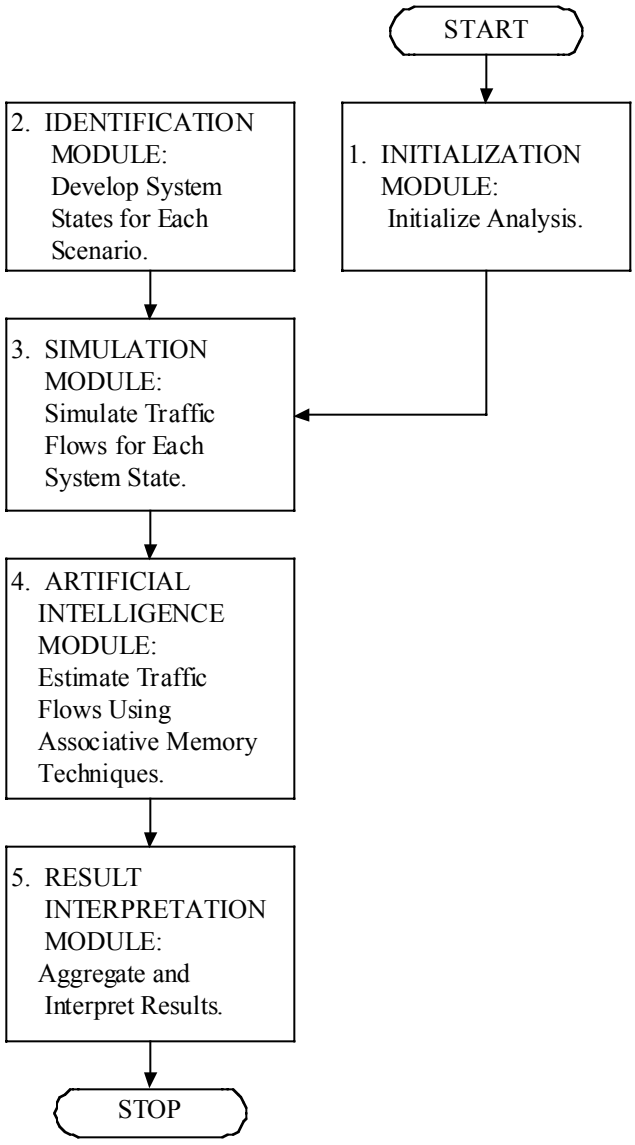

FIGURE 4: THE OVERALL FRAMEWORK OF GENERAL TRANSPORTATION NETWORK ANALYSIS PROCEDURE

The simulation module generates equilibrium traffic flows given both the three transportation system data determined in the initialization module and the network configurations of the sample system states selected in the identification module. A

conventional user equilibrium model is employed to simulate post-earthquake equilibrium traffic flows as well as equilibrium link travel times for all the sample system states.

The artificial intelligence module involves the application of associative memory models to efficiently estimate post-earthquake network flows for the remaining system states. The network configurations (stimulus vectors) and their associated equilibrium network flows (response vectors) of the sample system states are divided into two groups: training system states and test system states. Most of the stimulus and response vectors are used as training system states to compute different associative memory matrices. The remaining pairs of the vectors are used to evaluate the performance of the generated associative memory matrices. The associative memory matrix providing the closest estimates of test case network flows given the sample system states is applied to estimate network flows for the network configurations of the remaining system states.

The result interpretation module summarizes results of the associative memory approach. The results of associative memory models are gathered and interpreted. The performance of the associative memory models is evaluated by Root Mean Square Errors (RMSEs), scatter plots, and correlation coefficients between the link flows simulated by the conventional transportation network model and the flow estimates provided by the associative memory approach.

4-1-2. The Simplified Transportation Network Analysis Procedure

The simplified TNA procedure is developed based on the assumption that a set of post-earthquake link volumes is available. This procedure consists of four modules: (1) initialization of the procedure, (2) identification of link-failure system states, (3) application of artificial intelligence techniques for estimating network flows of additional link-failure system states, and (4) aggregation and interpretation of results. The key element of this procedure is the associative memory approach in the artificial intelligence module. The O-D trip estimation method, the conventional transportation network model, and the three transportation system data are not employed in this procedure because of the set of post-earthquake link volumes available from MPOs. The overall framework of the simplified TNA procedure is shown in Figure 5.

The initialization module is a pre-processor to the simplified TNA procedure. This module considers the extraction of variations from a set of post-earthquake link volumes. A study transportation network is defined from the actual transportation network. A link volume adjustment method is applied to identify seasonal and trend variations from a series of link volumes collected at all of the network links during a specific time period. Seasonal and trend parameters are determined by the method.

The identification module is another pre-processor to the simplified TNA procedure. This module defines link-failure system states based on different network configurations due to earthquakes. Observed link volumes are obtained from MPOs. Seasonal and trend

variations of the observed link volumes are extracted by using the seasonal and trend parameters identified in the initialization module. The network configurations (stimulus vectors) and their associated adjusted link volumes (response vectors) are structured as the pair of vectors.

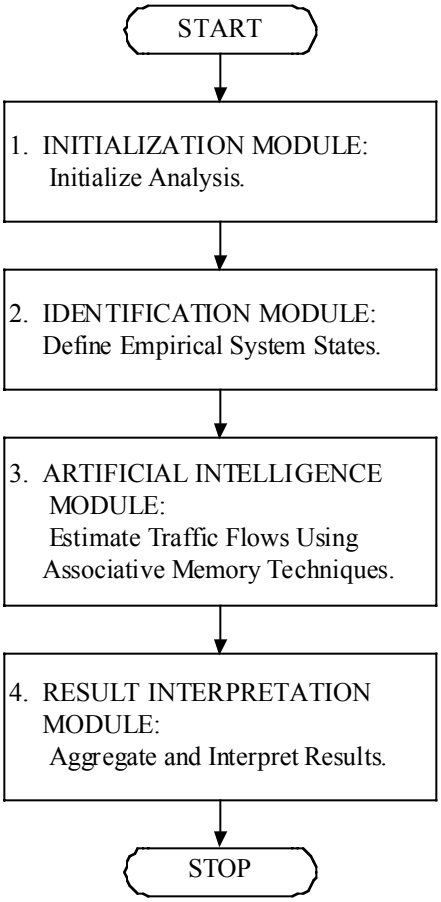

FIGURE 5: THE OVERALL FRAMEWORK OF SIMPLIFIED TRANSPORTATION NETWORK ANALYSIS PROCEDURE

The artificial intelligence module involves the application of associative memory models, mapping from the network configurations to the adjusted link volumes. The network configurations (stimulus vectors) and their associated link volumes (response vectors) are divided into two groups: training system states and test system states. Most of the stimulus and response vectors are used as training system states to compute different associative memory matrices. The remaining pairs of vectors are used to evaluate the performance of the generated memory matrices. The best performing associative memory matrix is applied to estimate network flows for additional system states.

The result interpretation module discusses and interprets results of associative memory models. The performance of the associative memory models is evaluated by Root Mean Square Errors (RMSEs), scatter plots, and correlation coefficients between the link volumes adjusted by the link volume adjustment method and the flow estimates provided by the associative memory approach.

The procedure modules and the relationships between the modules have been described for each of the two TNA procedures. Required data sets and model results are also demonstrated for each module. The application of the general TNA procedure to a simple synthetic transportation network will be described in more detail in the following sections. The applications of both the general and the simplified TNA procedures to an aggregated Los Angeles highway network will be presented in Chapters 6 and 7.

4-2. A Simple Synthetic Network

This section defines a simple synthetic transportation network to examine the applicability of the general TNA procedure. The synthetic transportation network includes seven zones and twenty-four directed links. The synthetic network is shown in Figure 6.

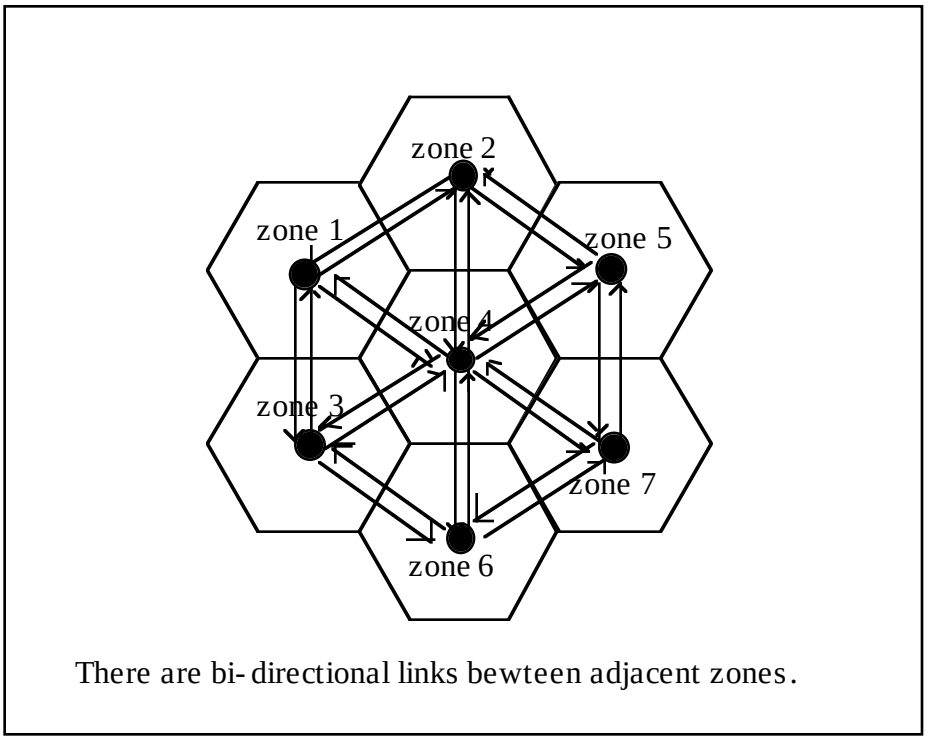

Figure 6: Synthetic Network and Zones

The general transportation network analysis procedure requires the following assumptions:

(1) the seven analysis zones are discrete;

(2) traffic flows are static, i.e., they do not change with time of day or time of year;

(3) drivers have perfect traffic information, i.e., their behaviors are predictable;

(4) there is only one transportation mode (cars), i.e., there is no mass transit etc.;

(5) each zone serves as both origin and destination of trips;

(6) the transportation network consists of only freeway links, i.e., there are neither signalized intersections nor waiting to turn at intersections;

(7) the freeway links are directed, i.e., adjacent nodes are connected by two links, one in each direction;

(8) the links are congestable, i.e., the time cost of traffic increases with volume of flow; and

(9) travel demand is inelastic, i.e., origin-destination requirements do not change even if the network changes, unless link failures make travel to some zones impossible in the case of seismic risk analysis.

This research employs the static user equilibrium model to simulate traffic flows given network configurations of different link-failure system states. The formulation of the static user equilibrium model is:

$$\textit{Minimize} \quad \sum_{a} \int_{0}^{v_a} t_a(w)\,dw \tag{46}$$

Subject to

$$v_a = \sum_s v_a^s \quad \textit{for all links } a \tag{47}$$

$$\sum_{a \text{ in Out}(r)} v_a^s - \sum_{a \text{ in In}(r)} v_a^s = \text{Demand}^{r->s} \quad \textit{for all origin-destination pairs (r,s)} \tag{48}$$

$$v_a^s \geq 0 \quad \textit{for all links a, and destinations s} \tag{49}$$

where

w = *the variable of integration,*
v_a = *the total flow on link a,*
$t_a(w)$ = *the link travel cost function for link a,*
v_a^s = *the total flow on link a bound for destination s*
Out(r) = *the set of link flows outbound from node r, and*
In(r) = *the set of link flows inbound to node r.*

This is a nonlinear minimization problem with a convex objective function subject to two sets of linear constraints and two sets of non-negativity conditions (Eash et al., 1979). Equation (46) is the objective function. The objective function is to minimize the area under the link travel cost function $t_a(w)$, satisfying the equilibrium conditions stated by Wardrop. Equation (47) represents the flow conservation rule that the flows on each link is equal to the sum of the flows from all zones *i* to zone *j* passing the link. Equation (48) represents the trip conservation rule that the total number of trips from zone *i* to zone *j* over all paths is equal to the specified number of trip demand. Equation (49) ensures that all flows are non-negative.

The Bureau of Public Roads (BPR) link travel cost function is used to describe link travel costs as a function of link flows in the static user equilibrium model. The BPR link travel cost function is

$$t = t_0 \times [\, 1 + 0.15\, (v/c)^4 \,], \tag{50}$$

where

t = *the link travel cost,*
t_0 = *the link travel cost when the link is not congested, and*
v/c = *the link volume to design capacity ratio.*

Free-flow link travel costs are used as parameters t_0 . The link volumes and link capacities are *v* and *c*, respectively.

The Frank-Wolfe algorithm is the standard method for solving the above convex mathematical programming problem. The application of the Frank-Wolfe algorithm involves the following steps (Eash et al., 1979; Boyce et al., 1981; Van Vliet, 1987):

Step 1. Compute the travel cost on each link corresponding to link flows in the current solution.

Step 2. Trace minimum skim trees from each origin to all destinations using the link travel costs computed in step 1.

Step 3. Assign all trips from each origin to each destination to the minimum cost paths computed in step 2 (all-or-nothing assignment). Call this link flow as w_a.

Step 4. Linearly combine the current solution's link flows (v_a) and the new all-or-nothing assignment's link flows (w_a) to obtain a new current solution (v_a') so as to minimize the objective function. The two flows are combined by the following equation:

$$v_a' = (1 - \lambda)\, v_a + \lambda\, w_a,$$ where λ is the value between 0 and 1.

Seep 5. If the solution has converged sufficiently, stop. Otherwise, return to step 1.

The transportation network flow model is codified by the UNIX version of the SPEAKEASY matrix manipulation program. The Speakeasy code is shown in Appendix 1.

Three synthetic input data sets of an O-D trip matrix, link capacities, and free-flow link travel times are randomly generated. They are regarded as noise-free input data sets.

The three synthetic input data sets are shown in Table 3. User equilibrium traffic flows and link travel times given the base line transportation network are generated by applying the static network equilibrium model. They are shown in Table 4. Baseline total system travel times can be computed by multiplying equilibrium travel times with their associated traffic flows.

Table 3: Synthetic Network Input Data Sets

(a). An Origin-Destination Trip Matrix (Trips Between Two Zones)

(UNIT: Passenger Car Unit)

		TO							
		ZONE 1	ZONE 2	ZONE 3	ZONE 4	ZONE 5	ZONE 6	ZONE 7	**SUM**
	ZONE 1	0	168	57	21	111	67	75	499
F	ZONE 2	94	0	27	108	58	127	188	602
R	ZONE 3	20	38	0	94	183	147	108	590
O	ZONE 4	57	86	197	0	102	49	208	699
M	ZONE 5	229	145	211	174	0	236	117	1112
	ZONE 6	112	161	200	16	18	0	13	520
	ZONE 7	146	182	287	321	236	102	0	1274
	SUM	658	780	979	734	708	728	709	5296

(b). Link Capacities

(UNIT: Passenger Car Unit)

	TO						
	ZONE 1	ZONE 2	ZONE 3	ZONE 4	ZONE 5	ZONE 6	ZONE 7
ZONE 1	0	254	215	262	0	0	0

F	ZONE 2	245	0	0	209	241	0	0
R	ZONE 3	230	0	0	244	0	261	0
O	ZONE 4	234	244	202	0	215	232	261
M	ZONE 5	0	286	0	257	0	0	232
	ZONE 6	0	0	214	233	0	0	218
	ZONE 7	0	0	0	260	226	277	0

NOTE 1: Link capacity is zero if there is no link between two zones.
NOTE 2: The link capacity is directed.

(c). Free-Flow Link Travel Times (Travel Times Under No Congestion).

(UNIT: Minute)

		TO						
		ZONE 1	ZONE 2	ZONE 3	ZONE 4	ZONE 5	ZONE 6	ZONE 7
	ZONE 1	INF	2.6	2.7	3	INF	INF	INF
F	ZONE 2	2.5	INF	INF	3.6	2.1	INF	INF
R	ZONE 3	2.7	INF	INF	3.3	INF	5.1	INF
O	ZONE 4	2.6	2.5	3.7	INF	4.2	2.3	5.1
M	ZONE 5	INF	3.2	INF	3.5	INF	INF	2.2
	ZONE 6	INF	INF	6.1	2.9	INF	INF	3.1
	ZONE 7	INF	INF	INF	3.6	4.7	2.4	INF

NOTE: "INF" stands for infinite link travel times.

Table 4: Baseline User Equilibrium Traffic Flows and Link Travel Times

(a) User Equilibrium Traffic Flows

(UNIT: Passenger Car Unit)

		TO						
		ZONE 1	ZONE 2	ZONE 3	ZONE 4	ZONE 5	ZONE 6	ZONE 7
	ZONE 1	0	324	236	167	0	0	0
F	ZONE 2	410	0	0	241	363	0	0
R	ZONE 3	71	0	0	269	0	253	0
O	ZONE 4	405	338	359	0	279	365	286

M	ZONE 5	0	529	0	446	0	0	419
	ZONE 6	0	0	386	405	0	0	139
	ZONE 7	0	0	0	539	349	521	0

NOTE: Traffic flow is zero if there is no link between two zones.

(b) User Equilibrium Link Travel Times

(UNIT: Minute)

		TO						
		ZONE 1	ZONE 2	ZONE 3	ZONE 4	ZONE 5	ZONE 6	ZONE 7
	ZONE 1	INF	3.64	3.29	3.07	INF	INF	INF
F	ZONE 2	5.44	INF	INF	4.55	3.72	INF	INF
R	ZONE 3	2.7	INF	INF	4.03	INF	5.77	INF
O	ZONE 4	6.09	3.88	9.27	INF	5.98	4.4	6.2
M	ZONE 5	INF	8.83	INF	8.28	INF	INF	5.72
	ZONE 6	INF	INF	15.83	6.85	INF	INF	3.18
	ZONE 7	INF	INF	INF	13.56	8.72	6.91	INF

NOTE: "INF" stands for infinite link travel times.

The user equilibrium model is also used to simulate post-earthquake traffic flows with respect to link-failure system states due to different scenario earthquakes. Post-earthquake total system travel times can be computed by using post-earthquake traffic flows and user equilibrium link travel times. The difference between the baseline total system travel time and post-earthquake total system travel times is computed. The system-wide travel time changes are used to determine the importance of network links in Caltrans' prioritization procedure.

4-3. Flow Simulation

This section generates traffic flows and link travel times for link-failure system states due to post-earthquake scenarios. The seven-zone synthetic network is used to

demonstrate traffic flow simulations. A subset of link-failure system states is randomly selected to represent all possible link-failure system states. The link-failure system states are based on the assumption that any link can be severed without damaging the opposite directional link. Network configurations of the link failures are represented discretely. Collapsed links are coded as "2," and unaffected links are coded as "1." The static network equilibrium model is applied to simulate post-earthquake link flows given the three input data sets. All link-failure system states are assumed to reflect the same pattern of travel demand.

The total number of possible link-failure system states can be calculated combinatorically. Combinations are defined by the number of subsets of size ***r*** that can be constructed from the population of ***n*** objects with no concern for the arrangement or order of the ***r*** objects (Kachigan, 1986). For example, the synthetic network has 24 links. The total number of ways to select one link (***r***) from the 24 links (***n***) is obviously 24. More generally, the combinatorial formula is

$$ {}_nC_r = \frac{n!}{r!(n-r)!} \tag{51} $$

where ***n*** is the total objects and ***r*** is the number of subsets to be taken.

The total number of possible link-failure system states in this synthetic network is ${}_{24}C_1 + {}_{24}C_2 + {}_{24}C_3 + {}_{24}C_4 + ... + {}_{24}C_{23} + {}_{24}C_{24} = 24 + 276 + 2{,}024 + 10{,}626 + ... + 24 + 1 =$

16,777,215. This total number of system states includes cases corresponding to one-link, two-link, three-link, ... 24-link closures. This link failure problem includes a huge number of system states. It is impossible to simulate all of these system states with any method. In addition, some system states have infeasible solutions in which at least one zone is completely disconnected from other zones.

Severe earthquakes tend to damage more links than minor earthquakes. The network flow simulation can be based on any number of disconnected links. The link failure system states can be grouped by the number of severed links. Our baseline simulations for the seven-zone synthetic network are summarized in two system state classes: single link failures and double link failures. The simulation of single link failures represents post-earthquake effects on traffic flows due to a minor earthquake. The double link failure system states represent more severe damage to the synthetic network due to more significant earthquakes.

4-3-1. Single Link Failures

The simulation of this class involves the failure of one link in the network. There are a total of twenty-four possible system states. User equilibrium traffic flows and their associated link travel times are simulated for all twenty-four system states. Network configurations of the twenty-four system states are shown in Appendix 2-A. Equilibrium

link flows and associated link travel times are computed by applying the static user equilibrium model, and are shown in Appendices 2-B and 2-C, respectively.

4-3-2. Double Link Failures

The total number of possible system states in this category is 276. This number is obtained from the combinatorial formula for selecting any two links out of 24 links:

$$ {}_{84}C_2 = \frac{24!}{2!(24-2)!} = \frac{24!}{2!\times 22!} = \frac{24\times 23\times 22!}{2\times 22!} = \frac{24\times 23}{2} = 276. \qquad (52) $$

Fifty system states are randomly selected. Network configurations of the fifty system states are shown in Appendix 3-A. Equilibrium link flows and associated link travel times are computed by applying the static user equilibrium model. They are shown in Appendices 3-B and 3-C, respectively.

4-4. Application of Associative Memory Models

Our objective is to generate good estimates of equilibrium link flows without using conventional network flow models. In section 4-3, post-earthquake traffic flows are simulated by using the static user equilibrium model. In this section, traffic flows are estimated based on the association between the network configurations of link failure system states (stimulus vectors) and simulated link flows (response vectors). Three types

of associative memory models described in section 3-4 are computed and used to map the network configurations to the associated link flows.

The network configurations (stimulus vectors) and their associated equilibrium link flows (response vectors) are divided into two groups: training system states and test system states. Most of the stimulus and response vectors are used as training system states. The stimulus and response vectors of the training system states are used to generate different associative memory matrices. The remaining pairs of the vectors are states used to test the system. They are used to evaluate the performance of the associative memory matrices. If the associative memory matrix test results do not satisfy our criteria, we have to increase the number of training system states by simulating more system states using the static network equilibrium model.

Three associative memory scenarios are considered based on the flow simulation scenarios: single-link failures, double-link failures, and the mixture of single-link and double-link failures. The associative memory models generate estimated traffic flows. Root Mean Square Error (RMSE) is used as the measure of performance. The RMSE results measure the difference between the estimated link traffic flows and the test (simulated) link traffic flows. They are used to compare the performances of the associative memory models. The difference between the estimated and target vectors of traffic flows is also described by scatter plots and correlation coefficients.

4-4-1. Single-Link Failures

The total number of possible system states is twenty-four. The twenty-four system states are randomly ordered. Three associative memory evaluations are conducted to test the performance of different associative memory models in the case of single-link failures. The multicriteria associative memories (MAM) have an additional parameter α. The estimation performance of the MAM procedure is varied by changing the α parameter. Since the α parameter takes values on the interval [0.1,0.9], at least nine different MAM procedures can be considered.

The first evaluation of associative memory models to the single-link failure system states uses each of the twenty-four system states as the test system state in rotation. The other twenty-three system states are used to create different memory matrices. Table 5 presents the RMSE results of SAM, RAM, and MAM in estimates in the case of single-link failures.

The first column represents the test system state. Twenty-four system states are used as the test system state in rotation. Numbers within the parentheses for each MAM column give the value of α. The first row represents RMSE results for "training" system states when the system state 1 is used as the test system state. The second row represents RMSE results for the system state 1 (the test system state) when different associative memory models are computed by using the other twenty-three system states.

Different associative memory models are applied. However, the RMSE results of estimated traffic flows do not significantly vary across the associative memory models in the case of test states. The training results of SAM and RAM are usually very good

Table 5: RMSEs of SAM, RAM, and MAM in Seven-Zone Network (Single Link Failure)

		MAM									SAM	RAM
	α	0.1	0.2	0.3	0.4	0.5	0.6	0.7	0.8	0.9	SAM	RAM
SS 1	Training	93.32	82.94	72.57	62.2	51.84	41.47	31.1	20.73	10.37	7.95E-13	4.95E-13
	Test	98.09	98.1	98.1	98.11	98.11	98.11	98.11	98.11	98.11	98.112	98.227
SS 2	Training	92.86	82.54	72.22	61.9	51.58	41.27	30.95	20.63	10.32	7.23E-13	7.08E-13
	Test	110	110	110	110.1	110.1	110.1	110.1	110.1	110.1	110.07	110.33
SS 3	Training	92.88	82.55	72.23	61.91	51.59	41.27	30.95	20.64	10.32	7.76E-13	7.94E-13
	Test	109.8	109.8	109.8	109.8	109.8	109.8	109.8	109.8	109.8	109.79	109.91
SS 4	Training	93.19	82.82	72.47	62.12	51.76	41.41	31.06	20.71	10.35	7.46E-13	4.01E-13
	Test	101.6	101.7	101.7	101.7	101.7	101.7	101.7	101.7	101.7	101.67	101.84
SS 5	Training	93.45	83.06	72.68	62.29	51.91	41.53	31.15	20.76	10.38	6.25E-13	3.27E-13
	Test	94.23	94.21	94.21	94.21	94.2	94.2	94.2	94.2	94.2	94.201	94.212
SS 6	Training	90.84	80.74	70.64	60.55	50.46	40.37	30.28	20.18	10.09	7.50E-13	3.97E-13
	Test	152.1	152.1	152.1	152.1	152.1	152.1	152.1	152.1	152.1	152.12	152.2
SS 7	Training	93.19	82.82	72.47	62.12	51.76	41.41	31.06	20.71	10.35	6.19E-13	3.85E-13
	Test	101.6	101.6	101.6	101.6	101.7	101.7	101.7	101.7	101.7	101.66	101.89
SS 8	Training	94.56	84.04	73.54	63.03	52.53	42.02	31.52	21.01	10.51	7.52E-13	3.63E-13
	Test	51.97	51.99	51.99	52	52	52	52.01	52.01	52.01	52.008	52.224
SS 9	Training	93.57	83.17	72.77	62.37	51.98	41.58	31.19	20.79	10.4	5.47E-13	4.29E-13
	Test	90.7	90.67	90.66	90.65	90.65	90.65	90.65	90.65	90.65	90.646	90.618
SS 10	Training	91.98	81.75	71.53	61.31	51.09	40.87	30.66	20.44	10.22	4.82E-13	5.80E-13
	Test	130.1	130.2	130.2	130.2	130.2	130.2	130.2	130.2	130.2	130.23	130.58
SS 11	Training	92.17	81.92	71.68	61.44	51.2	40.96	30.72	20.48	10.24	8.63E-13	7.51E-13
	Test	126.1	126.1	126.1	126.1	126.1	126.1	126.1	126.1	126.1	126.09	126.17
SS 12	Training	92.91	82.58	72.25	61.93	51.61	41.29	30.97	20.64	10.32	7.66E-13	9.11E-13
	Test	109	109	109	109	109	109	109	109	109	108.96	109
SS 13	Training	93.04	82.7	72.36	62.02	51.68	41.35	31.01	20.67	10.34	6.45E-13	5.58E-13
	Test	105.4	105.4	105.5	105.5	105.5	105.5	105.5	105.5	105.5	105.49	105.77
SS 14	Training	92.27	82.01	71.76	61.51	51.25	41	30.75	20.5	10.25	6.50E-13	4.93E-13
	Test	124.2	124.1	124.1	124	124	124	124	124	124	124.01	123.62
SS 15	Training	94.85	84.3	73.76	63.22	52.69	42.15	31.61	21.07	10.54	5.66E-13	5.21E-13
	Test	32.9	32.99	33.02	33.04	33.05	33.05	33.06	33.06	33.06	33.067	33.603
SS 16	Training	94.56	84.04	73.53	63.03	52.52	42.02	31.51	21.01	10.51	6.64E-13	4.36E-13
	Test	52.14	52.16	52.17	52.18	52.18	52.19	52.19	52.19	52.19	52.192	52.439
SS 17	Training	94.12	83.65	73.19	62.74	52.28	41.82	31.37	20.91	10.46	7.85E-13	6.67E-13

	Test	71.69	71.83	71.88	71.9	71.92	71.93	71.94	71.94	71.95	71.95	72.575
SS 18	Training	93.83	83.4	72.97	62.55	52.12	41.7	31.27	20.85	10.42	5.75E-13	5.92E-13
	Test	82.41	82.36	82.35	82.34	82.34	82.34	82.33	82.33	82.33	82.33	82.266
SS 19	Training	93.69	83.27	72.86	62.45	52.04	41.64	31.23	20.82	10.41	6.18E-13	4.15E-13
	Test	86.82	86.85	86.86	86.86	86.87	86.87	86.87	86.87	86.87	86.872	87.055
SS 20	Training	90.31	80.27	70.23	60.2	50.17	40.13	30.1	20.07	10.03	6.17E-13	3.75E-13
	Test	161.1	161.1	161.1	161.1	161.1	161.1	161.1	161.2	161.2	161.15	161.27

Table 5 (continued)

SS 21	Training	93.99	83.53	73.09	62.65	52.21	41.77	31.32	20.88	10.44	8.64E-13	3.82E-13
	Test	76.96	76.91	76.9	76.89	76.89	76.89	76.89	76.89	76.89	76.885	76.835
SS 22	Training	91.85	81.63	71.42	61.22	51.02	40.81	31.61	20.41	10.2	6.83E-13	5.89E-13
	Test	133.2	133.1	133.1	133.1	133.1	133.1	133.1	133.1	133.1	133.08	132.96
SS 23	Training	92.73	82.42	72.12	61.81	51.51	41.21	30.91	20.6	10.3	1.00E-12	4.96E-13
	Test	113.6	113.4	113.4	113.4	113.4	113.4	113.4	113.4	113.4	113.35	112.98
SS 24	Training	90.53	80.46	70.41	60.35	50.29	40.23	30.17	20.12	10.06	6.96E-13	8.83E-13
	Test	157.5	157.5	157.5	157.5	157.5	157.5	157.5	157.5	157.5	157.45	157.41

because the associative memory matrices are created based on the information from training system states. However, we try to estimate traffic flows of the system states that have not been used to create the associative memory matrices. Therefore, the results in the testing rows such as row 2 are much more important than the training figures. The RMSE results for test system states show that test system state 15 provides the lowest test case RMSE. Test system state 20 provides the highest test case RMSE, representing the worst estimate of traffic flows.

Figures 4-A to 4-F in Appendix 4 show the scatter plots and correlation coefficients for test system state 15. Each coordinate in the figures represents the comparison between the simulated (target) link flows provided by the static network equilibrium

model and the estimated link flows provided by an associative memory. Coordinates located close to the 45 degree line represent more accurate estimates. Figure 4-A presents the performance of SAM in estimating traffic flows of 23 training system states, excluding system state 15 (the target state). Figure 4-B presents the performance of SAM in estimating traffic flows for system state 15. Figure 4-C presents the performance of RAM for the same 23 training states. Figure 4-D presents the performance of RAM for system state 15. Figure 4-E presents the performance of MAM for the same 23 training system states when α is 0.9. Figure 4-F presents the performance of MAM in estimating traffic flows of system state 15 using the same α value.

The second evaluation of associative memories to the single-link failure system states varies the number of the test system states as well as the training system states. One of the advantages of associative memory techniques is that associative memory models can estimate a group of test system states simultaneously without significant cost. However, there is a trade-off between the number of simultaneously estimated test system states and the performance of associative memory models. For example, the simultaneous estimates of ten test system states may be worse than the estimate of only one test system state if the number of training system states are fixed. There is no rule in determining the optimal number of test system states that can be estimated simultaneously without considerably losing the estimation power.

This second evaluation investigates the relationship between the number of simultaneous test states and the performance of the associative memory models. The evaluation begins with the case that test system state 15 is the only test system state. System state 15 is selected because this state provides the lowest test state RMSE among the twenty-four test system states. This is referred to as the lower bound of the estimation performance. CASE 2 uses two test system states including state 15. The remaining twenty-two system states are used to create associative memory matrices. CASE 3 uses three test system states and twenty-one training system states. Thus, the number of test states increases as the number of training states decreases. Table 6 presents the RMSE results of SAM, RAM, and MAM in estimates, when the number of test system states increases with the decrease in training states.

Table 6: RMSEs of SAM, RAM, and MAM in Seven-Zone Network (Single Link Failure: the number of training and test system states varies, STUDY A)

		MAM									**SAM**	**RAM**
	α	0.1	0.2	0.3	0.4	0.5	0.6	0.7	0.8	0.9	SAM	RAM
CASE 1	Training: 23	94.85	84.3	73.76	63.22	52.69	42.15	31.61	21.07	10.54	5.66E-13	5.21E-13
	Test: 1	32.9	32.99	33.02	33.04	33.05	33.05	33.06	33.06	33.06	33.067	33.603
CASE 2	Training: 22	94.62	84.1	73.58	63.07	52.56	42.05	31.54	21.02	10.51	6.25E-13	1.01E-13
	Test: 2	83.49	83.42	83.4	83.38	83.38	83.37	83.37	83.37	83.37	83.365	83.209
CASE 3	Training: 21	93.33	82.95	72.58	62.21	51.84	41.47	31.11	20.74	10.37	4.40E-13	5.70E-13
	Test: 3	104.2	104.1	104.1	104.1	104.1	104.1	104.1	104.1	104.1	104.05	103.91
CASE 4	Training: 20	94.44	83.94	73.44	62.95	52.46	41.97	31.48	20.98	10.49	5.49E-13	4.11E-13
	Test: 4	98.11	98.04	98.02	98.01	98	98	97.99	97.99	97.99	97.989	97.862
CASE 5	Training: 19	91.3	81.14	71	60.85	50.71	40.57	30.43	20.28	10.14	4.78E-13	4.36E-13
	Test: 5	113.5	113.4	113.4	113.4	113.4	113.4	113.4	113.4	113.4	113.41	113.35
CASE 6	Training: 18	91.98	81.75	71.53	61.31	51.09	40.87	30.65	20.44	10.22	6.42E-13	5.62E-13
	Test: 6	110.2	110.2	110.2	110.2	110.2	110.2	110.2	110.2	110.2	110.15	110.13
CASE 7	Training: 17	92.88	82.55	72.22	61.91	51.59	41.27	30.95	20.64	10.32	5.11E-13	6.05E-13
	Test: 7	107.7	107.6	107.6	107.6	107.6	107.6	107.6	107.6	107.6	107.59	107.56

CASE 8	Training: 16	94.24	83.75	73.28	62.81	52.34	41.87	31.4	20.94	10.47	4.80E-13	3.58E-13
	Test: 8	105.1	105.1	105.1	105.1	105.1	105.1	105.1	105.1	105.1	105.09	105.14
CASE 9	Training: 15	96.37	85.65	74.94	64.23	53.53	42.82	32.12	21.41	10.71	4.34E-13	6.27E+13
	Test: 9	102.1	102	102	102.1	102.1	102.1	102.1	102.1	102.1	102.05	102.13
CASE 10	Training: 14	92.72	82.39	72.09	61.79	51.49	41.19	30.89	20.6	10.3	3.13E-13	5.40E-13
	Test: 10	109.1	109.1	109.1	109.1	109.1	109.1	109.1	109.1	109.1	109.06	109.12
CASE 11	Training: 13	91.66	81.45	71.26	61.08	50.9	40.72	30.54	20.36	10.18	5.76E-13	2.94E-13
	Test: 11	110	109.9	109.9	109.9	109.9	109.9	109.9	109.9	109.9	109.9	109.87
CASE 12	Training: 12	91.63	81.41	71.23	61.06	50.88	40.7	30.53	20.35	10.18	3.62E-13	3.68E-13
	Test: 12	109.9	109.9	109.9	109.9	109.8	109.8	109.8	109.8	109.8	109.84	109.84

The third evaluation is the same as the second application except that the initial test system state is system state 20. System state 20 provides the highest test state RMSE in Table 5. This can be regarded as the upper limit. The RMSE results of SAM, RAM, and MAM in this evaluation are shown in Table 7.

Table 7: RMSEs of SAM, RAM, and MAM in Seven-Zone Network (Single Link Failure: the number of training and test system states varies, STUDY B)

		MAM									**SAM**	**RAM**
	α	0.1	0.2	0.3	0.4	0.5	0.6	0.7	0.8	0.9	SAM	RAM
CASE 1	Training: 23	90.31	80.27	70.23	60.2	50.17	40.13	30.1	20.07	10.03	6.17E-13	3.75E-13
	Test: 1	161.1	161.1	161.1	161.1	161.1	161.1	161.1	161.2	161.2	161.15	161.27
CASE 2	Training: 22	89.78	79.79	69.82	59.84	49.87	39.89	29.92	19.95	9.974	6.97E-13	8.95E-13
	Test: 2	140.9	140.9	140.9	140.9	140.9	140.9	140.9	140.9	140.9	140.87	140.8
CASE 3	Training: 21	88.35	78.52	68.7	58.89	49.07	39.26	29.44	19.63	9.815	5.94E-13	4.24E-13
	Test: 3	137.5	137.5	137.5	137.5	137.5	137.5	137.4	137.4	137.4	137.44	137.33
CASE 4	Training: 20	89.26	79.33	69.42	59.5	49.58	39.67	29.74	19.83	9.916	5.02E-13	6.10E-13
	Test: 4	125.3	125.2	125.2	125.2	125.2	125.2	125.2	129.2	125.2	125.16	125.05
CASE 5	Training: 19	86.06	76.49	66.92	57.36	47.8	38.24	28.68	19.12	9.56	4.86E-13	6.23E-13
	Test: 5	131.4	131.3	131.3	131.3	131.3	131.3	131.3	131.3	131.3	131.25	131.15
CASE 6	Training: 18	86.44	76.82	67.22	57.61	48.01	38.41	28.81	19.2	9.602	6.17E-13	3.84E-13
	Test: 6	125.9	125.9	125.9	125.9	125.9	125.9	125.9	125.9	125.9	125.85	125.78
CASE 7	Training: 17	87.07	77.38	67.7	58.03	48.36	38.69	29.02	19.34	9.672	6.05E-13	4.30E-13
	Test: 7	121.6	121.5	121.5	121.5	121.5	121.5	121.5	121.5	121.5	121.46	121.38
CASE 8	Training: 16	88.12	78.31	68.52	58.73	48.94	39.15	29.37	19.58	9.788	5.46E-13	4.43E-13
	Test: 8	117.7	117.7	117.7	117.7	117.7	117.7	117.7	117.7	117.7	117.67	117.67

CASE 9	Training: 15	90	79.98	69.98	59.98	49.98	39.99	29.99	19.99	9.996	4.52E-13	6.27E-13
	Test: 9	113.6	113.6	113.6	113.6	113.6	113.6	113.6	113.6	113.6	113.6	113.63
CASE 10	Training: 14	92.72	82.39	72.09	61.79	51.49	41.19	30.89	20.6	10.3	3.13E-13	5.40E-13
	Test: 10	109.1	109.1	109.1	109.1	109.1	109.1	109.1	109.1	109.1	109.06	109.12
CASE 11	Training: 13	91.66	81.45	71.26	61.08	50.9	40.72	30.54	20.36	10.18	5.76E-13	2.94E-13
	Test: 11	110	109.9	109.9	109.9	109.9	109.9	109.9	109.9	109.9	109.9	109.87
CASE 12	Training: 12	91.63	81.41	71.23	61.06	50.88	40.7	30.53	20.35	10.18	3.62E-13	3.68E-13
	Test: 12	109.9	109.9	109.9	109.9	109.8	109.8	109.8	109.8	109.8	109.84	109.84

The outcomes of single-link failure studies demonstrate the applicability of associative memory models to the synthetic network. The simple and recurrent associative memory models are able to perfectly replicate the training flows, but this is expected. The test results of the associative memory models are somewhat disappointing. The associative memory models do not produce close estimates of test link flows in the case of most single-link failure test states except test state 8, 15, and 16. These results indicate that a training sample consisting of twenty-three different system states is not sufficient to train the associative memory models.

Traffic flow estimates for various training and test system states show that the performance of associative memory models seems to be more affected by the number of training and test system states. This is expected because the associative memory approach requires only sufficient training information to understand the association between network configurations and their simulated traffic flows. Additional information tends to make associative memory models produce more accurate estimates.

4-4-2. Double-Link Failures

The estimation of link flows becomes more complex if more links are severed. There are a total number of 276 system states in the case of double-link failures. Fifty system states are randomly selected to represent all the 276 system states of double link failures. Two associative memory evaluations are conducted to test the performance of different associative memory models in this scenario.

The first evaluation of associative memory models to the double-link failure system states examines the performance of associative memory models in the case of varying training and test system states. The number of test states increases as the number of training states decreases. For example, the first case uses 49 training states to estimate one test state, the second uses 48 training states to estimate two test states, the third uses 47 training states to estimate three test states, and so on. The RMSE results of the three associative memory models in this application are shown in Table 8. The SAM, RAM, and MAM scatter plots and correlation coefficients in the case of double-link failures are shown in Appendices 4-G to 4-L.

The second evaluation is the same as the first application except that the sequence of the pair data sets is different. The same sets of network configurations and their associated link flows are differently ordered to examine whether or not the associative memory models are independent from the order of training states. The same associative

memory models are applied to the differently ordered data sets. The RMSE results of the three associative memory models are shown in Table 9.

The outcomes of two double-link failure studies demonstrate that the associative memory models perform reliably with respect to the test states. The MAM replicates simulated traffic flows better than the SAM and RAM in most test cases. The MAM provides the reliable estimates of traffic flows up to a group of fifteen test states when the remaining system states are used to compute associative memory matrices. The RMSE results between the two double-link failure applications are not significantly different. This result indicates that the estimation performance of associative memory models is not sensitive to the order of training or test system states.

Fifty system states seem to be sufficient for the learning process of the associative memory models. The RMSE results from the two double-link failures are usually lower than those of the single-link failures. The reason may be that more system states are trained in the case of the double-link failure scenario. Further, each link has a higher chance of being selected as link failures. The RMSE results of test states tend to decrease when the alpha of MAM increases. Zero flow in severed links is predicted in the double link-failure scenarios unlike in the single-link failure applications.

Table 8: RMSEs of SAM, RAM, and MAM in Seven-Zone Network (Double Link Failure: the number of training and test system states varies, STUDY A)

		MAM									**SAM**	**RAM**
	α	0.1	0.2	0.3	0.4	0.5	0.6	0.7	0.8	0.9	SAM	RAM
CASE 1	Training: 49	101.7	76.4	60.3	49.12	41.09	35.31	31.29	28.71	27.32	26.906	4.232

	Test: 1	81.99	61.99	50.59	43.47	38.89	35.98	34.21	33.26	32.88	32.912	20.317
CASE 2	Training: 48	102.1	76.89	60.76	49.53	41.43	35.56	31.45	28.77	27.31	26.867	4.00E-10
	Test: 2	103.1	82.85	69.58	59.84	52.27	46.29	41.71	38.58	37.06	37.381	124.42
CASE 3	Training: 47	102.8	77.58	61.38	50.05	41.83	35.85	31.63	28.87	27.35	26.88	4.08E-12
	Test: 3	101	81.26	67.86	57.87	50.16	44.25	39.99	37.42	36.6	37.599	92.954
CASE 4	Training: 46	103.5	78.16	61.86	50.45	42.15	36.09	31.8	28.97	27.4	26.918	7.32E-13
	Test: 4	100.7	81.73	68.67	58.84	51.14	45.11	40.56	37.54	36.19	36.705	85.085
CASE 5	Training: 45	104.4	78.9	62.45	50.9	42.48	36.3	31.89	28.97	27.34	26.83	9.20E-13
	Test: 5	93.74	76.5	64.58	55.65	48.76	43.53	39.84	37.71	37.24	38.515	87.247
CASE 6	Training: 44	105	79.47	62.97	51.36	42.84	36.54	31.98	28.9	27.15	26.585	6.90E-13
	Test: 6	100.5	83.31	71.11	61.64	54.06	48.14	43.97	41.85	42.11	44.929	89.612
CASE 7	Training: 43	105.8	80.24	63.63	51.9	43.28	36.87	32.22	29.05	27.23	26.638	6.46E-13
	Test: 7	100.3	83.4	71.22	61.7	54.06	48.05	43.79	41.62	41.94	45.061	83.476
CASE 8	Training: 42	106.6	80.99	64.3	52.48	43.74	37.22	32.44	29.15	27.21	26.577	1.61E-11
	Test: 8	101.4	83.83	71.3	61.58	53.8	47.7	43.38	41.19	41.62	45.118	286.71
CASE 9	Training: 41	107.1	81.42	64.71	52.86	44.08	37.46	32.54	29.07	26.96	26.228	5.03E-11
	Test: 9	105.8	90.63	79.43	70.28	62.49	55.89	50.8	47.97	48.61	54.054	1154.6
CASE 10	Training: 40	108	82.2	65.38	53.41	44.51	37.76	32.69	29.07	26.84	26.068	1.34E-09
	Test: 10	105.2	90.44	79.48	70.48	62.84	56.47	51.74	49.39	50.5	56.123	18000
CASE 11	Training: 39	108.7	83.12	66.24	54.15	45.09	38.19	32.98	29.23	26.91	26.094	4.37E-11
	Test: 11	106.4	90.55	78.95	69.61	61.81	55.41	50.69	48.39	49.6	55.531	1001.4
CASE 12	Training: 38	109.7	84.03	67.01	54.76	45.56	38.52	33.19	29.34	26.94	26.098	4.98E-13
	Test: 12	105.2	89.37	77.78	68.49	60.76	54.42	49.73	47.37	48.39	53.928	79.422
CASE 13	Training: 37	110	84.53	67.62	55.42	46.2	39.09	33.64	29.64	27.1	26.185	6.40E-13
	Test: 13	110.2	94.77	83.07	73.3	64.82	57.51	51.73	48.35	48.75	54.465	79.525
CASE14	Training: 36	111.2	85.53	68.46	56.11	46.75	39.5	33.9	29.74	27.06	26.075	9.13E-13
	Test: 14	109	93.67	82.11	72.5	64.16	56.97	51.28	47.96	48.43	54.308	81.604
CASE 15	Training: 35	111.6	86.48	69.56	57.16	47.64	40.15	34.27	29.85	26.96	25.897	4.50E-13
	Test: 15	112.6	96.28	83.82	73.46	64.54	56.92	50.95	47.5	47.93	53.751	79.293
CASE 16	Training: 34	112.1	87.32	70.48	58	48.31	40.59	34.42	29.68	26.46	25.219	3.76E-13
	Test: 16	115.2	98.26	85.3	74.59	65.5	57.92	52.18	49.14	50.09	56.509	81.635
CASE 17	Training: 33	112.5	87.7	70.71	58.05	48.14	40.17	33.73	28.68	25.19	23.807	3.71E-13
	Test: 17	116.6	100.2	87.54	77.04	68.11	60.62	54.9	51.7	52.29	58.326	87.411
CASE 18	Training: 32	113.5	88.45	71.26	58.42	48.37	40.29	33.75	28.6	24.96	23.444	4.17E-13
	Test: 18	116.1	99.96	87.57	77.35	68.68	61.42	55.79	52.49	52.92	60.216	83.835

Table 8 (continued)

CASE 19	Training: 31	114.6	89.45	72.1	59.13	48.97	40.8	34.19	28.99	25.34	161.4	3346.8
	Test: 19	116.2	100.5	88.53	78.77	70.47	63.38	57.61	53.67	52.81	2.83E+16	2.96E+17

CASE 20	Training: 30	113.8	89.49	72.72	60.11	50.09	41.86	35.02	29.45	25.38	144.34	147.46
	Test: 20	123	107.3	94.52	83.54	73.82	65.26	58.15	53.29	52.28	6.82E+16	3.94E+15
CASE 21	Training: 29	114.7	90.5	73.67	60.89	50.64	42.12	34.94	29	24.56	411.31	5.66E-13
	Test: 21	122.8	107.1	94.42	83.51	73.88	65.49	58.63	54.1	53.49	1.69E+17	141.78
CASE 22	Training: 28	115.4	91.18	74.41	61.69	51.46	42.87	35.48	29.13	24.06	21.618	4.01E-13
	Test: 22	123.8	109	96.86	86.17	76.51	67.85	60.61	55.89	55.98	65.848	90.163
CASE 23	Training: 27	113	88.72	71.95	59.4	49.49	41.35	34.49	28.72	24.19	22.014	3.53E-13
	Test: 23	132	120.1	110.9	103.4	96.85	91.23	86.6	83.37	82.73	88.196	103.18
CASE 24	Training: 26	112.7	88.34	71.46	58.83	48.87	40.71	33.85	27.98	23.11	628.86	4.83E-13
	Test: 24	133.2	121.5	112.6	105.2	98.84	93.17	88.15	84.03	82.02	9.02E+16	149.87
CASE 25	Training: 25	114.1	89.63	72.62	59.83	49.68	41.32	34.18	27.93	22.4	544.14	3.42E-13
	Test: 25	133.5	122	113.1	105.6	98.98	93.06	87.81	83.67	82.64	4.21E+16	170.91

Table 9: RMSEs of SAM, RAM, and MAM in Seven-Zone Network (Double Link Failure: the number of training and test system states varies, STUDY B)

		MAM									**SAM**	**RAM**
	α	0.1	0.2	0.3	0.4	0.5	0.6	0.7	0.8	0.9	SAM	RAM
CASE 1	Training: 49	101.7	76.4	60.3	49.12	41.09	35.31	31.29	28.71	27.32	26.906	4.232
	Test: 1	81.99	61.99	50.59	43.47	38.89	35.98	34.21	33.26	32.88	32.912	20.317
CASE 2	Training: 48	102	76.81	60.7	49.47	41.32	35.38	31.18	28.43	26.92	26.46	7.85E-06
	Test: 2	102.4	84.32	71.74	62.33	55.26	50.28	47.32	46.37	47.31	49.893	1.09E+09
CASE 3	Training: 47	102.5	77.31	61.17	49.87	41.64	35.61	31.32	28.47	26.88	26.388	2.78E-11
	Test: 3	108.6	89.71	76.57	66.58	58.79	52.83	48.68	46.44	46.24	48.142	138.48
CASE 4	Training: 46	103	77.82	61.6	50.2	41.88	35.75	31.34	28.4	26.74	26.216	1.29E-12
	Test: 4	108.2	90.09	77.38	67.66	60.03	54.13	49.92	47.48	46.98	48.549	94.599
CASE 5	Training: 45	102.5	77.38	61.2	49.85	41.55	35.42	30.97	27.94	26.19	25.618	3.49E-10
	Test: 5	121.8	106.1	94.91	85.82	77.93	70.9	64.7	59.6	56.19	55.397	53303
CASE 6	Training: 44	103.2	78.01	61.76	50.32	41.93	35.7	31.15	28.02	26.18	25.555	7.93E-04
	Test: 6	120.6	104.3	92.75	83.5	75.58	68.59	62.45	57.38	54.04	53.672	7.93E+10
CASE 7	Training: 43	104.2	78.79	62.38	50.8	42.27	35.9	31.22	27.99	26.07	25.427	5.39E-09
	Test: 7	113.9	98.49	87.53	78.8	71.43	65.03	59.54	55.16	52.45	52.447	447925
CASE 8	Training: 42	104.6	79.39	62.99	51.35	42.72	36.21	31.37	27.97	25.91	25.214	2.15E-05
	Test: 8	114.6	99.2	88.05	79.12	71.62	65.3	60.2	56.66	55.33	57.117	2.44E+09

Table 9 (continued)

CASE 9	Training: 41	104.2	78.97	62.51	50.78	41.99	35.29	30.22	26.59	24.35	23.574	5.47E-13
	Test: 9	121.3	106.4	95.31	86.36	78.81	72.41	67.18	63.37	61.51	62.379	104.53

CASE 10	Training: 40	104.6	79.29	62.74	50.83	41.82	34.83	29.45	25.49	23	22.12	6.01E-13
	Test: 10	121.6	106.7	95.74	86.93	79.65	73.64	68.92	65.71	64.41	65.69	121.03
CASE 11	Training: 39	104	79.29	63.01	51.22	42.22	35.16	29.64	25.51	22.85	21.889	7.11E-07
	Test: 11	128.3	112.5	100.5	90.68	82.46	75.59	70.09	66.18	64.35	65.386	39144396
CASE 12	Training: 38	104.8	79.99	63.58	51.68	42.57	35.41	29.79	25.57	22.84	21.836	1.10E-10
	Test: 12	126.2	110.5	98.55	88.89	80.8	74.02	68.54	64.57	62.56	63.345	4336.7
CASE 13	Training: 37	105.1	80.5	64.14	52.22	43.05	35.8	30.08	25.74	22.9	21.848	2.54E-10
	Test: 13	128.3	112.4	100.3	90.36	82	74.89	69	64.53	61.94	62.097	8944.9
CASE 14	Training: 36	106.1	81.29	64.77	52.72	43.44	36.1	30.27	25.82	22.87	21.766	4.04E-13
	Test: 14	126	110.7	99.11	89.6	81.5	74.54	68.68	64.11	61.29	61.153	112.43
CASE 15	Training: 35	105.1	80.84	64.56	52.57	43.24	35.75	29.73	25.04	21.86	20.64	5.73E-13
	Test: 15	133	117.3	105.1	95.03	86.37	78.85	72.45	67.33	63.97	63.379	109.51
CASE 16	Training: 34	105.9	81.64	65.27	53.18	43.75	36.19	30.08	25.3	21.99	20.669	9.05E-13
	Test: 16	131.2	115.8	103.8	93.92	85.41	78.01	71.6	66.3	62.55	61.681	108.82
CASE 17	Training: 33	105.8	81.92	65.7	53.64	44.16	36.51	30.31	25.46	22.1	20.687	4.10E-13
	Test: 17	134.1	119	107	96.96	88.32	80.78	74.22	68.59	64.04	62.184	105.33
CASE 18	Training: 32	106.6	82.57	66.2	54.01	44.45	36.71	30.4	25.39	21.81	20.137	4.43E-13
	Test: 18	132.9	118.4	107.1	97.69	89.46	82.15	75.64	70.01	65.74	68.028	113.72
CASE 19	Training: 31	107.4	83.21	66.67	54.34	44.68	36.88	30.57	25.6	22.07	297.12	61.37
	Test: 19	132.3	117.9	106.9	97.8	89.94	83.02	76.89	71.56	67.35	7.07E+16	5.78E+15
CASE 20	Training: 30	108.5	84.15	67.44	55	45.24	37.35	30.9	25.73	21.94	84.801	1.21E-12
	Test: 20	130.9	117	106.3	97.47	89.76	82.85	76.64	71.23	67.31	3.00E+16	202.12
CASE 21	Training: 29	109.8	85.17	68.17	55.5	45.58	37.6	31.11	25.89	21.93	309.94	2210.6
	Test: 21	129.5	115.8	105.5	97.07	89.83	83.37	77.47	72.12	67.91	9.83E+16	1.36E+17
CASE 22	Training: 28	111.2	86.4	69.08	56.06	45.81	37.52	30.73	25.23	20.97	18.402	4.58E-13
	Test: 22	128.6	114.9	104.8	96.74	89.97	84.05	78.73	73.97	70.45	81.737	111.92
CASE 23	Training: 27	112.6	87.55	69.95	56.64	46.08	37.44	30.24	24.21	19.35	16.233	3.91E-13
	Test: 23	127.2	113.7	103.8	96.02	89.54	83.99	79.2	75.22	72.85	85.699	111.41
CASE 24	Training: 26	113.6	88.64	70.97	57.55	46.86	38.07	30.7	24.5	19.46	355.51	6.98E-13
	Test: 24	127	113.5	103.5	95.51	88.86	83.1	78.06	73.8	71.19	1.00E+17	121.62
CASE 25	Training: 25	113.4	88.24	70.53	57.13	46.51	37.81	30.53	24.43	19.54	16.594	5.50E-13
	Test: 25	129.2	117.3	108.7	102.1	96.71	92.16	88.29	85.21	83.62	93.501	116.11

4-4-3. The Mixture of Single-Link and Double-Link Failures

The applications of associative memory models to the same level of system states has been performed in terms of the number of damaged links. This scenario examines the performance of associative memory models from mixed system states of single-link and double-link failures. The single-link failure scenario contains twenty-four system states. The double-link failure scenario includes fifty system states. Consequently, seventy-four system states are used in this scenario.

This evaluation of associative memory models to the combined link failure system states investigates the performance of associative memory models in the case of varying training and test system states. The seventy-four data sets are combined and re-arranged. Several associative memory models are applied to this combined link failure system states. The RMSE results of the three associative memory models in estimates in the case of the combined link failures are shown in Table 10. The scatter plots and correlation coefficients between the simulated and the estimated traffic flows are shown in Appendices 4-M to 4-R.

This mixed link failure evaluation provides the lowest RMSE results among the three link failure scenarios. This may be due to the increased number of system states available for training. The estimation performance of SAM, RAM and MAM ($\alpha = 0.9$) is very close. The RMSE results do not vary significantly as the number of training system states decreases. The MAM procedure indicates that this approach is noise tolerant,

when the number of training system states decreases and the number of test states increases.

Table 10: RMSEs of SAM, RAM, and MAM in Seven-Zone Network (Single and Double Link Failure)

		MAM									SAM	RAM
	α	0.1	0.2	0.3	0.4	0.5	0.6	0.7	0.8	0.9	SAM	RAM
CASE 1	Training: 73	87.94	64.56	50.56	41.45	35.38	31.38	28.84	27.37	26.65	26.445	15.031
	Test: 1	118.5	90.52	70.48	55.43	43.92	35.21	28.92	24.89	22.95	22.761	23.842
CASE 2	Training: 72	88.34	65.03	50.98	41.78	35.61	31.5	28.89	27.36	26.61	26.403	13.994
	Test: 2	108.2	81.49	62.68	49.08	39.43	33.1	29.68	28.65	29.33	31.043	27.59
CASE 3	Training: 71	88.5	65.34	51.28	42.03	35.77	31.6	28.92	27.35	26.57	26.358	12.147
	Test: 3	114.8	87.77	69.06	55.6	45.93	39.26	35.07	32.91	32.31	32.804	38.922
CASE 4	Training: 70	88.92	65.71	51.59	42.28	35.98	31.75	29.04	27.44	26.65	26.426	12.021
	Test: 4	106	81.58	64.64	52.43	43.62	37.49	33.56	31.45	30.74	31.043	36.668
CASE 5	Training: 69	89.38	66.12	51.95	42.56	36.19	31.9	29.14	27.5	26.69	26.464	11.829
	Test: 5	101.5	78.92	62.92	51.28	42.83	36.95	33.22	31.27	30.72	31.156	36.024
CASE 6	Training: 68	89.56	66.43	52.27	42.82	36.35	31.94	29.07	27.35	26.49	26.246	12.825
	Test: 6	105.2	82.91	67.01	55.31	46.81	40.98	37.45	35.86	35.77	36.748	35.936
CASE 7	Training: 67	89.98	66.89	52.68	43.16	36.6	32.11	29.16	27.39	26.49	26.242	13.029
	Test: 7	104.2	81.81	65.96	54.31	45.85	40.06	36.59	35.09	35.11	36.214	34.299
CASE 8	Training: 66	90.57	67.4	53.06	43.42	36.75	32.16	29.14	27.32	26.39	26.131	12.763
	Test: 8	100.9	78.76	63.38	52.27	44.38	39.17	36.24	35.2	35.56	36.892	35.83
CASE 9	Training: 65	91.07	67.8	53.4	43.7	36.97	32.33	29.26	27.39	26.45	26.174	12.457
	Test: 9	97.59	76.6	61.97	51.34	43.73	38.62	35.67	34.53	34.81	36.085	34.518
CASE 10	Training: 64	91.64	68.28	53.76	43.95	37.12	32.4	29.26	27.35	26.37	26.096	12.027
	Test: 10	96.03	75.23	60.96	50.74	43.54	38.79	36.13	35.18	35.53	36.784	36.576
CASE 11	Training: 63	92.19	68.8	54.19	44.28	37.37	32.57	29.37	27.41	26.41	26.128	11.882
	Test: 11	95.33	74.46	60.17	49.95	42.75	38.01	35.38	34.46	34.85	36.148	35.311
CASE 12	Training: 62	92.31	69.14	54.59	44.65	37.64	32.72	29.4	27.34	26.28	25.969	12.318
	Test: 12	98.39	77.08	62.33	51.65	44	38.87	35.94	34.87	35.25	36.677	35.83
CASE 13	Training: 61	92.58	69.49	54.89	44.85	37.71	32.65	29.2	27.05	25.93	25.601	12.691
	Test: 13	100.3	78.83	64.04	53.33	45.65	40.5	37.54	36.44	36.8	38.216	179.57
CASE 14	Training: 60	93.14	69.95	55.23	45.07	37.83	32.69	29.17	26.96	25.8	25.469	12.378
	Test: 14	98.99	77.96	63.53	53.15	45.74	40.81	37.99	36.96	37.32	38.679	45.558
CASE 15	Training: 59	93.71	70.46	55.67	45.42	38.04	32.72	29.02	26.66	25.4	25.028	10.683
	Test: 15	97.59	77.25	63.12	52.84	45.54	40.83	38.47	38.14	39.41	41.793	50.486
CASE 16	Training: 58	94.05	70.84	56.05	45.75	38.31	32.92	29.13	26.68	25.36	24.966	152.42
	Test: 16	98.54	78.52	64.46	54.1	46.59	41.6	38.97	38.46	39.71	42.269	169.02
CASE 17	Training: 57	94.49	71.29	56.46	46.11	38.61	33.15	29.3	26.8	25.45	25.045	306.02
	Test: 17	98.53	78.8	64.84	54.48	46.88	41.74	38.91	38.2	39.26	41.665	319

CASE 18	Training: 56	94.76	71.66	56.8	46.36	38.75	33.19	29.25	26.68	25.28	24.856	43.409
	Test: 18	100.6	80.72	66.62	56.11	48.34	42.96	39.82	38.76	39.46	41.555	67.544
CASE 19	Training: 55	94.87	71.84	57.01	46.59	38.97	33.38	29.39	26.77	25.33	24.889	7.1233
	Test: 19	102.5	83.39	69.75	59.37	51.43	45.58	41.69	39.74	39.61	41.144	2.85E+08
CASE 20	Training: 54	95.07	72.18	57.41	47	39.34	33.68	29.61	26.9	25.4	24.943	28.618
	Test: 20	103.7	84.95	71.27	60.7	52.46	46.26	42.04	39.8	39.49	40.944	7.21E+15

4-5. Conclusions

The results of different link failure cases demonstrate the applicability of associative memory models to seismic risk analysis in the synthetic network. The SAM, RAM, and MAM procedures provide good overall estimates of traffic flows, if the number of the training system states is sufficient (greater than fifty). There is not much difference in the performance among the three associative memory models. However, MAM demonstrates an advantage with respect to the test flows, being less sensitive to error terms than SAM and RAM. Both SAM and RAM provide poor estimates of traffic flows in the cases of CASE 19 and 20 in Table 8. On the other hand, MAM produces reliable estimates in the same cases due to MAM's built-in penalty function for overfitting. The results of the MAM procedure indicate the best value of α is in the neighborhood of 0.9.

The accurate estimates made by associative memory models from the combined data sets demonstrate that the post-earthquake system states derived from the different link failure scenarios can be combined and used to train the associative memory matrices. The performance of the associative memory models mostly depends on the number of training system states as well as the number of test system states. The addition of more

training states used in the learning process tend to increase the performance of associative memory models. The results of applying associative memory models with varying training and testing system states indicate that the associative memory models are able to estimate a group of test system states simultaneously without significant loss of the estimation power, if the number of training system states is sufficiently large. This will result in significant time savings for computing estimates of link flows in the case of large number of link-failure system states.

The seven-zone synthetic network is simple, but captures several elements of a freeway system. This exercise measures the performance of different associative memory models by comparing the flow estimates provided by the associative memory approach with the noise-free numerical solutions to the corresponding network equilibrium model. Observed link volumes are not available in the synthetic network. Thus, simulated user equilibrium flows are used as benchmarks for evaluating the quality of alternative associative memories to the static network equilibrium model.

The associative memory approach is a heuristic process. Associative memory models produce heuristic solutions to conventional transportation models. The major point of this exercise is not to predict link flows on an individual link, but for the entire system. The objective is to generate an inexpensive, but reliable prediction of system-wide traffic flow changes with respect to given alternative network configurations related to different earthquake or congestion pricing scenarios.

The quality of the associative memory outputs is evaluated by RMSE measures, scatter plots, and correlation coefficients. In most cases, the procedure performs very well in this dimension. The outputs from the associative memory models provide good estimates of individual link flows. This result indicates the applicability of such techniques to the network flow modeling problem. The associative memory applications demonstrate the possibility of computational time savings by estimating the link flows of many system states simultaneously.

Conventional transportation network models may require huge computational times to generate exact solutions for a large-scale transportation network. The cheap, heuristic solutions of the associative memories can be used as good starting points for the conventional models. This is conducted in two steps. Associative memory solutions are adjusted for feasible solutions, satisfying all the network flow constraints. After a feasible solution is obtained, the conventional network flow models are applied to improve the feasible solution to an exact solution.

In an empirical context, this is second best. Both sets of flows are predictions. The standard network equilibrium model is an incomplete representation of the process that simulates link volumes. Empirical studies indicate that there are significant differences between simulated flows of conventional network flow models and observed link volumes. The comparison against observed link volumes will be presented for the case of seismic risk analysis in Chapter 7.

5. Estimation of an O-D Trip Matrix from Observed Traffic Volumes for a Synthetic Network

5-1. Motivation

An origin-destination (O-D) trip matrix describes the intensity of travel demand for service over space. This travel demand varies over time due to a number of factors. Transportation planners have developed various methods for estimating an O-D trip matrix using observed traffic volumes to avoid expensive and time consuming O-D trip generation methods such as home-interview surveys.

The application of the associative memory approach to traffic flow estimation requires a set of post-earthquake traffic flows as training input data. The post-earthquake traffic flows can be simulated using a static user equilibrium model if observed link volumes for link-failure system states are neither available nor sufficient. This traffic flow simulation requires transportation system data sets including an O-D trip matrix.

O-D trip matrices are often outdated. They may not be consistent with observed traffic volumes. One of the standard approaches to estimating O-D trip matrices is to use the LINKOD model (Gur, 1983). The LINKOD model updates O-D trip elements to be consistent with observed link volumes via an iterative sequence of nonlinear optimization procedures.[2]

---

[2] The LINKOD model was developed by Gur et al. (1980). The validity and applicability of the LINKOD model have been evaluated by Han et al. (1981), Han and Sullivan (1983), Gur (1983), Dowling and May (1984), and Easa and McColl (1987).

The LINKOD model consists of two components: a trip distribution model for small areas (SMALD) developed by Kurth et al. (1979) and an adaptable O-D trip matrix assignment model (ODLINK) based on the work of Nguyen (1977a, 1977b). This research employs the assignment model of the LINKOD model to adjust an O-D trip matrix until it is consistent with observed link volumes. Prior to applying the LINKOD model to the aggregated Los Angeles highway network, the following sections evaluate the performance of the LINKOD model in the case of the simple synthetic transportation network. The FORTRAN code of the LINKOD model is presented in Appendix 5.[3]

The LINKOD model requires equilibrium traffic volumes, free-flow link travel times, link capacities, and an initial O-D trip matrix as transportation system data sets. Free-flow link travel times and link capacities in Table 3 are used as the system input data sets. User equilibrium traffic flows in Table 4 are also used as the system input data. We evaluate the LINKOD model by injecting noise into the true O-D trip table corresponding to equilibrium traffic flows on the synthetic network

5-2. Testing the LINKOD Model

The equilibrium link flows can be obtained by assigning the target O-D trip matrix to the synthetic network under user equilibrium conditions. Tests on the validity of the

[3] The FORTRAN code of the LINKOD program was presented by Gur et al. (1980b, 1980c). A modified FORTRAN code for the assignment model (ODLINK) of the LINKOD program was introduced by Seongkil Cho.

LINKOD model are conducted by comparing the O-D trip matrix provided by the LINKOD model (the estimated O-D trip matrix) against the original O-D trip matrix (the target O-D trip matrix).

5-2-1. Testing Cases

Two different initial trip matrices are used to compare relative differences between the estimated O-D trip matrices as a function of data quality. Test 1 uses a good initial trip table identical to the target O-D trip matrix. Even though the target O-D trip matrix is used in the LINKOD model as an initial trip table, the LINKOD model does not immediately terminate because the LINKOD model must iterate until equilibrium link flows are obtained from the target matrix. Test 2 uses a poor initial trip table in which trip interchanges are uniformly distributed. This uniformly distributed O-D trip matrix means that almost no prior information about the true trip table is available.

5-2-2. Measurement of the Model Validity

Percent Mean Absolute Error (%MAE) is used to quantify the quality of LINKOD's outputs,

$$\%MAE = \frac{\sum_{ij} |t_{ij} - T_{ij}|}{\sum_{ij} T_{ij}} \times 100 \quad (52)$$

where t_{ij} and T_{ij} are the estimated and solution trip interchanges, respectively.

%MAE for volume estimations is calculated in the same manner.

5-2-3. Test Results

Results are summarized in Table 11.

Table 11: Percent Mean Absolute Errors

	Link Volume Error (%)	Trip Interchange Error (%)
Case 1	2.9	15.8
Case 2	4.3	29.0

Figure 7 depicts the correlation between target and estimated volumes for Case 1 and Case 2. Figure 8 presents the same information for the target and estimated trip interchanges.

The following results are apparent.

(1) The LINKOD model results in good quality volume assignments regardless of the accuracy of the initial trip table.

(2) Lower volume errors are observed when the initial estimate of the trip table is of higher quality.

(3) Errors in trip interchange estimates are more sensitive to the accuracy of the initial trip table than volume errors.

(4) A better initial estimate of the trip table produces a better final estimate of the trip table, though differences between the final estimate and the target persist.

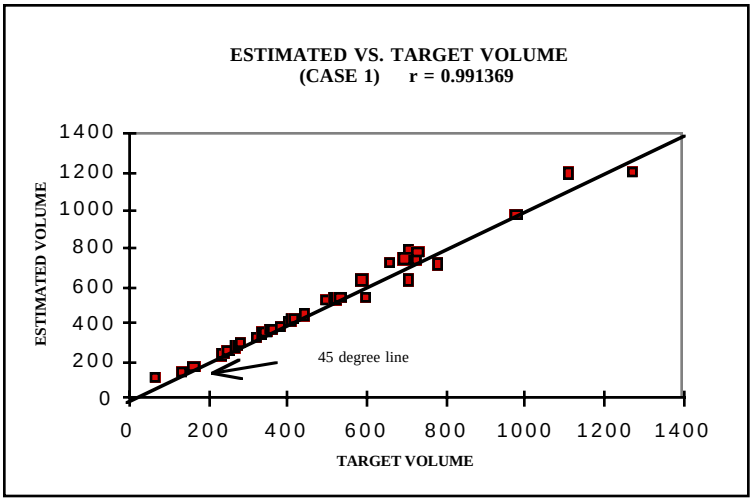

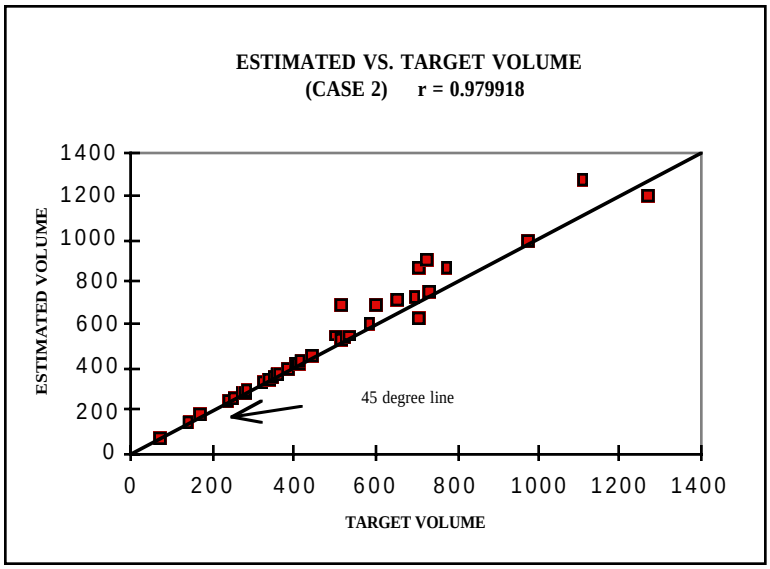

Figure 7: Link Volume Correlation

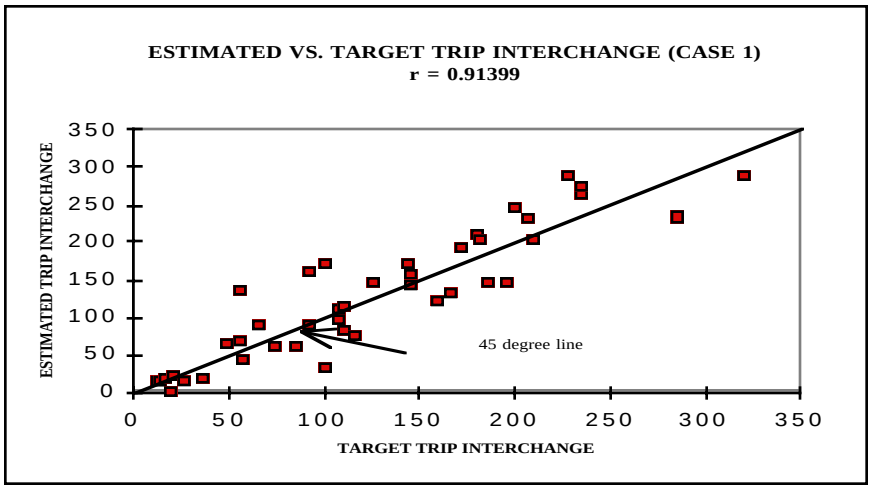

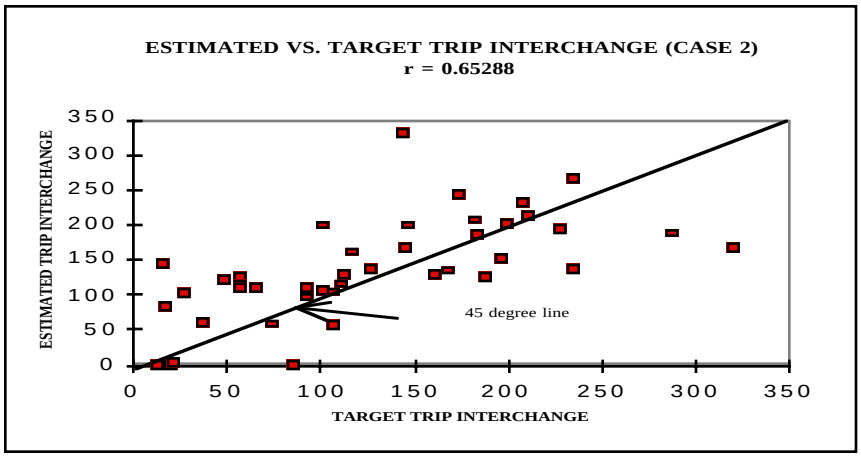

Figure 8: Trip Interchange Correlation

6. Preparation of Empirical Data

6-1. Background

Results from the application of the general TNA procedure to the simple synthetic network demonstrate that the associative memory approach offers considerable potential. Applying this approach to the Los Angeles highway system in a way that combines user equilibrium concepts with Caltrans' multi-attribute decision procedure requires the following fourteen steps:

(1) construct a representation of the Los Angeles highway network;

(2) collect or generate initial transportation system data sets including observed link volumes, free-flow link travel times, link capacities, and a Los Angeles highway O-D trip matrix;

(3) adjust observed link volumes to exclude seasonal and trend variations;

(4) reduce the lack of uniformity between the Los Angeles O-D trip matrix and adjusted link volumes using the LINKOD PLUS model;[4]

(5) adjust free-flow link travel times and link capacities to minimize the difference between observed and simulated traffic flows under the perfect condition of the Los Angeles highway network;

(6) identify empirical link-failure system states;

(7) apply associative memory models to estimate link volumes for empirical link-failure system states;

(8) define additional synthetic link-failure system states;

[4] This LINKOD PLUS model is a modified version of the FORTRAN code based on the assignment model of the LINKOD program described in Chapter 5. It was developed by Geunyoung Kim to estimate an O-D trip matrix for the aggregated representation of the Los Angeles highway network.

(9) simulate traffic flows for additional synthetic link-failure system states by using the static user equilibrium model and the adjusted system data sets;

(10) extend the number of link-failure system states by combining the empirical link-failure system states with the synthetic system states;

(11) apply associative memory models to the combined data sets to determine the best associative memory model;

(12) estimate traffic flows for additional link-failure system states using the best associative memory matrix;

(13) compute total system travel times by multiplying estimated traffic flows with their associated link travel times; and

(14) employ the total system travel time changes to Caltrans' multi-attribute decision procedure for the priority rating of each freeway link.

The following sections define the Los Angeles highway network and empirical transportation system data that will be used for transportation network analysis procedures. A system of compact freeway traffic analysis zones is built up by aggregating 1990 US census tracts. An aggregated representation of the Los Angeles highway network is developed based on the arrangement of the Caltrans District 7 freeway system and traffic count stations. Five empirical link-failure system states are identified due to the opening of the Glen Anderson Freeway (I-105) and the 1994 Northridge earthquake.

Four empirical highway system data sets are constructed to perform the traffic flow analyses for the aggregated Los Angeles highway network. They are: (1) free-flow link

travel times, (2) link capacity data, (3) traffic volumes, and (4) an origin-destination trip matrix. It is assumed that observed traffic volumes obtained from Caltrans' traffic counts include seasonal and trend variations. It is also assumed that the origin-destination trip matrix extracted from SCAG's 1991 Southern California Origin-Destination Survey data is not consistent with Caltrans' traffic volumes. Thus, the initialization module of the general transportation network analysis procedure is applied to adjust the O-D trip matrix as well as the observed traffic volumes. The development of the aggregated Los Angeles highway network and its empirical system data is described in the following sections.

6-2. Aggregated Los Angeles Highway System

Structuring the Los Angeles urban system and transportation network is one of the essential tasks in this research. It requires a thorough understanding for the Los Angeles metropolitan area and its transportation system, an appropriate decision-making for defining traffic analysis zones and transportation network links, and a data acquisition process for the defined zones and network links.

The Los Angeles metropolitan area consists of five counties; Los Angeles, Orange, Riverside, San Bernardino, and Ventura Counties. The Los Angeles region includes the nation's second largest city, Los Angeles, and more than 180 other municipalities. The region has 10.6 million residents and 5.3 million jobs in 1980 (Guiliano and Small, 1994).

The Los Angeles metropolitan area contains a variety of transportation systems: the highway/roadway system, the public transit system, the aviation system, the maritime system, and the non-motorized transportation system. The Los Angeles freeway/roadway system is the backbone of regional mobility among the transportation systems, carrying out a huge amount of trips on a daily basis. The existing Los Angeles freeway/roadway system consists of approximately 3,380 miles of federal and state highways, 3,450 miles of major arterials, and massive secondary arterials and local streets (SCAG, 1994).

The Los Angeles freeway system is the principal facility for both regional and local automobile trips. The freeway system comprises only 15 percent of the total freeway/roadway system mileage. However, the freeway system carries slightly more than 50 percent of total vehicle miles traveled (VMT) within the Los Angeles region. The freeway system includes approximately 1,100 centerline miles of a high-occupancy vehicle (HOV) network for carpools, vanpools, and express buses. The freeway system also includes 14.5 miles of the Santa Monica Freeway Smart Corridor and 10 miles of two toll lanes in each direction within the median of State Route 91. Federal and state highways in the five counties of the Los Angeles region are managed by three districts of Caltrans: Los Angeles and Ventura Counties by District 7, Riverside and San Bernardino Counties by District 8, and Orange County by District 12. Arterials and local streets are managed by city governments.

Modeling system-wide traffic flows for the Los Angeles region requires the development of a large-scale transportation network. However, solving a large-scale network equilibrium problem such as the Los Angeles transportation network is computationally elaborate. Consequently, the idea of transportation network aggregation has been applied to reduce the computational burden associated with the network equilibrium problem by simplifying the actual Los Angeles transportation network.

This research develops an aggregated representation of the Los Angeles highway network for the area of Caltrans District 7, including Los Angeles and Ventura Counties. It is partially because the Los Angeles County is the core of the Los Angeles metropolitan area, and partially because the Caltrans District 7 is the major source of data in this study. The area of Caltrans District 7 includes over 8.4 million population, 26 freeways, 597 freeway miles, 790 traffic count stations, and over 6 million registered vehicles (Caltrans, _).

The highways of Caltrans District 7 serve 81 million vehicles daily, 1 million vehicle trips during morning rush hours (6-9 am), and 1.5 million vehicle trips during evening rush hours (3-6 PM). An average of 3.5 trips are made daily by each person. Around 62 percent of total trips and 60 percent of vehicle driver trips in the Los Angeles region occurred in the Los Angeles and Ventura Counties (SCAG, 1993). Average vehicle occupancies in the Los Angeles and Ventura Counties were 1.45 and 1.47, respectively.

An aggregated representation of the Los Angeles highway network is constructed based on Caltrans' traffic count stations. Arterials, local streets, and railway systems are not considered in the aggregated Los Angeles highway network.[5] Traffic analysis zones are defined by aggregating 1990 US Census tracts after considering the area of Caltrans District 7 and the Los Angeles highway network. Each zone serves as both origin and destination of trips. Different link segments of a highway link between two adjacent zones are combined to a representative link.[6] An origin-destination trip matrix for the aggregated Los Angeles highway network is estimated using SCAG's 1991 origin-destination survey data and Caltrans' 1993 traffic count data.

The aggregated Los Angeles highway network consists of 105 zones and 292 network links. A GIS map for the actual Los Angeles freeway network with traffic count stations is shown in Figure 9. A GIS map for the Los Angeles traffic analysis zones is presented in Figure 10. The defined network is shown in Figure 11.

---

[5] This research applies associative memory models that use observed link volumes as an input data set. Observed traffic volumes before and after the Northridge earthquake were available in only a few links of local streets near the Smart Corridor of the Santa Monica Freeway. Thus, this research excludes arterials and local streets from the study network. For detailed information regarding the local street traffic volumes, refer to Caltrans (1994). [5] The network aggregation method will be described in section 6-5.

[6] The network aggregation method will be described in section 6-5.

Figure 9: Los Angeles Highway Network and Traffic Count Stations

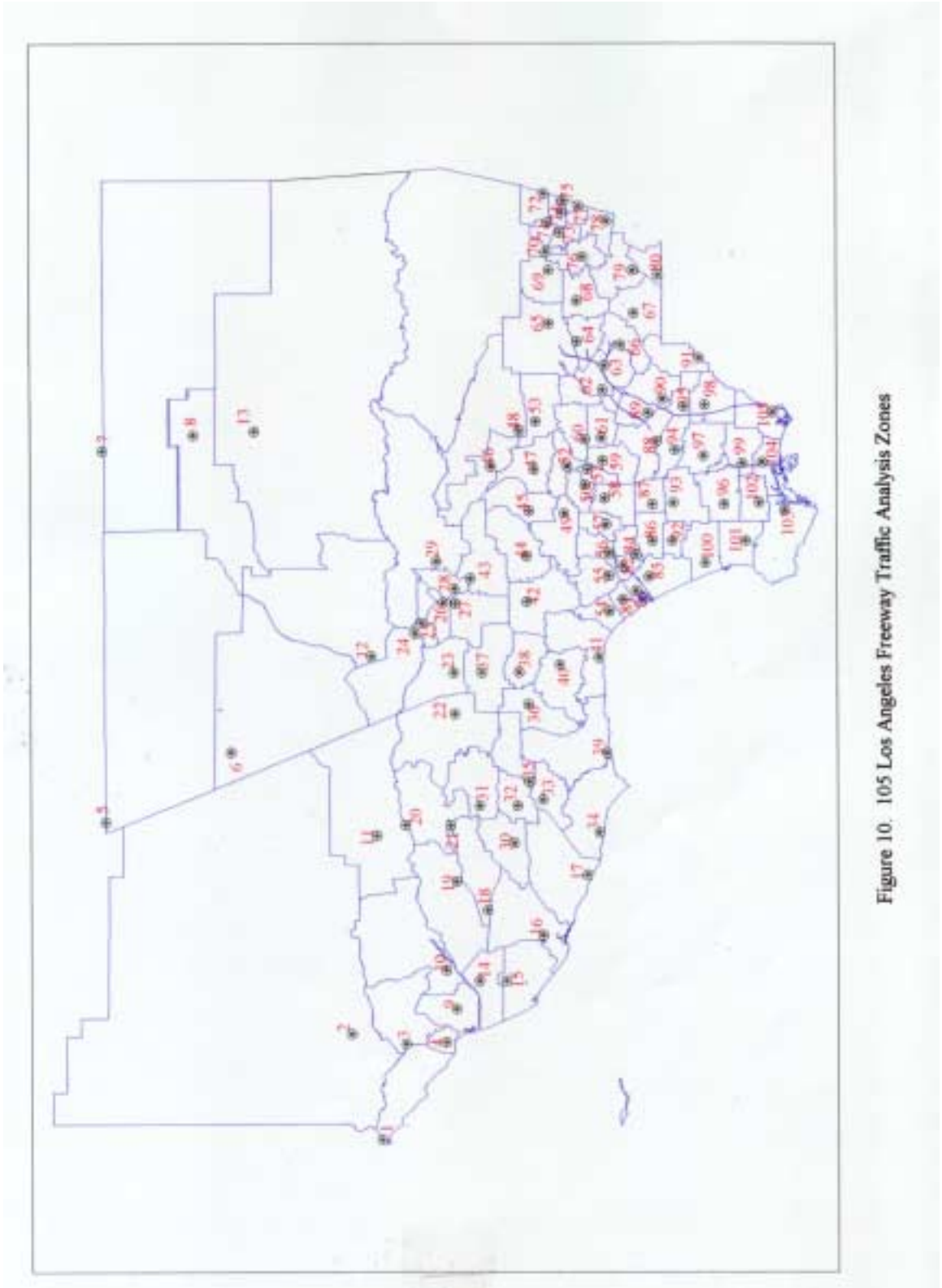

Figure 10. 105 Los Angeles Freeway Traffic Analysis Zones

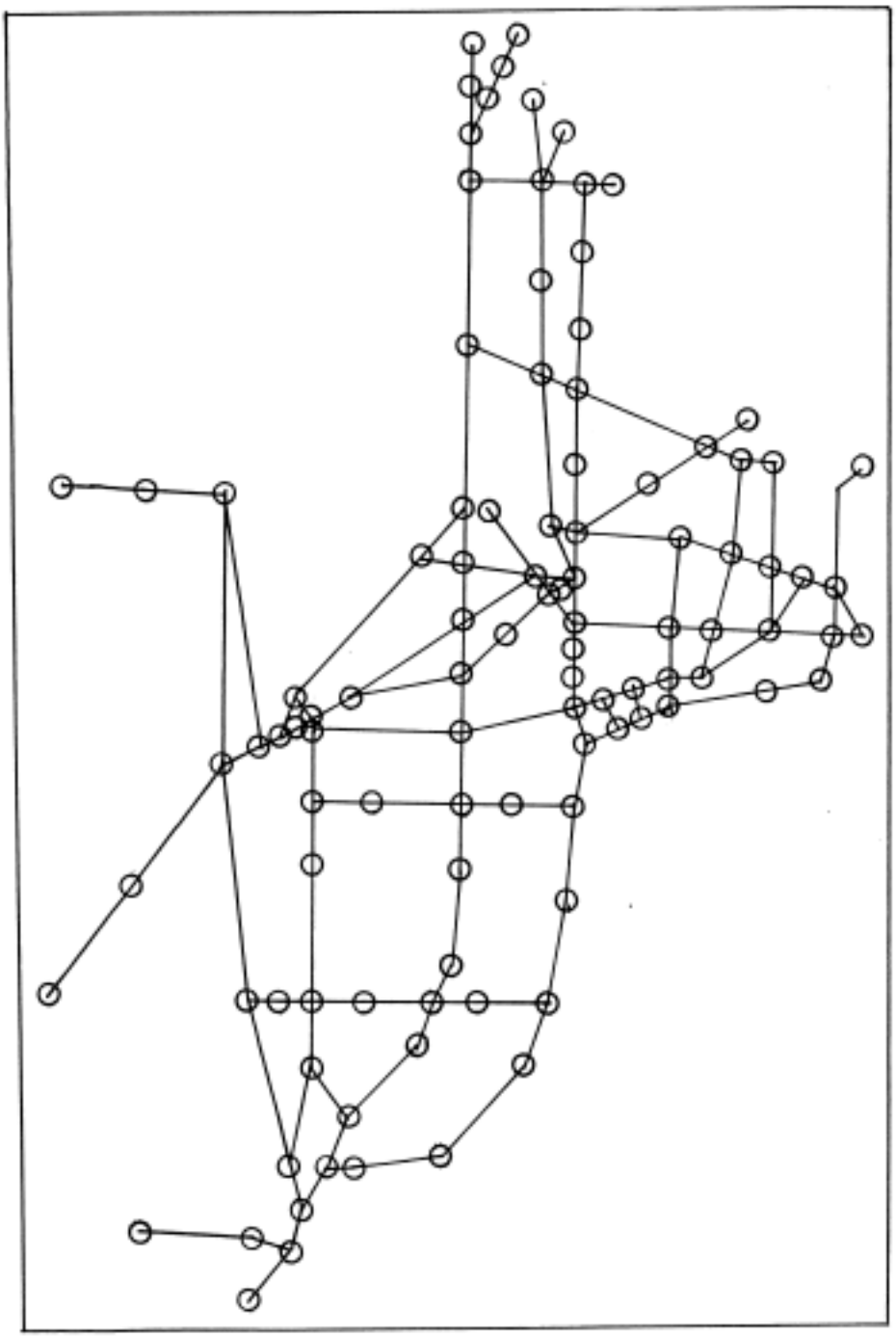

Figure 11: The Aggregated Representation of The Los Angeles Highway Network

6-3. Five Empirical System States

This research identifies empirical link-failure system states based on changes of network configurations in the Los Angeles highway system. The Los Angeles region experienced a range of unique events during the period of October 1993 to September 1994. The Glen Anderson Freeway (I-105) opened on October 14, 1993. The 6.8 magnitude Northridge earthquake struck Southern California on January 17, 1994. The earthquake simultaneously damaged several links of the Golden State Freeway (I-5), the Santa Monica Freeway (I-10), the Antelope Valley Freeway (SR-14), and the Simi Valley Freeway (SR-118). The disconnected links due to the Northridge earthquake gradually returned to service through several months.

A variety of mechanisms can be used to codify network configurations of link failures. The network configurations of link failures can be represented discretely. Collapsed links are coded as "2," and undamaged links are coded as "1." Alternatively, continuous numbers such as the weighed average number of lanes or link capacities can be used as values of the network configurations. This research employs the discrete network configuration mechanism for representing link-failure system states.

At least three sets of average monthly daily traffic volumes can be referred to observed link volumes of the Los Angeles highway network under perfect condition: (1)

average daily traffic volumes collected during the month of November 1993, (2) average daily traffic volumes during the month of December 1993, and (3) average daily traffic volumes during the month of October 1994 or later.

Theoretically, deseasonalized and detrended traffic volumes derived from the above three months should be identical because they are the outcomes of the perfect system state. The three sets of link volumes are associated with the same network configuration whose all elements are coded to "1." This research selects the observed link volumes collected in November 1993 as the representative traffic volumes for the perfect network system.

Five empirical link-failure system states including the perfect system state are identified based on different network configurations of the aggregated Los Angeles highway system. They are:

(1) empirical system state 1: July 1993 system state representing the pre-opening of the Glen Anderson Freeway (I-105),

(2) empirical system state 2: November 1993 system state representing the post-opening of the Glen Anderson Freeway and the pre-1994 Northridge earthquake,

(3) empirical system state 3: February 1994 system state representing the post-Northridge earthquake, and the pre-recovery of the damaged links,

(4) empirical system state 4: May 1994 system state representing the post-recovery of the damaged links in the Santa Monica Freeway, and

(5) empirical system state 5: August 1994 system state representing the post-recovery of the damaged links in the Golden State Freeway and the Antelope

Valley Freeway, but the pre-recovery of the Simi Valley Freeway's links.

Six links of the aggregated Los Angeles highway system were closed before the opening of the Glen Anderson Freeway. Thus, empirical system state 1 is referred to a six-link-failure system state. Empirical system state 2 represents the perfect system state with links in perfect condition. Seven links of the aggregated Los Angeles highway system were closed due to the Northridge earthquake. Empirical system state 3 is regarded as a seven-link-failure system state.

Three links in the Santa Monica Freeway returned to service on April 13, 1994. Empirical system state 4 is considered as a four-link-failure system state. Damaged links in the Golden State Freeway were recovered on May 18, 1994. The damaged junction of the Antelope Valley Freeway to the Golden State Freeway was opened on July 9, 1994. Thus, empirical system state 5 is referred to a double-link-failure system state. The damaged links of the Simi Valley Freeway were returned to service on September 7, 1994. All the physical damage of the Los Angeles transportation network caused by the Northridge earthquake was thus repaired. Appendix 6 summarizes the network configurations for the five empirical link-failure system states.

6-4. Free-Flow Travel Times

Speeds and travel times vary over time, space, and across modes. Free-flow speed is defined as speed when density approaches zero under free-flow conditions. A free-flow

link travel time is the time that a vehicle takes to traverse a link under free-flow conditions. The free-flow link travel time is obtained by dividing each link's distance by the link's free-flow speed. The equation for obtaining free-flow travel times is

$$FFTT = D / FFS \tag{53}$$

where

FFTT = free-flow link travel time,
D = link distance, and
FFS = free-flow speed.

Link distances for the aggregated Los Angeles highway network are obtained from post-mile information of the California State highway system in the 1993 California State Highway Log (Caltrans, 1993). Free-flow speed data for SCAG's Southern California Regional Transportation Model are used as the free-flow travel speed for each aggregated highway link. It is assumed that the free-flow link travel time of a directed link is identical to that of the corresponding reverse link. Tables 12, 13, and 14 show the facility type of roadway systems, area types, and free-flow speed and link capacity per lane per hour, respectively. Area-type boundaries in the Los Angeles region are shown in Figure 12. The free-flow link travel times by hour and by minute are summarized in the last two columns of Appendix 7.

6-5. Link Capacity Data

6-5-1. Methods for Obtaining Link Capacities

The capacity of a freeway/roadway link is defined as the maximum hourly rate at which persons or vehicles can be reasonably expected to traverse a point or uniform section of a lane or roadway during a given time period under prevailing roadway, traffic, and control conditions (TRB, 1985). The transportation network analysis procedure in this research uses hourly-based link capacities instead of daily-based values because the travel behavior of drivers are more accurately represented by the hourly-based values.

There are many ways of determining link capacities in the traffic engineering field. Pignataro (1973) provided a widely used formula for obtaining freeway link capacities by multiplying the Level of Service E service volume (2,000 passenger cars per hour per lane) by appropriate adjustment factors. Pignataro's equation for obtaining freeway link capacities is

Table 12: Types of Roadways

Code No	Facility Types
1	Freeways (mixed flow)
2	Major arterials and expressways (6-lane divided)
3	Primary arterials (4-lane divided)
4	Secondary arterials (4-lnae Undivided)
5	HOV facility for carpool/bus
6	Cordon and zone connectors

Source: 1990 Validation of the Southern California Regional Transportation Model.

Table 13: Types of Areas

Code No	Areas
1	CBD
2	CBD fringe
3	Suburban
4	Mountain
5	Rural

Source: 1990 Validation of the Southern California Regional Transportation Model.

Table 14: Free-Flow Travel Speed and Link Capacity for Lane by Area and Roadway Types

Area Type	Roadway	Free-Flow Speed (MPH)	Capacity/Lane/Hr
1	1	60	1900
	2	20	625
	3	20	575
	4	20	500
	5	65	1900
	6	20	10000
2	1	60	1950
	2	25	650
	3	25	600
	4	25	525
	5	65	1950
	6	25	10000

3	1	60	1950
	2	35	675
	3	35	625
	4	30	550
	5	65	1950
	6	30	10000
4	1	60	1950
	2	40	800
	3	40	800
	4	35	800
	5	65	1950
	6	40	10000
5	1	65	1950
	2	50	1250
	3	50	900
	4	50	900
	5	70	1950
	6	40	10000

Source: 1990 Validation of the Southern California Regional Transportation Model.

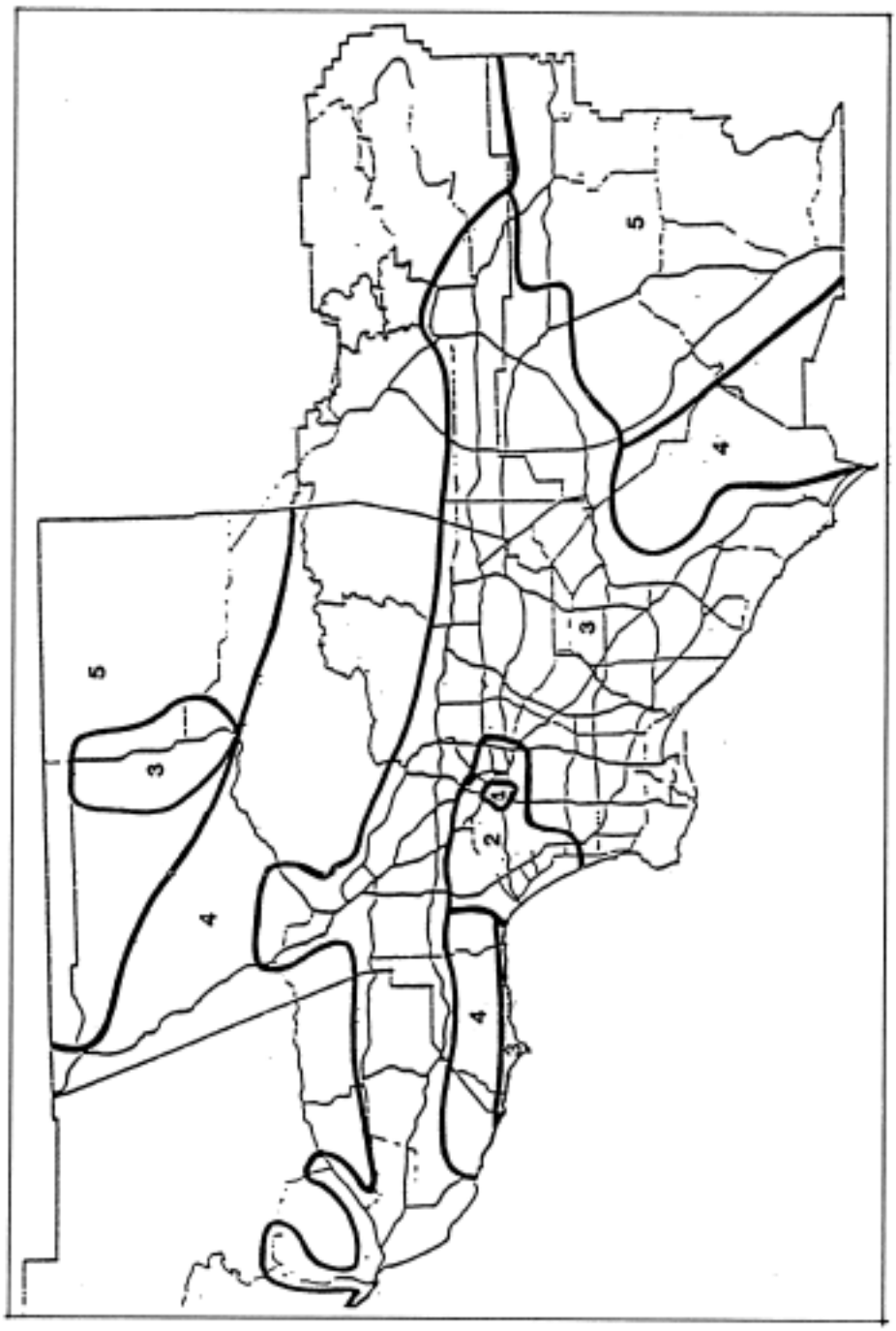

Figure 12: Area-Type Boundaries in the Los Angeles Metropolitan Area

$$C = 2000\,NWT_c \tag{54}$$

where

C = *capacity (mixed vehicle per hour, total for one direction),*
N = *number of lanes (in one direction)*
W = *adjustment for lane width and lateral clearance,*
T_c = *truck factor at capacity.*

Pignataro also presented different values of W and T_c in terms of freeway conditions. The values of W and T_c factors are set equal to value one because detailed information for these factors in the case of the Los Angeles highway network is not available. The number of lanes is obtained from The 1993 California State Highway Log (Caltrans, 1993).

Determining link capacities for aggregated network links is more than simply applying equation (53). First, the service is different according to area and roadway types of the Los Angeles highway links. Pignataro used 2,000 passenger cars per hour as the value of freeway link capacity per lane in equation (53). This research uses values of link capacity per hour per lane for SCAG's Southern California Regional Transportation Model. They are shown in Table 14.

Second, an aggregated network link may be comprised of several link segments with different segment lengths and number of lanes. Four capacity computing methods are considered to compute representative link capacities for the aggregated Los Angeles

network links; (1) a link length weighted average capacity (LLWAC) method, (2) a minimum capacity (MC) method, (3) a link segment capacity (LSC) method, and (4) an equivalent capacity (EC) method.

The LLWAC method first computes a weighted average number of lanes for an aggregated link by multiplying the number of lanes of each link segment with its proportional length and by summing up the weighted values. The LLWAC link capacity of a link is obtained by multiplying the weighted average number of lanes with the value of link capacity per lane per hour. The MC method identifies the minimum number of lanes among different link segments of a link. The MC method multiplies the minimum lane number with the value of link capacity per lane per hour. The LSC method treats all the link segments as network links. The EC method uses the BPR link travel cost function to compute a link capacity, representing the performance of all segments of a link.

An example network link with different link segments is shown in Figure 13. The representative link capacity for the link computed from the EC method is as follows. The total link travel time (T) of the link is

$$T = t_1 + t_2 + \ldots + t_n$$

$$= t_{01} \times \left[1 + 0.15\left(\frac{v}{c_1}\right)^4\right] + t_{02} \times \left[1 + 0.15\left(\frac{v}{c_2}\right)^4\right] + \ldots + t_{0n} \times \left[1 + 0.15\left(\frac{v}{c_n}\right)^4\right]. \qquad (55)$$

We assume the existence of a representative link travel cost function with a representative link capacity for the link. We can write

$$T = T_0 \left[1 + 0.15 \left(\frac{v}{C} \right)^4 \right], \tag{56}$$

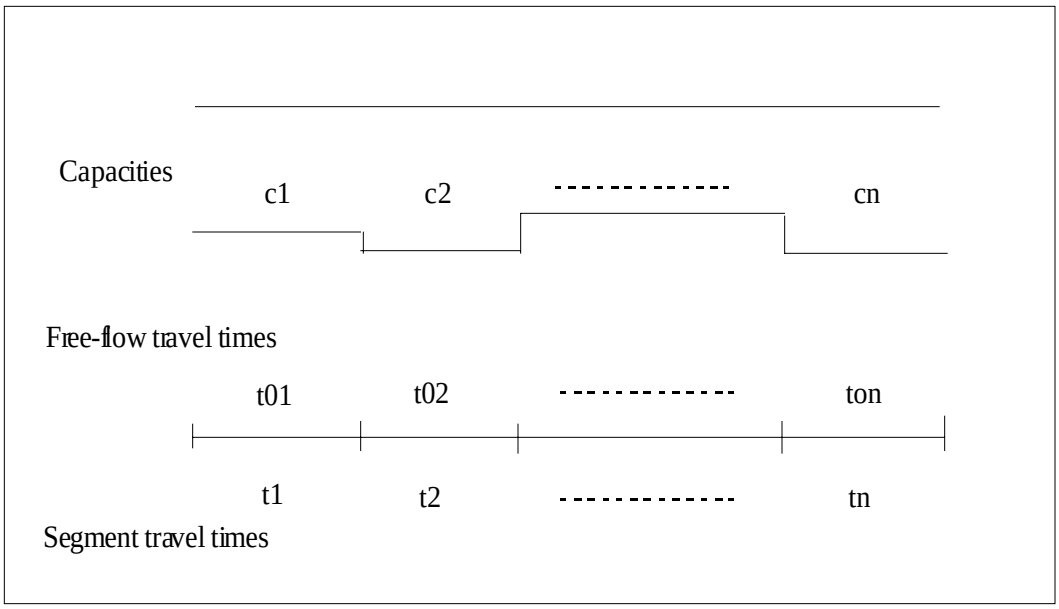

Figure 13: A Directed Network Link with Several Link Segments

where

$T_0 = t_{01} + t_{02} + \ldots + t_{0n}$.

We can write

$$t_{01} + t_{02} + \ldots + t_{0n} + 0.15v^4\left(\frac{t_{01}}{c_1^4} + \frac{t_{02}}{c_2^4} + \ldots + \frac{t_{0n}}{c_n^4}\right) = T_0 + 0.15T_0 \times v^4\left(\frac{1}{C^4}\right). \quad (57)$$

Since $T_0 = t_{01} + t_{02} + \ldots + t_{0n}$, equation (57) becomes

$$\frac{t_{01}}{c_1^4} + \frac{t_{02}}{c_2^4} + \ldots + \frac{t_{0n}}{c_n^4} = \frac{T_0}{C^4}. \quad (58)$$

The representative capacity (C) for the link is

$$C = \sqrt[4]{\frac{T_0}{\left(\frac{t_{01}}{c_1^4} + \frac{t_{02}}{c_2^4} + \ldots + \frac{t_{0n}}{c_n^4}\right)}}. \quad (59)$$

6-5-2. The Comparison between the Four Link Capacity Methods

The performance of the four capacity computing methods can be evaluated by using an example network link with four link segments. The example link is shown in Figure 14. The free-flow travel speed is assumed to be 75 mph (0.8 min/mile) through the entire link.

Two test cases are considered to evaluate the performance of the four capacity computing methods in predicting the actual total link travel time. The first test case assumes 3,000 vph (vehicles per hour) as the link volume. The second test case assumes

5,500 vph as the link volume. The actual link travel time is computed by using the link segment capacity (LSC) method. The actual travel time of the first test case is

$$T = 8.02 + 3.23 + 1.68 + 4.89 = 17.82 \text{ (min)}. \quad (60)$$

The link capacity using the LLWAC method becomes

$$C = (10*8000 + 4*6000 + 2*4000 + 6*5000) / 22$$
$$= 6455 \text{ (vph)}. \quad (61)$$

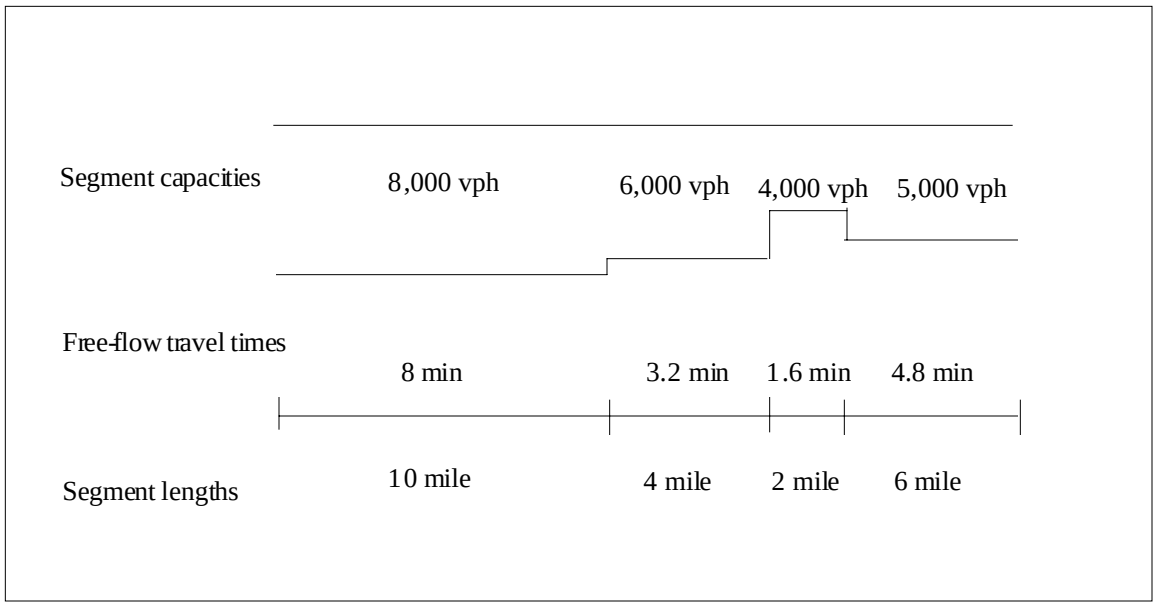

Figure 14: A Directional Link with Four Link Segments

Applying the LLWAC link capacity to the BPR function, the total link travel time is

$$T = 17.6 * \left[1 + 0.15\left(\frac{3000}{6455}\right)^4\right]$$

$$= 17.72 \text{ (min)}. \tag{62}$$

The minimum segment capacity among the four link segments is 4,000 vph. Applying the minimum capacity to the BPR function, we get

$$T = 17.6 * \left[1 + 0.15\left(\frac{3000}{4000}\right)^4\right]$$

$$= 18.44 \text{ (min)}. \tag{63}$$

The equivalent capacity method first computes the link capacity as

$$\frac{1}{C^4} = \frac{\frac{8}{8000^4} + \frac{3.2}{6000^4} + \frac{1.6}{4000^4} + \frac{4.8}{5000^4}}{17.6}$$

$$= \frac{0.018352261 \times 1000^{-4}}{17.6}. \tag{64}$$

Applying this equivalent link capacity to the BPR function, the total link travel time is

$$T = 17.6 + 0.15 \times (3000)^4 \times 0.018352261 \times 1000^{-4}$$

$$= 17.6 + 0.22$$

$$= 17.82 \text{ (min)}. \quad (65)$$

The results from the first test case are verified by the second test case. The actual link travel time is computed as 20.12 minutes by using the LSC method. The LLWAC method estimates the total travel time as 18.99 minutes. The minimum capacity method estimates the total travel time as 27.04 minutes. The EC method provides 20.12 minutes which is identical to the actual travel time. The performance of three capacity computing methods is shown in Table 15.

TABLE 15: The Comparison of Link Travel Times by Three Link Capacity Methods

Test Case	Volume = 3000	Volume = 5500	Comments
Actual Travel Times*	17.82	20.12	NA
LLWAC Method	17.72	18.99	underestimate
MC Method	18.44	27.04	overestimate
EC Method	17.82	20.12	same as actual

* The actual link travel times are computed by using the LSC method.

The results from the application of the three capacity computing methods to a network link with four link segments demonstrate that the EC method provides the actual link travel time. The LLWAC method underestimates the actual link travel time. In contrast, the MC method overestimates the actual link travel time. Thus, this research applies the EC method for computing representative link capacities for the aggregated Los Angeles network links. The representative link capacities for 292 links of the aggregated Los Angeles highway network are shown in the last column of Appendix 8.

6-6. Origin-Destination Trip Matrix

6-6-1. Background

This section intends to generate an origin-destination trip matrix for the aggregated Los Angeles highway network. There are two data sources in generating an origin-destination trip matrix for the Los Angeles network: Caltrans' O-D survey data and SCAG's O-D survey data. Caltrans sponsored a California State O-D survey in 1991. Caltrans' O-D survey data includes useful information such as the number of trucks and the number of vehicles taking freeways. However, the size of Caltrans' survey data is much smaller than that of SCAG's data. Only 3,000 households were surveyed for the Los Angeles region in the case of Caltrans' O-D survey data.

Southern California Association of Governments (SCAG) contracted with the Applied Management and Planning Group in April, 1991 to conduct an origin-destination survey

from 15,700 households in the Los Angeles region. The survey area included five counties of the Los Angeles region: Los Angeles, Orange, Riverside, San Bernardino, and Ventura Counties. Travel information was collected by a one-day, activity-focused diary from all persons aged five or older of sampled households via a Computer-Assisted Telephone Interviewing (CATI) system. Only weekday travel information was surveyed. All five weekdays were surveyed evenly to exclude daily bias. The survey data was collected from 16,086 households, slightly greater number of households than the planned.

6-6-2. Creating Origin-Destination Trip Matrices

The aggregated Los Angeles highway network contains 105 traffic analysis zones. Our origin-destination (O-D) trip matrices are of dimension 105*105. Four different types of hourly origin-destination trip matrices are created from SCAG's 1991 Southern California Origin-Destination Survey data for the aggregated network: (1) automobile/van/pick-up truck O-D trip matrices, (2) express bus O-D trip matrices, (3) school bus O-D trip matrices, and (4) taxi/shuttle bus O-D trip matrices.

The 5-6 PM O-D trip matrices are selected as peak-hour O-D trip matrices after observing the hourly distribution of total trips of the four O-D trip matrices. The hourly distribution of automobile trips including trips with incomplete information is shown in Figure 15. The hourly distribution of automobile trips with complete information is

shown in Figure 16.[7] The peak-hour automobile O-D trip matrix, the express bus O-D trip matrix, the school bus O-D trip matrix, and the taxi/shuttle bus O-D trip matrix are shown in Appendices 9, 10, 11, and 12, respectively. A listing of the SAS program used to aggregate SCAG's data files, and to generate the peak-hour O-D trip matrices is reported in Appendix 13.

All trips in the peak-hour O-D trip matrices are converted to passenger cars unit (PCU). The peak-hour automobile O-D trip matrix represents the number of passenger cars traveling between zones because only drivers are selected to create the automobile O-D trip matrix. Other peak-hour O-D trip matrices include passenger flows. According to Hu and Young (1993), the average vehicle occupancy of passenger van is 2.55. Thus, the peak-hour taxi/shuttle bus O-D trip matrix is converted to passenger cars by dividing values of all elements by 1.55, the average number of passengers per vehicle. The peak-hour school bus O-D trip matrix is disregarded because it comprises only a small number of passenger trips.

The average number of passengers per vehicle is not available in the case of express bus trips. Thus, the express bus O-D trip matrix is generated by observing routes and schedules of commuter express buses. The route and schedule information was provided

[7] Some trips have neither trip origin information nor trip destination information. The hourly distribution in Figure 15 includes these trips, whereas the hourly distribution in Figure 16 contains trips with both origin and destination information.

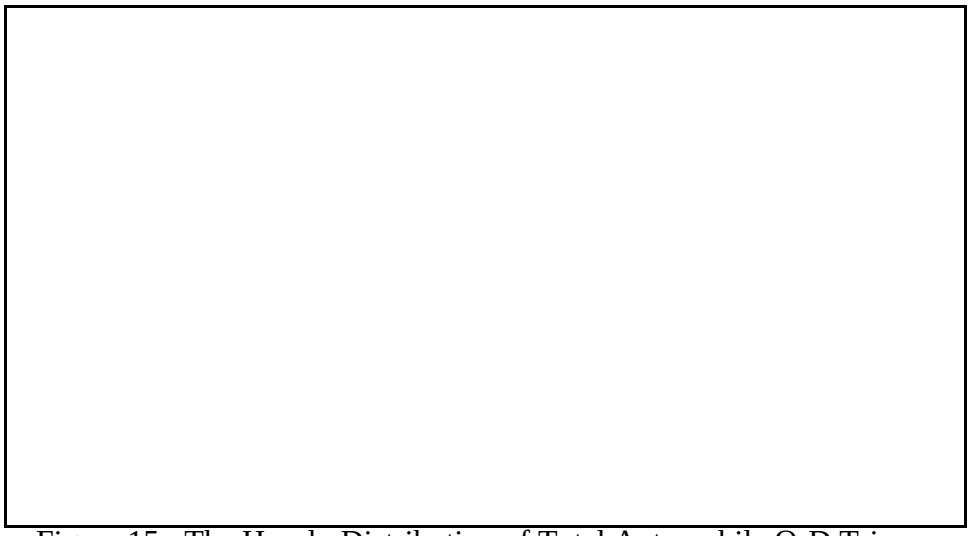

Figure 15: The Hourly Distribution of Total Automobile O-D Trips with Incomplete Origin and Destination Zone Information in 105 Zone Network

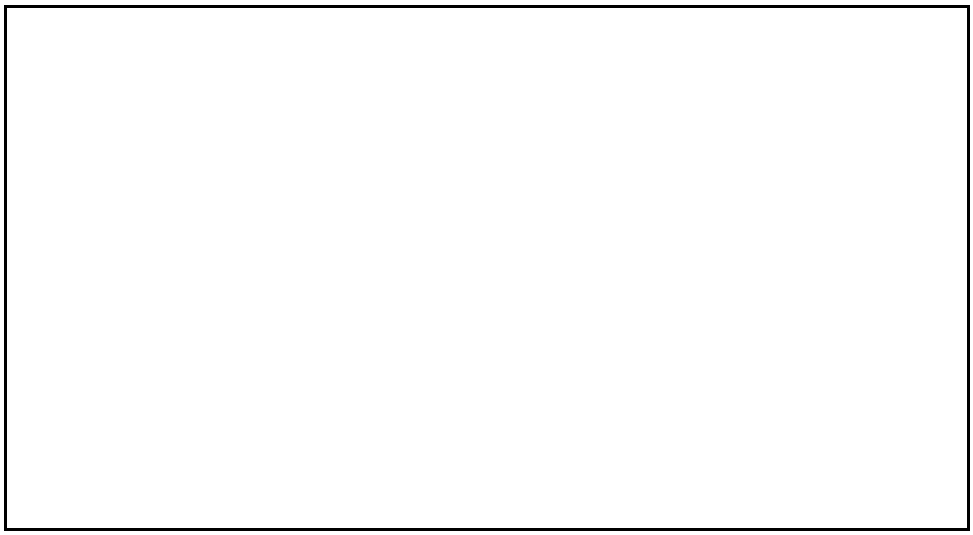

Figure 16: The Hourly Distribution of Total Automobile O-D Trips with Complete Origin and Destination Zone Information in 105 Zone Network

by the Los Angeles Department of Transportation (LADOT). The number of express buses is converted to passenger cars by multiplying values of all elements by 1.5. The value of 1.5 is the passenger-car equivalent number for buses provided by the 1985 Highway Capacity Manual. The three peak-hour O-D trip matrices are combined to an O-D trip matrix for the aggregated Los Angeles highway network. Values of diagonal elements of the combined O-D trip matrix become zero because intrazonal flows are assumed to be zero. Appendices 14 and 15 show the converted express bus O-D trip matrix and the combined O-D trip matrix, respectively.

6-7. Observed Traffic Volume

6-7-1. Traffic Counting Data

Traffic counts are a major source for traffic volume data. California Department of Transportation (Caltrans) continuously collects traffic counts at designated traffic count stations installed on freeways and state highways. Caltrans' STATEWIDE traffic count program provides two types of traffic volumes computed from traffic count data: hourly-based traffic volumes and monthly average daily traffic volumes. Our study is based on the monthly average daily traffic volumes to exclude hourly and daily variations from traffic counts. Hourly-based traffic volumes are also considered to compute K-factors (ratios between peak-hour traffic volumes and daily traffic volumes) used for expanding

simulated peak-hour traffic flows to daily traffic flows as well as for computing peak-hour traffic volumes from monthly average daily traffic volumes.

Monthly average daily traffic volumes from October 1986 to December 1994 were obtained from Caltrans District 7. Variational features of a time series traffic volumes such as trend or seasonality can be identified by plotting the traffic volumes against time. Thus, monthly average daily traffic volumes from October 1986 to June 1993 are standardized by setting the column of September 1992 to 100, and then by converting other months' traffic volumes relative to the September 1992's column.[8] Figure 17 summarizes the mean, standard deviation, minimum value, and maximum value of the standardized values derived from the monthly average daily traffic volumes between October 1986 and June 1993. The figure shows a clear feature of seasonality and trend embedded in the traffic volumes from October 1986 to June 1993.

Five sets of traffic volumes are structured based on the five empirical link-failure system states identified in section 6-3. They are monthly average daily traffic volumes collected in July of 1993, in November of 1993, in February of 1994, in May of 1994, and in August of 1994. We assumed that the five sets of traffic volumes are associated

---

[8] The standardized values are good indicators in presenting seasonal and trend variations of traffic volumes collected from different locations. We may use the total number of traffic volumes instead of the standardized values. Suppose that traffic volumes collected from a few links dominate the total number of traffic volumes of all links. Variations of the traffic volumes from the small number of major links will dominate the variations of the total traffic volumes. The use of standardized values prevents this problem. All links equally influence seasonal and trend variations of the mean standardized value. This approach is applicable, even though the number of observations (traffic volumes) varies from month to month.

The number of observations varied throughout the study months from October 1986 to June 1993. The month of September 1992 had the highest number of observations. Thus, the month of September 1992 is selected as the standard month.

with the five sets of network configurations due to the opening of the Glen Anderson Freeway and the 1994 Northridge Earthquake.

Missing data appeared in several links. Traffic volumes for the links with missing data are estimated from adjacent months of the same year or from the same month of different years.[9] They are used to complete the five sets of traffic volumes. Of 292 network links, 16 links had no traffic volume information available except for the month of November 1993. Thus, traffic volumes collected in November 1993 are directly used as four other sets of traffic volumes.

[9] Seasonal and trend indices estimated in the following sections are used to adjust traffic volumes collected from different months or years.

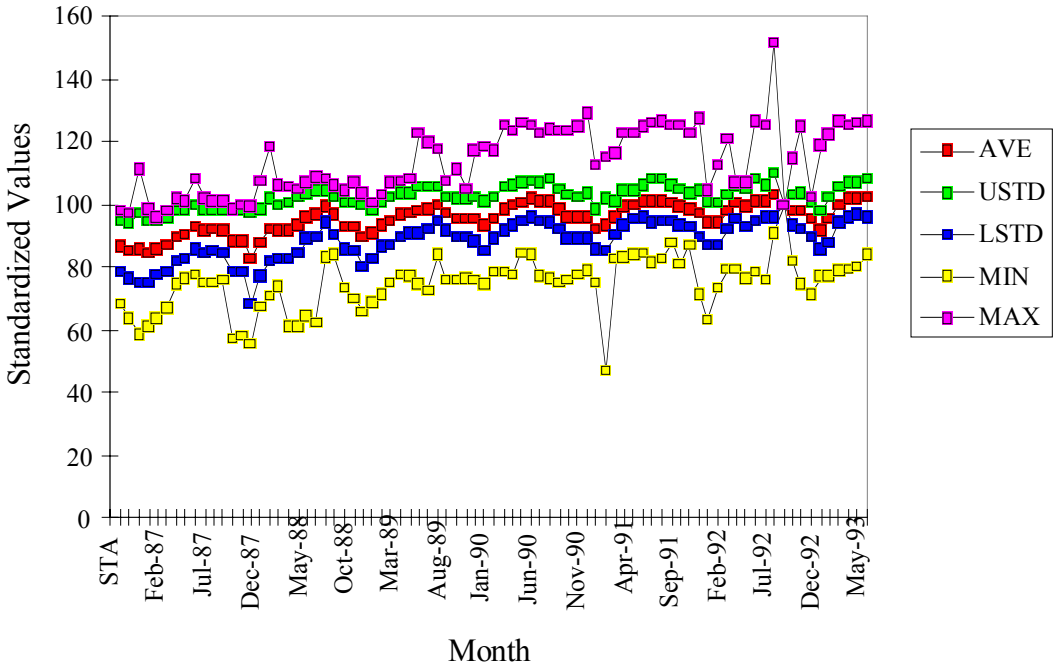

Figure 17: Average, Upper-Limit, Lower-Limit, Maximum, and Minimum Values of Standardized (100) Monthly Average Daily Traffic Volume Data from October 1986 to June 1993

6-7-2. Data Modification

A time series data is a set of sequentially collected observations in time. A time series data contains trend, seasonality, outliers, irregular components, and discontinuities.

Traffic counts continuously collected at automatic traffic recorder stations are the typical time series data. Traffic volumes are representative values of traffic counts. Thus, the traffic volumes possess the time series characteristic of the traffic counts.

Traffic volumes contain trend, seasonal variation, monthly variation, daily variation, hourly variation, and sub-hourly variation. This research is based on peak-hour weekday traffic flow analyses. Thus, the sub-hourly variation is not considered. This research computes the average daily link volumes of a standard month,[10] the average weekday link volumes of the month, and the average hourly link volumes of the month.

These three average link volumes are assumed to exclude the monthly variation, daily variation, and hourly variation. The ratios between the average daily link volumes and the average weekday link volumes of the standard month are used to convert the average daily link volumes of any month to the average weekday link volumes of the month. The ratios between the average weekday link volumes and the average hourly link volumes of the standard month are used to convert the average weekday link volumes of any month to the average hourly link volumes of the month.

6-7-3. Seasonal Adjustment

[10] This research selects November 1993 as the standard month. Empirical studies for traffic volumes have shown that November 1993 daily link volumes are close to average annual daily traffic (AADT) volumes. The Los Angeles highway system was under the perfect condition in November, 1993 because the Glen Anderson Freeway was opened on October 14, 1993, and the Northridge earthquake struck the LA highway network on January 17, 1994.

Seasonality is a cyclical pattern that regularly recurs over a 12-month period. The seasonal index is a measure of how much the value of the variable in a particular period deviates from the average of the variable over the 12-month period (Johnson et al., 1987). Seasonality provides information about regularity in the series that can aid in making a forecast (Pindyck and Rubinfeld, 1991). Seasonal adjustment is an important process when traffic volumes significantly fluctuate on a monthly. Strong seasonal fluctuations in link volumes may reflect the dynamic change of social and economic activities of the region (TRB, 1985).

Identifying seasonal variations from observed link volumes has been the subject of interest to traffic engineers. A variety of seasonal adjustment approaches has been introduced and evaluated. Two seasonal adjustment methods become dominant: a regression analysis method introducing seasonal dummy variables and an *ad hoc* structure of decomposition model.

The regression analysis method uses dummy variables to estimate seasonal indices from Ordinary Least Squares (OLS) coefficients. The use of seasonal dummy variables along with the other regressors eliminates seasonal influences on the intercept term (Kennedy, 1992). The basic seasonal model is

$$y_t = b_0 + b_1 M_1 + b_2 M_2 + \ldots + b_{11} M_{11} + e \qquad (66)$$

where

y_t = *a time-series traffic volume collected at a traffic count station,*
b_0 = *the constant term for December observations,*
b_i = *the amount that traffic volume deviates from the December observations,*
M_i = *the* i^{th} *month. 1 if the season is the* i^{th} *month. Otherwise, 0,*
e = *the error term.*

The dummy variable for December observations is omitted to avoid the dummy variable trap. This method has been studies by Fuller (1976), Wonnacott and Wonnacott (1979), Johnston (1984), Johnson et al. (1987), and Ramanathan (1992).

Alternatively, the decomposition method may be used to compute seasonal indices. The decomposition method is the *ad hoc* method derived from moving average techniques (Pindyck and Rubinfeld, 1991). The *ad hoc* method is based on the idea that the variations of a time series link volume can be represented as the product of the following four components:

$$y_t = L \times S \times C \times I \tag{67}$$

where

y_t = *directed time series traffic volume,*
L = *value of the long-term secular trend in series,*
S = *value of seasonal component,*
C = *(long-term) cyclical component, and*
I = *irregular component.*

The decomposition method isolates each of the components, and attempts to measure both the seasonal and the trend variations in the series. The decomposition method is described by Pindyck and Rubinfeld (1991)

An *ad hoc* smoothing model is used to remove the combined seasonal and irregular components $S \times I$ from the original series y_t. The smoothing model computes the 12-month average $y_t^{\sim}$ as an estimate of $L \times C$:

$$y_t^{\sim} = \boxed{} \tag{68}$$

The value $y_t^{\sim}$ is relatively free of seasonal and irregular fluctuations.

The original data is now divided by the 12-month average $y_t^{\sim}$ to generate an estimate of the combined seasonal and irregular components $S \times I$:

$$\boxed{} = z_t \tag{69}$$

The irregular component I is eliminated by computing the average values of $S \times I$ corresponding to the same month. Suppose that there are 48 months of traffic volume data. The average values of $S \times I$ for the same month are computed as follows:

$$\text{average value } z_1^{\sim} = \boxed{} \tag{70}$$

$$\text{average value } z_2^{\sim} = \boxed{} \tag{71}$$

. . . . . .

$$\text{average value } z_{12}^{\sim} = \boxed{} \tag{72}$$

The irregular fluctuations are smoothed out by averaging the seasonal-irregular percentages z_t for each month.

The twelve average values $z_1^{\sim}, \ldots, z_{12}^{\sim}$ are the estimates of the seasonal indices. The sum (T) of the twelve average values $z_1^{\sim}, \ldots, z_{12}^{\sim}$ is usually close to 12. If the sum of the twelve averages is not close to 12, the average values should be adjusted as follows:

$$\text{adjusted average } z_1^{\wedge} = \boxed{} \qquad (73)$$

$$\text{adjusted average } z_2^{\wedge} = \boxed{} \qquad (74)$$

. . . . . .

$$\text{adjusted average } z_{12}^{\wedge} = \boxed{} \qquad (75)$$

These twelve adjusted average values $z_1^{\wedge}$ ... $z_{12}^{\wedge}$ are the seasonal indices. The original series y_t can be deseasonalized by dividing each value in the series by its corresponding seasonal index. The *ad hoc* smoothing model has been developed by Fuller (1976), Wonnacott and Wonnacott (1979), Chatfield (1989), Granger (1989), Pindyck and Rubinfeld (1991), and Ramanathan (1992).

We apply the *ad hoc* smoothing model to compute the seasonal indices from monthly average daily traffic volumes of 138 traffic count stations from October 1986 to June 1993. The seasonal indices are reported in Appendix 16. The SAS code for the *ad hoc* smoothing model is presented in Appendix 17.

6-7-4. Trend Analysis

Identifying trends in time series traffic volumes is another important task. Trends may be linear, growing by a constant absolute amount over time, in exponential form growing by at a constant rate over time, or in a more complicated nonlinear form.

The regression analysis approach is the dominant method in trend analysis of link volumes. Johnson et al. (1987) and Lardaro (1993) introduced two types of linear trend models using an OLS method: simple regression models, and multiple regression models. Kennedy (1992) explained two more sophisticated methods: autoregressive integrated model average (ARIMA) models and the structural econometric time series approach (SEMTSA).

Granger (1989) classified trend models into six groups in terms of functional forms: the straight line, the exponential curve, the parabolic curve, the modified exponential curve, the Gompertz curve, and the logistic curve. Pindyck and Rubinfeld (1991) and Ramanathan (1992) categorized them into six groups: linear trend models, exponential growth models, autoregressive trend models, logarithmic autoregressive trend models, quadratic trend models, and logistic growth models. Faghri and Chakroborty (1994) applied the simple linear regression model to examine the trend of link volumes. Benjamin (1986) introduced logistic models in trend analysis.

The link volume trend is investigated after the observed link volumes are deseasonalized by the *ad hoc* smoothing model. The time series deseasonalized link volumes are assumed to have a linear form of trend, growing by a constant absolute amount over time. A simple linear regression model is applied to predict the long-term

growth pattern of the deseasonalized link volumes in each link. The first month in the time series is assigned to value 1. We assign value one to the month of October 1986. The value is increased by 1 for each month until the month of June 1993. This time variable is used as an explanatory variable in the simple regression model for each link. Regression coefficients are interpreted as the trends of the deseasonalized link volumes. Appendix 18 shows parameters representing trend of deseasonalized link traffic volumes.

6-7-5. K-factors and AWTV/ADTV Ratio Study

Another important task for traffic demand analysis is to investigate the distribution pattern of hourly-based traffic volumes. Identifying peak-hours from traffic volumes is important in traffic flow analyses regarding a facility design, traffic operation, or traffic control. Peak-hours represent the most critical period for traffic flow operations. Rural transportation networks often show no pronounced peak-hours. In contrast, urban transportation networks suffer from traffic demands exceeding capacity during morning and evening peak hours. Peak-hours are recurrent in most urban transportation networks because the hourly distribution of a daily traffic demand in a network does not vary significantly. Urban peak-hour traffic volumes are often directional.

Representative hourly distributions of daily traffic volumes for the aggregated Los Angeles highway links are computed by using hourly-based traffic volumes of thirty days in November 1993. The representative hourly distributions of daily traffic volumes are computed by averaging hourly-based traffic volumes collected for at least fourteen days.

If the number of observations (hourly-based traffic volumes) in November 1993 is less than fourteen, hourly-based traffic volumes collected in October 1993 or in December 1993 are added to the hourly-based traffic volumes of November 1993. The sum of 282 representative hourly-based traffic volumes is computed for all days including weekdays and weekends.[11] The sum is also computed for weekdays only. Figures 18 and 19 show the average values of 282 representative hourly-based traffic volumes for all days and weekdays, respectively.

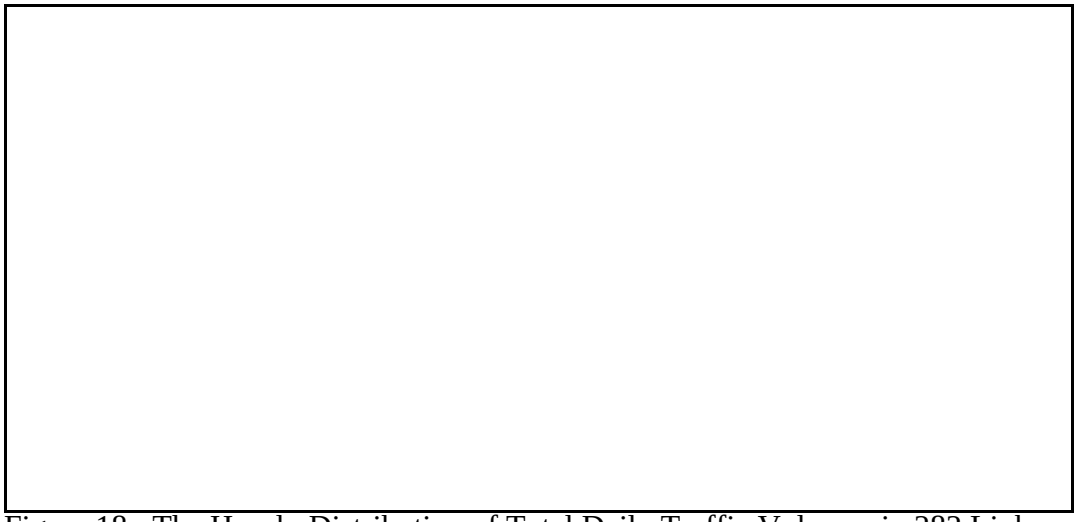

Figure 18: The Hourly Distribution of Total Daily Traffic Volumes in 282 Links (Weekdays & Weekends, Missing Data in 10 Links)

[11] The aggregated Los Angeles highway network includes 292 directed links. The hourly-based traffic volumes were not available in ten links. This research computes the representative hourly-based traffic volumes for 282 links.

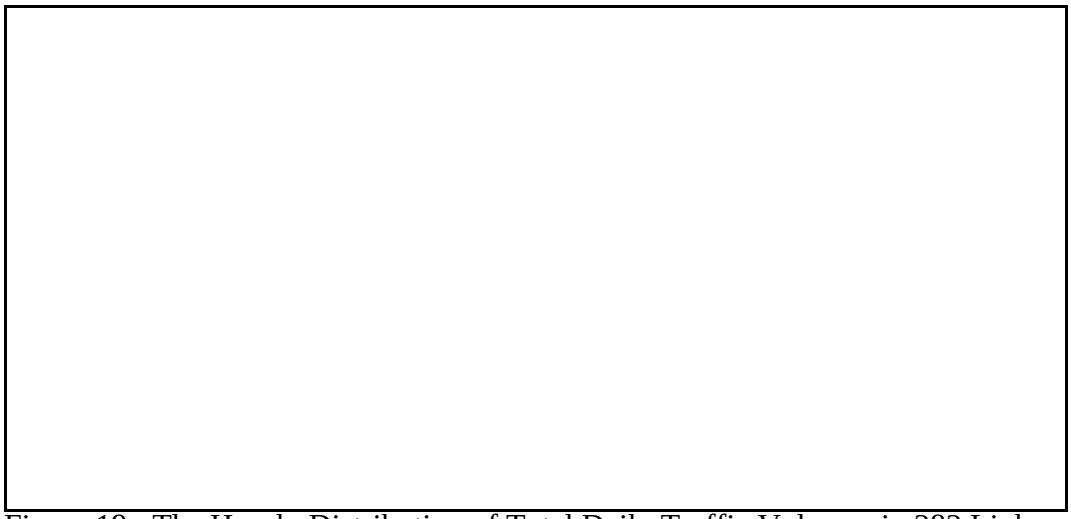

Figure 19: The Hourly Distribution of Total Daily Traffic Volumes in 282 Links (Weekdays Only, Missing Data in 10 Links)

Our research is based on peak-hour weekday traffic flow analyses. A peak-hour origin-destination trip matrix derived from SCAG's 1991 origin-destination survey data is based on weekday survey data. Caltrans' monthly average daily traffic volumes are based on weekday and weekend traffic volumes. Thus, ratios between average weekday traffic volumes (AWTV) and average daily traffic volumes (ADTV) in November 1993 are computed to convert the average daily link volumes to the average weekday traffic volumes for the five sets of empirical link-failure system states. Average daily traffic volumes, average weekday traffic volumes, and AWTV/ADTV ratios are shown in Appendix 19.

K-factor is defined as the proportion of average annual daily traffic (AADT) volume occurring in the peak hour. The distribution figures of hourly-based traffic volumes in the aggregated Los Angeles highway network demonstrate that network links of the Los

Angeles highway network experience heavy traffic congestion. The peak period persists for at least 12 hours. Traffic volumes build rapidly in the early morning, remain near capacity throughout the day, then decline after evening peak hours. The hourly distribution figure of weekday traffic volumes indicates the period of 5-6 P.M. as the peak-hour. Peak-hour (5-6 P.M.) traffic volumes and K-factors are also shown in Appendix 19.

7. Empirical and Simulation Modeling the Los Angeles Urban System

7-1. Application of the LINKOD PLUS Model - Adjustments between SCAG's O-D Trip Matrix and Caltrans' Traffic Volumes

Travel demand is defined as activities of moving from one zone to another in a transportation network during a given time period. The travel demand is usually structured in the form of a two dimensional matrix called an origin-destination trip matrix. A combined peak-hour origin-destination trip matrix of dimension 105*105 is generated based on the SCAG's 1991 Southern California Origin-Destination Survey data and LADOT's commuting express bus schedules in section 6-6-2.

Our traffic flow analyses for empirical link-failure system states are based on the five sets of traffic volumes collected from July 1993 to August 1994. Our traffic flow analyses for synthetic post-earthquake system states require traffic flow simulations using three Los Angeles highway system data sets including the Los Angeles origin-destination trip matrix. We found that traffic volumes in November 1993 represent traffic volumes under perfect condition of the aggregated Los Angeles highway network. However, it is not certain that the combined Los Angeles O-D trip matrix based on the 1991 O-D survey data is consistent with the November 1993 traffic volumes. Consequently, an O-D trip estimation method is required to reconcile the combined Los Angeles O-D trip matrix with the November 1993 traffic volumes.

The LINKOD PLUS model is one of the O-D trip estimation methods estimating an origin-destination trip matrix from link volumes given network system data such as free-flow link travel times and link capacities. The LINKOD PLUS model requires an initial O-D trip matrix as input data. The model produces an estimated O-D trip matrix and simulated link traffic flows consistent with the adjusted O-D trip matrix.

The combined peak-hour Los Angeles O-D trip matrix is referred to the initial O-D trip matrix for the LINKOD PLUS model. Adjusted peak-hour weekday traffic volumes in November 1993 are used as link volumes for the perfect Los Angeles highway network. The number of 1,000 iterations is selected to adjust the initial Los Angeles O-D trip matrix. The performance of the LINKOD PLUS model is evaluated by two performance measures: (1) the sum of absolute link volume errors, and (2) the percent volume errors between November 1993 link volumes and simulated link flows provided by the LINKOD PLUS model.

The results from the application of the LINKOD PLUS model to the aggregated Los Angeles highway network indicate a reduction of total trips in the Los Angeles O-D trip matrix. Total trips decreased from 902,441 to 663,730 trips, resulting in around 26.5 percent trip reduction from the total trips of the initial O-D trip matrix. The reduced trips may be interpreted as trips taking arterials and local streets.

The sum of absolute volume errors between link volumes and simulated link flows is 32,660 PCU/hr. The percent volume error is 2.36 percent. The absolute volume errors

between link volumes and simulated link flows can be further reduced if transportation system data such as link capacities and/or free-flow link travel times are modified. This modification for the transportation system data may result in the development of a peak-hour O-D trip matrix that is consistent with peak-hour weekday link volumes. Transportation system data for 31 links among 292 links are modified iteratively to minimize the sum of absolute volume errors.

The results from the application of the LINKOD PLUS model using modified transportation system data reduced the sum of absolute volume errors to 2,070 PCU/hr. The difference between link volumes and simulated link flows in all links becomes less than 100 PCU/hr. Total trips for the Los Angeles O-D trip matrix further decreased to 629,330 trips, resulting in 30.26 percent trip reduction from the total trips of the initial O-D trip matrix. The final Los Angeles O-D trip matrix is shown in Appendix 20. Transportation system data sets after the modification are shown in Appendix 21. Figure 20 shows the difference between adjusted November 1993 traffic volumes and simulated traffic flows consistent with the final O-D trip matrix. The final Los Angeles O-D trip matrix will be used for simulating traffic flows in the case of synthetic post-earthquake system states in section 7-3.

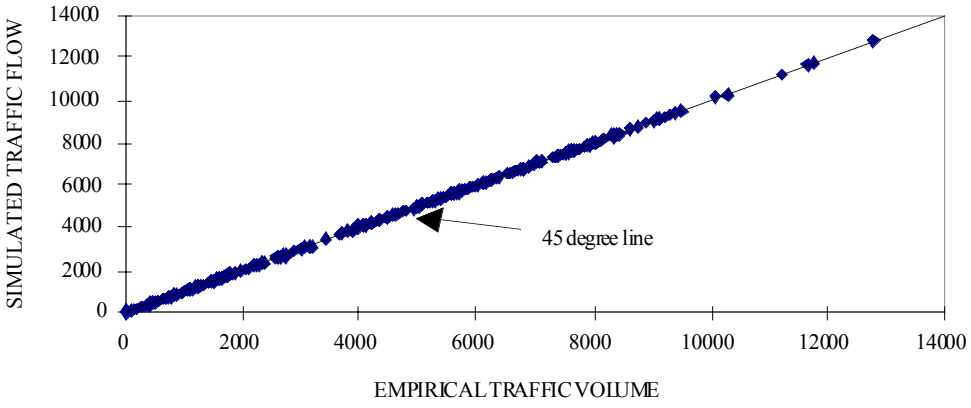

Figure 20: Simulated vs. Empirical Link Volumes in 105 Zone Network (Using the LINKOD PLUS Model, Iteration Number: 1000, 292 Links, r= 0.9999784, Target State: November 1993)

7-2. Application of the Associative Memory Approach - Empirical Flows

7-2-1. Application of Associative Memory Models

Modeling the behavior of drivers in roadways is a highly complex process. Transportation network equilibrium models are widely used approaches in modeling travel behaviors of drivers in transportation networks. Transportation planners and traffic engineers have developed a variety of transportation network equilibrium models to predict system wide changes of traffic flows with given changes in network configurations or network environments. As an alternative to the conventional network equilibrium models, we apply the simplified transportation network analysis (TNA) procedure to estimate empirical link volumes in the aggregated Los Angeles highway network.

The aggregated Los Angeles transportation highway system contains 105 traffic analysis zones and 292 network links. As described in section 6-7-1, observed link volumes are not available from Caltrans District 7 at sixteen links for four link-failure system states except empirical system state 2. Thus, link traffic volumes collected in November 1993 are used as traffic volumes for the remaining four empirical system states. Network configurations for the five empirical system states in the case of 292 links were shown in Appendix 6. Network configurations for the five empirical system states in the case of 276 links are shown in Appendix 22. They are used as stimulus vectors.

Response vectors of associative memory models are link volumes associated with the network configurations. The link volumes are peak-hour weekday traffic volumes derived from Caltrans' traffic count data. They are adjusted by extracting seasonal and trend variations from observed link volumes.

Scenario A: Five Empirical Link-Failure System States with 292 Links

This exercise uses each of the five empirical link-failure system states as the test system state in rotation. The other four empirical system states are used to create associative memory matrices. Associative memory models are applied to map network configurations of the four training system states to associated link volumes. The RMSE results of SAM, RAM, and MAM in estimates are shown in Table 16.

Table 16: RMSEs of SAM, RAM, and MAM in 105 Zone Network with Five Empirical System States (292 Links)

		MAM									SAM	RAM
α		0.1	0.2	0.3	0.4	0.5	0.6	0.7	0.8	0.9	SAM	RAM
State 1	Training	501.7	410	340.7	283.2	232.4	185.1	139.6	94.32	48.15	2.18E-11	4.24E-11
	Test	1022	979.8	955.6	940.3	930.1	923.3	919	916.9	916.8	918.94	910.89
State 2	Training	506.2	390.1	312	251.3	200.4	155.3	114	75.03	37.28	2.46E-11	4.56E-11
	Test	683.4	660.1	651.3	649.2	651.2	655.9	662.7	671.1	681	692.38	698.28
State 3	Training	432.2	344	284.6	237.6	196.3	157.8	120	81.75	42.06	2.24E-11	4.46E-11
	Test	1127	1111	1100	1093	1089	1086	1084	1083	1084	1085.8	1177.6
State 4	Training	523.3	400.2	318.4	256	204.3	158.2	116.9	77.12	38.41	2.43E-11	4.26E-11
	Test	556.9	550.7	552.9	556.8	561.2	566	571.3	577.2	583.9	591.53	553.91
State 5	Training	501.7	383.2	303.7	241.9	190.1	144.9	104.2	66.95	32.4	2.76E-11	4.49E-11
	Test	677.8	655.3	643	636.1	632.4	631.1	631.3	632.6	634.7	637.35	737.71

Different associative memory models are applied. However, the RMSE results from empirical link volume estimation do not vary significantly across the associative memory models in the case of test states. The training results of SAM and RAM are very good. But, this is expected because the associative memory matrices are created based on the information from training system states. The RMSE results for test system states demonstrate that empirical link-failure system state 4 provides the lowest test case RMSE. Empirical system state 3 provides the highest test case RMSE, describing the worst estimate of link volumes.

Figures in Appendix 23 show the scatter plots and correlation coefficients for each empirical link-failure system state used as the test case. Each coordinate in the figures represents the comparison between the link volumes derived from Caltrans' traffic count

data and the estimated link flows provided by an associative memory. Coordinates located close to the 45 degree line represent more accurate estimates.

Scenario B: Five Empirical Link-Failure System States with 276 Links

Good link volume estimation may result in using link volumes of empirical system state 2 to other four system states in the sixteen links whose observed volumes were not available from Caltrans. This exercise uses network configurations and their associated link volumes for only 276 links to evaluate the influence of identical link volumes to the performance of associative memory models.

Each of the five empirical link-failure system states is used as the test system state in rotation. Network configurations and their associated link volumes of the remaining four system states are used to compute associative memory matrices in the case of 276 links. The RMSE results of SAM, RAM, and MAM in estimates are presented in Table 17. Figures in Appendix 24 show the scatter plots and correlation coefficients for each empirical link-failure system state used as the test case.

Table 17: RMSEs of SAM, RAM, and MAM in 105 Zone Network with Five Empirical System States (276 Links)

		MAM									SAM	RAM
	α	0.1	0.2	0.3	0.4	0.5	0.6	0.7	0.8	0.9	SAM	RAM
State 1	Training	516.5	422.1	350.7	291.5	239.2	190.5	143.7	97.06	49.55	2.16E-11	4.36E-11
	Test	1051	1008	982.8	967.1	956.2	949.6	945.3	943.2	943.2	945.46	936.91
State 2	Training	521	401.6	321.2	258.8	206.3	159.9	117.4	77.24	38.38	2.18E-11	4.07E-11
	Test	703	678.9	669.7	667.5	669.4	674.2	681.1	689.7	699.8	711.45	718.08
State 3	Training	444.6	353.9	292.8	244.4	202	162.3	123.5	84.13	43.28	2.26E-11	3.92E-11

	Test	1160	1144	1133	1126	1121	1118	1116	1116	1116	1118	1212.5
State 4	Training	538.7	412.1	327.9	263.7	210.4	163.5	120.4	79.41	39.55	2.11E-11	4.28E-11
	Test	573.1	566.6	568.8	572.7	577.3	582.2	587.6	593.7	600.6	608.44	569.63
State 5	Training	516.4	394.6	312.8	249.2	195.8	149.2	107.3	68.97	33.37	2.14E-11	3.97E-11
	Test	697.7	674.3	661.6	654.3	650.6	649.1	649.3	650.7	652.8	655.56	758.82

The RMSE results in the case of 276 links do not significantly differ from those in the case of 292 links. The RMSEs become slightly higher. The RMSE results of estimated link volumes do not significantly vary across the associative memory models in the case of test cases. The same empirical link-failure system states provide the lowest test case RMSE (empirical system state 4) and the highest test case RMSE (empirical system state 3).

7-2-2. The Comparison between the Static User Equilibrium Model and Associative Memory Models

The results from traffic flow analyses in section 7-2-1 indicate that traffic volumes of a link-failure system state can be estimated from the information of empirical link-failure system states by applying associative memory models. Alternatively, link volumes of an empirical link-failure system state can be predicted by using conventional transportation network equilibrium models. This exercise compares associative memory models with a static network equilibrium model in terms of link volume estimation. The comparison is made against observed link volumes.

The static user equilibrium model is applied to simulate traffic flows with given defined network configurations of the same empirical link-failure system states except empirical system state 2. Empirical system state 2 represents the system state under the perfect transportation network condition. The peak-hour weekday O-D trip matrix was generated based on link volumes of empirical system state 2. Thus, the simulated traffic flows given the network configuration of empirical system state 2 would be very close to empirical link volumes.

Three transportation system data sets including link capacities, free-flow link travel times, and a peak-hour weekday Los Angeles O-D trip matrix are used to simulate traffic flows in the static user equilibrium model as system input data. The number of 200 iterations is selected to produce equilibrium traffic flows.

A comparison is made between link volumes derived from Caltrans' traffic counts and flow estimates provided by associative memory models as well as traffic flows simulated by the static user equilibrium models. The performance of the static user equilibrium model and associative memory models is evaluated by four measures of performance (MOP): (1) total volume errors between link volumes and estimated (or simulated) traffic flows, (2) mean volume errors, (3) correlation coefficients, and (4) scatter plots. The first three MOP results in the case of 292 links are shown in Table 18. Figures in Appendix 25 show the scatter plots and correlation coefficients between link volumes derived from

Caltrans' traffic counts and simulated traffic flows provided by the static user equilibrium model for each empirical link-failure system state.

Table 18: The Comparison Study of Estimating Equilibrium Traffic Volumes Using the User Equilibrium Model and Associative Memories Under Five Empirical System States (292 Links)

SYSTEM STATE 1 (JUL 93)	UE model (IT# 200)	SAM	RAM	MAM (α=0.9)
TOTAL VOLUME ERROR:	103732 PCU	102611 PCU	100185 PCU	101046 PCU
MEAN VOLUME ERROR:	7.83%	7.75%	7.57%	7.63%
CORRELATION COEFF:	0.973525	0.955433	0.955633	0.955572
SYSTEM STATE 2 (NOV 93)	UE model (IT# 200)	SAM	RAM	MAM (α=0.4)
TOTAL VOLUME ERROR:	NA	90363 PCU	89314 PCU	86622 PCU
MEAN VOLUME ERROR:	NA	6.80%	6.72%	6.52%
CORRELATION COEFF:	NA	0.972207	0.971809	0.975911
SYSTEM STATE 3 (FEB 94)	UE model (IT# 200)	SAM	RAM	MAM (α=0.8)
TOTAL VOLUME ERROR:	286926 PCU	114263 PCU	122279 PCU	115559 PCU
MEAN VOLUME ERROR:	22.96%	9.14%	9.78%	9.25%
CORRELATION COEFF:	0.88458	0.9385	0.925665	0.938848
SYSTEM STATE 4 (MAY 94)	UE model (IT# 200)	SAM	RAM	MAM (α=0.2)
TOTAL VOLUME ERROR:	210900 PCU	67641 PCU	65359 PCU	70322 PCU
MEAN VOLUME ERROR:	16.02%	5.14%	4.97%	5.34%
CORRELATION COEFF:	0.897719	0.980695	0.982828	0.983665
SYSTEM STATE 5 (AUG 94)	UE model (IT# 200)	SAM	RAM	MAM (α=0.6)
TOTAL VOLUME ERROR:	176418 PCU	82538 PCU	93870 PCU	83015 PCU
MEAN VOLUME ERROR:	13.29%	6.22%	7.07%	6.25%
CORRELATION COEFF:	0.930171	0.977077	0.969182	0.977673

The results from the comparison show that associative memory models provide better estimates of empirical link volumes than the static user equilibrium model. This is expected. The conventional user equilibrium model is constructed by mathematical formulations based on assumptions for travel behaviors of drivers. The conventional

approach may fail to capture behavioral characteristics of drivers in its functional forms. In contrast, the associative memory approach does not require the identification of the functional forms that link stimulus vectors (network configurations of link-failure system states) with response vectors (empirical link volumes). Thus, associative memory models may be more flexible in capturing the association between the network configurations and empirical link volumes.

There is no significant difference of estimation performance across the associative memory models. Associative memory estimates and traffic flows predicted by the static user equilibrium model covary very close to the empirical link volumes in the cases of empirical system states 1. This can be observed. The opening of the Glen Anderson Freeway (I-105) was scheduled. Drivers were informed about the opening of the freeway links. Consequently, the state of flow equilibrium can be easily obtained from the known change of the Los Angeles highway network.

On the other hand, traffic flows provided by the static user equilibrium model are significantly different from empirical link volumes in the case of empirical system state 3, whereas associative memory models still provide reliable flow estimates. Static user equilibrium outputs in the cases of empirical system state 4 and 5 become close to empirical link volumes. However, associative memory models still dominate the static user equilibrium model in the same cases in terms of link volume prediction. This is also expected. The outputs of the conventional network equilibrium model are based on the

constrained optimization framework and assumptions. The conventional model assumes that drivers change their travel behaviors and routes until state of equilibrium is reached.

Link volumes of empirical system state 3 seem to be far from the state of equilibrium due to the occurrence of the 1994 Northridge earthquake. Link volumes are more stable in the cases of empirical system state 4 and 5. However, some drivers seem to be still adjusting their travel behaviors. A new equilibrium state may not be reached yet. Drivers need time to adjust their travel patterns whose outcomes will be different from empirical link volumes before the occurrence of the Northridge earthquake.

In contrast, associative memory models are simply mapping stimulus vectors to response vectors without considering the nature of relationships between two sets of vectors. Hidden relationships that the conventional approach fails to address seem to be captured by using associative memory models. We have no information about the hidden relationships. However, associative memory models successfully construct associative memory matrices that provide sufficiently accurate estimates of empirical link volumes.

The same procedure is applied to the case of 276 links. The three MOP results in the case of 276 links are shown in Table 19. Figures in Appendix 26 show the scatter plots and correlation coefficients between link volumes derived from Caltrans' traffic counts and simulated traffic flows provided by the static user equilibrium model for each empirical link-failure system state.

This exercise confirms findings from the comparison between the associative memory models and the static user equilibrium model. The MOP results are slightly different compared to the MOP results in the case of 292 links. However, the same pattern is observed from the traffic flow analyses in the case of 276 links.

Our empirical link-failure system states were limited to only five states. Thus, synthetic network flows will be simulated to increase the number of link-failure system states. Additional exercises will be performed by using the synthetic network flows in the following sections.

Table 19: The Comparison Study of Estimating Equilibrium Traffic Volumes Using the User Equilibrium Model and Associative Memories Under Five Empirical System States (276 Links)

SYSTEM STATE 1 (JUL 93)	UE model (IT# 200)	SAM	RAM	MAM (α=0.8)
TOTAL VOLUME ERROR:	90867 PCU	100499 PCU	98918 PCU	98624 PCU
MEAN VOLUME ERROR:	7.53%	8.33%	8.20%	8.17%
CORRELATION COEFF:	0.979843	0.952113	0.952345	0.952188
SYSTEM STATE 2 (NOV 93)	UE model (IT# 200)	SAM	RAM	MAM (α=0.4)
TOTAL VOLUME ERROR:	NA	88688 PCU	88669 PCU	84586 PCU
MEAN VOLUME ERROR:	NA	7.32%	7.32%	6.98%
CORRELATION COEFF:	NA	0.970019	0.969575	0.973967
SYSTEM STATE 3 (FEB 94)	UE model (IT# 200)	SAM	RAM	MAM (α=0.8)
TOTAL VOLUME ERROR:	277671 PCU	113459 PCU	121218 PCU	114667 PCU
MEAN VOLUME ERROR:	24.52%	10.02%	10.70%	10.13%
CORRELATION COEFF:	0.885446	0.933568	0.919437	0.933933
SYSTEM STATE 4 (MAY 94)	UE model (IT# 200)	SAM	RAM	MAM (α=0.2)
TOTAL VOLUME ERROR:	208766 PCU	67641 PCU	64947 PCU	70133 PCU
MEAN VOLUME ERROR:	17.41%	5.64%	5.42%	5.85%
CORRELATION COEFF:	0.893084	0.979212	0.981485	0.982457
SYSTEM STATE 5 (AUG 94)	UE model (IT# 200)	SAM	RAM	MAM (α=0.6)
TOTAL VOLUME ERROR:	174126 PCU	82537 PCU	93466 PCU	82699 PCU

MEAN VOLUME ERROR:	14.39%	6.82%	7.72%	6.83%
CORRELATION COEFF:	0.925887	0.975296	0.966775	0.975952

7-3. Synthetic Flow Simulation

The results from associative memory applications using five empirical link-failure system states demonstrate the potential of applying associative memory models to flow estimation in large-scale transportation networks such as the aggregated Los Angeles highway network. Exercises in section 7-2 indicate that associative memory models provide better estimates of traffic volumes than the static user equilibrium model. However, empirical link-failure system states were limited to only five cases. The five empirical system states may not be sufficient for representing all possible system states of different link-failures.

Generating additional link-failure system states in the empirical study means collecting traffic count data after closing network links from the actual transportation network. Unlike the fields of natural science, it is impossible to experiment this scenario in traffic flow analyses. Additional link-failure system states can be obtained from the occurrence of another earthquake in the Los Angeles region. Thus, the general transportation network analysis procedure is applied to simulate post-earthquake traffic flows for synthetic link-failure system states.

The link failure simulation in the aggregated Los Angeles highway network can be based on either directed link failures or couple link failures. Directed link failures are

general cases of coupled link failures. The total number of link-failure system states can be obtained from the combinatorial formula for selecting any number of links out of 292 links. The total number of system states in the case of directed link failures is ${}_{292}C_1 + {}_{292}C_2 + {}_{292}C_3 + {}_{292}C_4 + {}_{292}C_5 + \ldots + {}_{292}C_{292} = 292 + 42{,}486 + 4{,}106{,}980 + 296{,}729{,}305 + 17{,}091{,}607{,}968 + \ldots + 1$.

Alternatively, coupled link failures can be exercised. The coupled link failures represent the system states that two links sharing origin and destination zones are closed simultaneously. The total number of system states in the case of coupled link failures is ${}_{146}C_1 + {}_{146}C_2 + {}_{146}C_3 + {}_{146}C_4 + {}_{146}C_5 + \ldots + {}_{146}C_{146} = 146 + 10{,}585 + 508{,}080 + 18{,}163{,}860 + 515{,}853{,}624 + \ldots + 1$.

This exercise is based on post-earthquake flow simulations in the case of one couple link failure. The total number of possible system states in this category is 146. Seventy coupled link-failure system states are randomly selected for representing all possible system states of one couple link failure. A static user equilibrium model is applied to simulate traffic flows given network configurations of the seventy synthetic link-failure system states.

Three system input data sets including link capacities, free-flow link travel times, and a peak-hour weekday Los Angeles origin-destination trip matrix are used as input data in the static user equilibrium model. All the seventy link-failure system states are assumed to share the same O-D trip matrix. Network configurations and their associated link

flows for the seventy coupled link-failure system states are shown in Appendices 27 and 28, respectively.

7-4. Application of Associative Memory Models to Synthetic Flows Computed for the Aggregated Los Angeles Highway Network

This exercise examines the application of associative memory models to the seventy synthetic coupled link-failure system states. Each of the last ten synthetic system states is used as the test system state in rotation. Network configurations and their equilibrium traffic flows for the remaining sixty-nine synthetic system states are used to compute associative memory matrices in each case. The RMSE results of SAM, RAM, and MAM in estimates in the case of synthetic coupled link-failure system states are shown in Table 20.

The RMSE results of estimated traffic flows do not significantly vary across associative memory models in the case of test states. The RMSE results for test system states show that test system state 64 provides the lowest test case RMSE. Test system state 69 provides the highest test case RMSE, describing the worst estimate of traffic flows. Figures in Appendix 29 show the scatter plots and correlation coefficients for test system states 64 and 69.

Table 20: RMSEs of SAM, RAM, and MAM in 105 Zone Network with 70 Synthetic System States (292 Links)

		MAM									SAM	RAM
	α	0.1	0.2	0.3	0.4	0.5	0.6	0.7	0.8	0.9	SAM	RAM
State 61	Training	683.6	557	449.9	358.1	278.5	208.9	147.4	92.83	43.97	3.06E-11	2.93E-11
	Test	914.1	914	914	914	914	914	914	914	914	913.96	913.22
State 62	Training	688.9	561.3	453.4	360.8	280.7	210.5	148.6	93.55	44.31	3.38E-11	3.45E-11
	Test	278.7	278.7	278.8	278.9	278.9	278.9	278.9	278.9	278.9	278.91	281.78
State 63	Training	683.7	557.1	450	358.1	278.5	208.9	147.5	92.85	43.98	3.24E-11	3.10E-11
	Test	905.7	905.6	905.6	905.6	905.6	905.6	905.6	905.6	905.6	905.54	904.78
State 64	Training	689.1	561.5	453.5	361	280.8	210.6	148.6	93.58	44.33	3.12E-11	3.09E-11
	Test	202.3	202.6	202.7	202.8	202.8	202.8	202.8	202.8	202.8	202.85	206.98
State 65	Training	689	561.4	453.4	360.9	280.7	210.5	148.6	93.57	44.32	2.92E-11	3.08E-11
	Test	246.3	246.4	246.5	246.5	246.5	246.6	246.6	246.6	246.6	246.57	248.38
State 66	Training	685	558.1	450.8	358.8	279.1	209.3	147.7	93.02	44.06	3.24E-11	2.82E-11
	Test	797.8	797.9	797.9	797.9	797.9	797.9	798	798	798	797.96	799.37
State 67	Training	683	556.5	449.5	357.7	278.2	208.7	147.3	92.75	43.93	3.02E-11	2.98E-11
	Test	961.9	961.9	961.9	961.9	961.9	961.9	961.9	961.9	961.9	961.93	961.91
State 68	Training	682.6	556.2	449.2	357.6	278.1	208.6	147.2	92.7	43.91	3.09E-11	2.87E-11
	Test	987.8	987.8	987.9	987.9	987.9	987.9	987.9	987.9	987.9	987.91	988.69
State 69	Training	679.3	553.5	447.1	355.8	276.8	207.6	146.5	92.25	43.7	2.90E-11	2.97E-11
	Test	1203	1203	1203	1203	1203	1203	1203	1203	1203	1203.2	1202.5
State 70	Training	683.8	557.2	450	358.2	278.6	209	147.5	92.87	43.99	3.21E-11	3.00E-11
	Test	894.6	894.7	894.7	894.7	894.7	894.7	894.7	894.7	894.7	894.71	895.37

The RMSE results from the synthetic system state exercise demonstrate the applicability of associative memory models to the aggregated Los Angeles highway network in estimating simulated link flows. The RMSE results from synthetic system state 64 are lower than any RMSE result from five empirical link-failure system states. The RMSE results from synthetic system state 69 are close to the RMSE results from the empirical link-failure system states. Correlation coefficients between simulated traffic flows and flow estimates are at least 0.9 in all ten test system states.

The sample size of 69 training system states seems to be sufficiently large to compute good associative memory matrices for the aggregated Los Angeles highway network.

The computed associative memory matrices produce reliable estimates of traffic flows by capturing the relationships between the stimulus and response vectors. The results from MAM models show that the estimation performance of MAM is not sensitive to the value of α.

7-5. Application of Associative Memory Models to Empirical and Synthetic Flows

Earthquakes may damage more than two links simultaneously. Three empirical link-failure system states among the five system states represent the events of multiple link failures. However, building associative memory matrices based on various events of multiple link failures would be extremely expensive. The results from associative memory applications to the combined sets of single link-failure system states and double link-failure system states examined in section 4-4 demonstrated the applicability of the associative memory approach to traffic flow estimation for combined data sets.

This exercise examines the application of associative memory models to predict empirical link volumes based on two scenarios of training system states: (1) a set of only seventy synthetic coupled link-failure system states, and (2) combined sets of seventy synthetic coupled link-failure system states and five empirical link-failure system states.

The first exercise of associative memory models uses each of the five empirical link-failure system states as the test system state in rotation. The seventy synthetic coupled link-failure system states are used to create associative memory matrices. The computed

memory matrices are used to estimate link volumes of each empirical link-failure system states. The RMSE results of associative memory models in estimates are shown in Table 21.

Table 21: RMSEs of SAM, RAM, and MAM in 105 Zone Network with 75 Empirical and Synthetic System States (292 Links, Training System States: 70 Synthetic System States)

		MAM									SAM	RAM
	α	0.1	0.2	0.3	0.4	0.5	0.6	0.7	0.8	0.9	SAM	RAM
Em State 1	Training	684.5	557.7	450.5	358.5	278.9	209.1	147.6	92.95	44.03	2.97E-11	2.94E-11
	Testing	756.8	641.7	594.7	600.7	640.1	696.4	759.3	823.2	885.4	944.62	1613.9
Em State 2	Training	684.5	557.7	450.5	358.5	278.9	209.1	147.6	92.95	44.03	2.97E-11	2.94E-11
	Testing	124.8	125	125.1	125.1	125.1	125.2	125.2	125.2	125.2	125.17	134.24
Em State 3	Training	684.5	557.7	450.5	358.5	278.9	209.1	147.6	92.95	44.03	2.97E-11	2.94E-11
	Testing	1255	1212	1237	1301	1385	1476	1567	1656	1740	1819.7	2576.9
Em State 4	Training	684.5	557.7	450.5	358.5	278.9	209.1	147.6	92.95	44.03	2.97E-11	2.94E-11
	Testing	823.7	827	837.9	852.9	870.1	888	905.9	923.4	940.3	956.41	842.61
Em State 5	Training	684.5	557.7	450.5	358.5	278.9	209.1	147.6	92.95	44.03	2.97E-11	2.94E-11
	Testing	891.6	891.7	891.8	891.8	891.8	891.8	891.8	891.8	891.8	891.81	893.21

The results from the associative memory applications demonstrate that flow estimates are still reliable. Associative memory matrices are trained by using the seventy noisy-free, synthetic system states within the framework of network equilibrium. The computed memory matrices are applied to estimate five noisy, empirical link-failure system states based on the different number of closed links. However, the estimation performance of the associative memory models does not vary significantly in the case of synthetic training system states compared with the performance in the case of empirical training system states. The performance of MAM seems to be slightly sensitive to the

value of α compared to the exercise for synthetic test system states. The value of α is in the neighborhood of 0.2.

The second exercise of associative memory models also uses each of the five empirical link-failure system states as the test system state in rotation. The remaining four empirical link-failure system states and seventy synthetic coupled link-failure system states are used to compute associative memory matrices as training system states. The RMSE results from associative memory models estimated in the case of the combined data sets are shown in Table 22.

Table 22: RMSEs of SAM, RAM, and MAM in 105 Zone Network with 75 Empirical and Synthetic System States (292 Links, Training System States: 70 Synthetic System States and 4 Empirical System States)

		MAM									**SAM**	**RAM**
	α	0.1	0.2	0.3	0.4	0.5	0.6	0.7	0.8	0.9	SAM	RAM
Em State 1	Training	676	551.3	448.7	362.3	288.6	225.2	170.1	121.5	77.44	373.41	6.55E-11
	Testing	756.3	643.2	596.9	602.8	641.8	698.2	762.1	828.6	895.5	1256.50	926.29
Em State 2	Training	677.2	551.8	449.8	364.4	292	230.2	177.2	131.5	91.43	208.87	1.49E-10
	Testing	121.2	122.3	123.4	124.5	125	127.5	129.7	133.3	141	415.94	460.78
Em State 3	Training	674.4	548.9	444.6	356.2	280.7	215.8	160.6	115	80.85	1224.50	3.85E-11
	Testing	1061	942.9	947	1016	1114	1221	1329	1433	1539	1926.00	1495.9
Em State 4	Training	676.1	550.7	447.9	361.4	287.8	224.7	170.5	123.7	82.25	230.93	6.10E-11
	Testing	574.4	503.4	493.4	515.5	551.3	588.7	619.7	637.1	635.5	778.92	813.35
Em State 5	Training	674.1	549.4	447.5	361.9	289	226.3	172.1	124.6	81.39	180.26	7.93E-11
	Testing	745.1	687.6	651.1	628.2	616.9	616	623.8	638.3	659.3	703.48	784.04

The results from associative memory applications using the combined training data sets provide best flow estimates compared to the previous three exercises. A difference exists between the empirical link-failure system states and the synthetic coupled link-

failure system states in terms of flow errors. Simulated traffic flows of the synthetic system states are noise-free. Link volumes of the empirical system states contain unknown noise despite exclusion of daily, seasonal, and trend variations from observed link volumes. However, associative memory models seem to reconcile the difference between two data sets, and provide very close estimates to empirical link volumes.

7-6. The Study of Los Angeles Origin-Destination Trip Changes Due to the Northridge Earthquake and the Opening of I-105 Freeway

7-6-1. Background

Traffic flow simulations using the static user equilibrium model assume that a travel demand for the aggregated Los Angeles highway network do not change across different network configurations. The same peak-hour weekday Los Angeles O-D trip matrix consistent with November 1993 traffic volumes is used to all seventy synthetic link-failure system states to simulate equilibrium link flows. However, travel demand may vary as the condition of network links is changed. The opening or closure of network links may change link travel times for certain links so that increased or decreased link travel times influence travel behaviors of drivers. Drivers not only try to find new shortest routes, but also change their trip starting times. Similarly, drivers also change origins and/or destinations of their trips.

Our objective in this section is to predict trip changes in the peak-hour weekday Los Angeles O-D trip matrix due to the opening of the Glen Anderson Freeway and the closure of seven links caused by the 1994 Northridge earthquake. Empirical link-failure system state 1 represents the six-link-failure system state before the opening of the Glen Anderson Freeway. Empirical link-failure system state 3 represents the seven-link-failure system state after the Northridge earthquake, and before the recovery of the damaged links. The LINKOD PLUS model is applied to estimate O-D trip changes given different empirical link volumes for the two empirical link-failure system states.

The LINKOD PLUS model estimates an origin-destination trip matrix given network information and link volumes. The LINKOD PLUS model requires four system input data sets including a seed O-D trip matrix, link capacity data, free-flow link travel times, and link volumes. The model produces an estimated O-D trip matrix modified from the seed O-D trip matrix, and simulated traffic flows consistent with the estimated O-D trip matrix.

The November 1993 O-D trip matrix consistent with peak-hour weekday link volumes of the month of November 1993 is used as the seed O-D trip matrix. One-thousand iterations are selected to produce equilibrium O-D trip matrices from empirical link volumes. The performance of the LINKOD PLUS model is evaluated by comparing empirical link volumes with simulated traffic flows consistent with the estimated O-D trip matrix.

7-6-2. Travel Demand Change Due to the Opening of the Glen Anderson Freeway (I-105)

This exercise investigates O-D trip changes due to the opening of the Glen Anderson Freeway. Six links were opened among 292 links of the aggregated Los Angeles highway network. The July 1993 O-D trip matrix is estimated from the November 1993 O-D trip matrix and the July 1993 link volumes. A comparison is made between the July 1993 O-D trip matrix and the November 1993 O-D trip matrix. It is assumed that the difference between the two O-D trip matrices results from the opening of the Glen Anderson Freeway.

The total number of O-D trips increased from 614,635 trips to 629,330 trips due to the opening of the six network links. There was an increase of 2.33 percent in trips. The origins and/or destinations changed 12.2 percent of the trips, excluding the net trip increase. Of the total November 1993 O-D trips, 14.53 percent changed. Errors between July 1993 link volumes and estimated traffic flows are 0.44 percent.

Figure 21 shows trip changes between the July 1993 O-D trip matrix and the November 1993 O-D trip matrix. Figure 22 shows the difference between July 1993 link volumes and simulated traffic flows consistent with the July 1993 O-D trip matrix. A table in Appendix 30 presents positive, negative, and net trip changes between the July 1993 O-D trip matrix and the November 1993 O-D trip matrix.

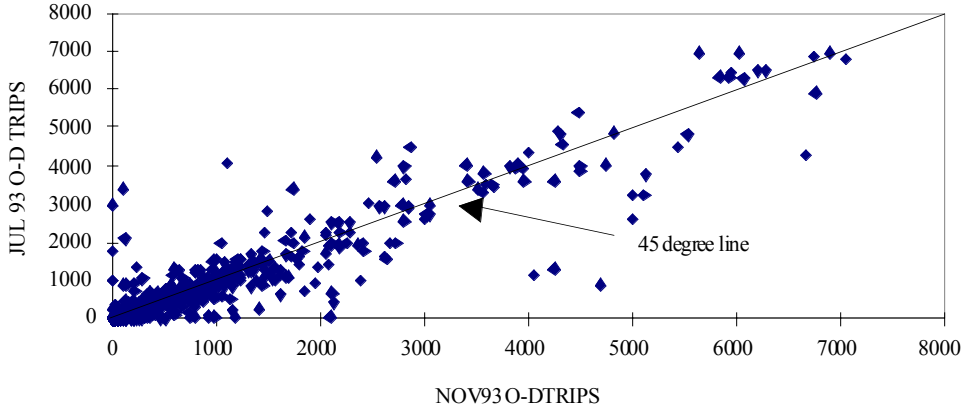

Figure 21: The November 1993 vs. the July 1993 Origin-Destination Trip Matrix (1279 Data Points, r=0.937727, Input O-D: the November 1993 O-D Trip Matrix)

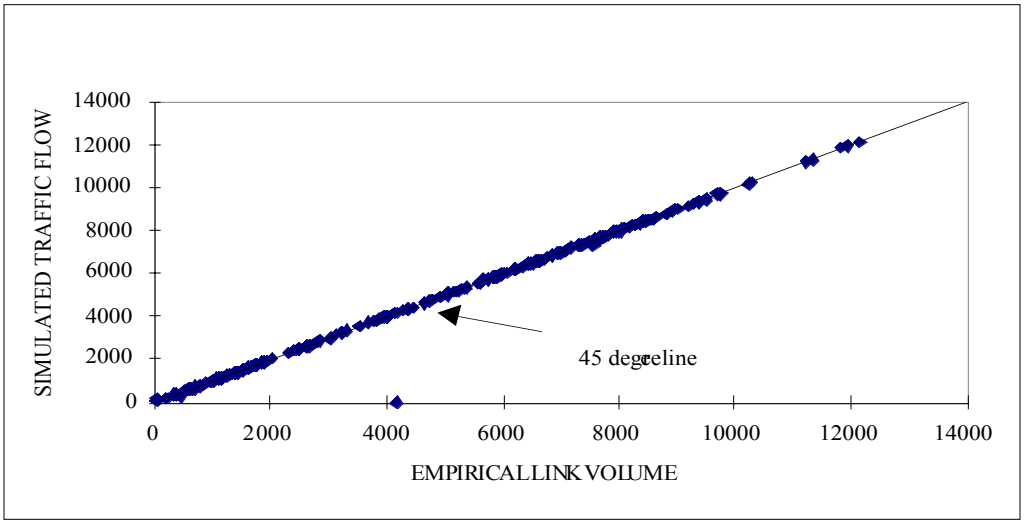

Figure 22: July 1993 Link Volumes vs. Simulated Link Flows in 105 Zone Network (Using the LINKOD PLUS model, Iteration Number: 1000, Input O-D: the November 1993 O-D Trip Matrix, Target: July 1993 Link Volumes, 286 Links, r=0.9967658, Six Links Failed)

7-6-3. Travel Demand Change Due to the Northridge Earthquake

This exercise investigates O-D trip changes due to the occurrence of the Northridge earthquake. The Northridge earthquake damaged seven network links. The February 1994 O-D trip matrix is estimated from the November 1993 O-D trip matrix and the February 1994 link volumes. A comparison is made between the November 1993 O-D trip matrix and the February 1994 O-D trip matrix. It is assumed that the difference between two O-D trip matrices results from the closure of seven network links due to the Northridge earthquake.

The total number of O-D trips decreased from 629,330 trips to 612,078 trips due to the closure of the highway links. There was a decrease of 2.74 percent in trips. The origins and/or destinations changed 12.06 percent of the trips, excluding the net trip increase. Of the total November 1993 O-D trips, 14.8 percent changed. Errors between July 1993 link volumes and estimated traffic flows are 16.97 percent. The February 1994 traffic volumes are far from the equilibrium state.

Figure 23 shows trip changes between the November 1993 O-D trip matrix and the February 1994 O-D trip matrix. Figure 24 shows the difference between February 1994 link volumes and simulated traffic flows consistent with the February 1994 O-D trip

matrix. A table in Appendix 31 presents positive, negative, and net trip changes between the November 1993 O-D trip matrix and the February 1994 O-D trip matrix.

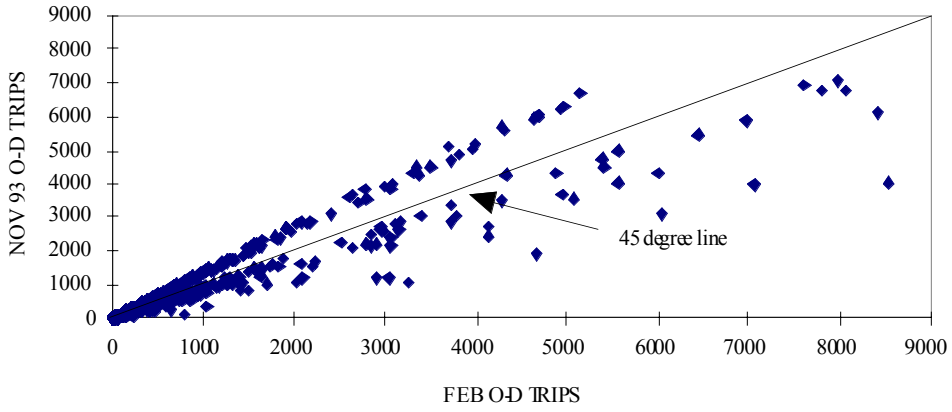

Figure 23: The February 1994 vs. the November 1993 Origin-Destination Trip Matrix (1246 Data Points, r=0.946428, Input O-D: the November 1993 O-D Trip Matrix)

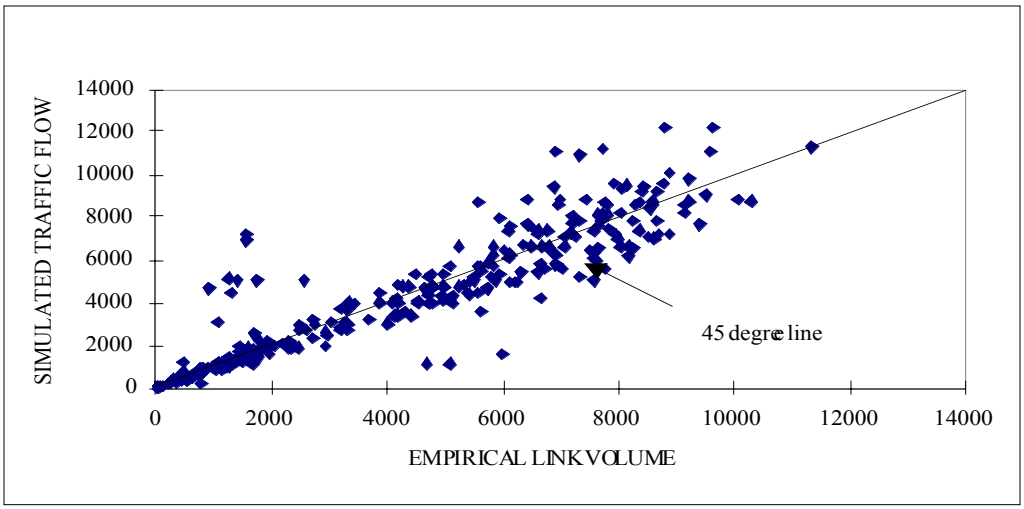

Figure 24: February 1994 Link Volumes vs. Simulated Link Flows in 105 Zone Network (Using the LINKOD PLUS model, Iteration Number: 1000, Input O-D:the November 1993 O-D Trip Matrix, Target: February 1994 Link Volumes, 285 Links, r=0.9169279, Seven Links Failed)

7-6-4. Conclusion

It is often assumed that travel demand increases as additional transportation facilities are provided. The results from two comparisons support our general hypothesis for O-D trip changes. The opening of Freeway 105 provided additional six network links to the aggregated Los Angeles highway network. Peak-hour trips increased up to 14,695 trips after the opening of the highway links. The 1994 Northridge earthquake damaged seven links of the aggregated Los Angeles highway network. Peak-hour trips decreased up to 17,292 trips with respect to the closure of the network links.

The opening or closure of few links in a transportation network may cause significant changes in travel demand of the network. The opening of the Glen Anderson Freeway provided additional six network links in service. This 2.1 percent change of network links resulted in 14.53 percent change of total O-D trips. The Northridge earthquake damaged seven links out of 292 network links. This 2.4 percent closure of network links resulted in 14.8 percent change of total O-D trips. Consequently, a small change in a transportation network causes significant impacts on behavioral changes of drivers.

The above comparisons are made between two peak-hour weekday O-D trip matrices. The results from the peak-hour O-D trip comparisons lack information for sources of O-D trip changes. The O-D trip changes may result from changes in trip start-times, trip origins or destinations. The total number of daily trips from an origin point to a destination point does not vary in the case of trip start-time changes. The total number of daily trips between two zones does vary in the case of trip origin and/or destination changes. Thus, further travel demand analyses are recommended to investigate dynamic O-D trip changes over the entire 24 hours time period.

8. Extensions

8-1. Policy Implications

This research has successfully demonstrated a transportation network analysis (TNA) procedure that provides rapid and reliable flow estimates used for bridge retrofit decisions in the Los Angeles highway network. The objective of this research is to predict system-wide traffic flow changes inexpensively with respect to the closure of network links. The TNA procedure developed here can be also applied to other transportation problems that require a large number of system-wide traffic flow analyses. Examples are: (1) new transportation policies such as congestion pricing, (2) infrastructure investments such as High-Occupancy Vehicle (HOV) lane construction, (3) and temporary road closures due to traffic accidents or road reconstruction.

Traffic congestion in urban transportation systems is one of the primary concerns of transportation planners. Traffic congestion occurs due to the failure to price access in current transportation systems. Traffic congestion not only causes inefficiencies in transportation systems, but also has impacts on many economic and environmental aspects in urban and suburban areas.

Congestion pricing is one of the demand management transportation policies proposed for reducing traffic congestion problems. Congestion pricing includes the use of the price mechanism as a means of inducing the efficient use of freeway/roadway spaces by reducing travel demand. It involves the imposition of congestion tolls on heavily congested highway/roadway systems like in the case of SR-91 Express Lanes in Southern California. The system-wide traffic impacts of congestion pricing applications are difficult to predict because of the complexity of drivers' behavioral changes. Further, determining the exact location and optimal number of toll instruments (or booths) requires the study of numerous congestion pricing system states. The results from the

applications of the TNA procedure to link-failure system states demonstrate the applicability of the TNA procedure to congestion pricing cases.

The performance of transportation facilities may be improved by public and private investments in transportation sector. Constructing additional freeway lanes or converting existing freeway lanes to HOV lanes may improve the efficiency of a transportation network. Our TNA procedure can be applied to evaluate the system-wide traffic impacts of such transportation investments.

A temporary road closure due to traffic accidents or road reconstruction is referred to a short-term link-failure system state. The TNA procedure can be applied to estimate traffic flows in the case of short-term link-failure system states. The flow estimates can be used to provide rapid traffic signal adjustments or traffic incident information.

8-2. The Procedure Improvements

TNA procedures developed in this research provide rapid and reliable estimates of traffic flows in a large-scale transportation network. However, the general TNA procedure is based on the static network equilibrium model, assuming a fixed travel demand. This section presents research directions for improving the current TNA procedures to a more technically advanced and empirically applicable procedure. The following three models are recommended for the further development of the TNA procedures: (1) a dynamic network equilibrium model predicting dynamic travel behaviors, (2) artificial neural network (ANN) models as alternatives to associative memory (AM) models, and (3) a procedure predicting O-D trip changes due to future earthquakes.

The dynamic network equilibrium model is a generalized form of static network equilibrium model. Results from this research indicate that the static network

equilibrium model provided reliable estimates of link volumes during a peak-hour period. However, traffic flow analyses will be more accurate if a dynamic pattern of travel behaviors is incorporated with TNA procedures.

TNA procedures developed here employ the AM approach as the alternative to the static network equilibrium model. An alternative to the AM approach is the ANN approach, especially backpropagation ANN models. The usefulness of backpropagation ANN models has been addressed by transportation planners. Further research is recommended to compare ANN models with AM models with respect to traffic flow estimation.

The general TNA procedure assumes the same pattern of travel demand in different system states. However, the results from travel demand studies in section 7-6 indicated that travel demand varies as network links are opened or closed. An improved O-D trip estimation procedure is required in TNA procedures to predict post-earthquake O-D trip matrices consistent with estimated post-earthquake traffic flows.

9. Conclusions

The California Department of Transportation (Caltrans) has developed bridge seismic retrofit programs that include a decision-making procedure for the structural reinforcement of existing freeway bridges. This decision-making procedure known as the multi-attribute decision procedure includes a priority rating for California's existing freeway bridges due to state and local governments' limited bridge retrofit funds.

Caltrans' multi-attribute decision procedure addresses average daily traffic (ADT) volumes as a major attribute for determining the importance of a bridge. However, the closure of a freeway bridge caused by earthquakes influences travel behaviors of drivers, resulting in a state of new network equilibrium. The importance of the bridge may be accurately demonstrated by changes in total system travel times than by ADT volumes. The total system travel time is computed by adding up all aggregated link travel times obtained by multiplying link travel times with link flows.

The objective of this research is to develop a transportation network analysis (TNA) procedure that serves as a cost-effective tool for predicting system-wide traffic flows with respect to the opening or closure of freeway links. Flow estimates produced by the TNA procedure can be used to estimate associated link travel times by applying the BPR link travel cost function to the flow estimates. The importance of a freeway bridge can be evaluated by observing the amount of total system travel time changes with respect to the closure of the bridge.

The research began with the literature review on Caltrans' bridge prioritization procedures, current traffic analysis technology, and artificial intelligence approaches. Two versions of the TNA procedure have been developed based on the quantity and quality of transportation system data: the general TNA procedure and the simplified TNA procedure.

An important feature of these two transportation network analysis procedures is the use of an associative memory (AM) approach as an efficient means for predicting network flows. The AM approach is a heuristic method that provides rapid and reliable estimates of traffic flows to network equilibrium problems. The general TNA procedure contains other analytical methods for: (1) extracting seasonal and trend variations from observed link volumes, (2) estimating origin-destination trip matrices from link volumes,

and (3) simulating network flows. The decomposition method, the LINKOD PLUS model, and the static user equilibrium model are selected to perform the above tasks.

The transportation network analysis procedure has been applied to both a simple synthetic transportation network and an aggregated representation of the Los Angeles highway network. The following tasks have been performed:

(1) a simple synthetic network with seven zones and twenty-four links was developed;

(2) the general TNA procedure was applied to simulate traffic flows of given synthetic system states with respect to single-link and double-link failures;

(3) the performance of associative memory models was evaluated by comparing simulated traffic flows provided by a static user equilibrium model and flow estimates produced by different associative memory models;

(4) an aggregated Los Angeles highway network with 105 zones and 292 links was defined;

(5) five empirical link-failure system states were identified based on the opening of the Glen Anderson Freeway, the closure of seven links due to the Northridge earthquake, and the gradual repair of closed links;

(6) transportation system data sets including observed link volumes, an origin-destination trip matrix, link capacities, and free-flow link travel times were developed from relevant empirical data sources;

(7) the decomposition method was employed to exclude seasonal and trend variations from the observed link volumes. Other important indicators such as K-Factors and AWTV/ADTV ratios were identified;

(8) the LINKOD PLUS model was applied to extract a peak-hour weekday origin-destination trip matrix consistent with adjusted peak-hour weekday link volumes for the aggregated Los Angeles highway network;

(9) associative memory models were applied to estimate link volumes for each of five empirical link-failure system states in rotation;

(10) the static user equilibrium model was applied to simulate traffic flows for the same five empirical link-failure system states;

(11) the estimates of traffic flows provided by different associative memory models were compared with the simulated traffic flows provided by the static user equilibrium model;

(12) the static user equilibrium model was applied to simulate traffic flows for seventy sets of synthetic coupled link-failure system states;

(13) associative memory models were applied to estimate synthetic traffic flows for each of the last ten coupled link-failure system states using the remaining sixty-nine system states;

(14) associative memory models were applied to estimate link volumes for each of the five empirical link-failure system states using seventy synthetic coupled link-failure system states;

(15) associative memory models were also applied to estimate link volumes for each of the five empirical system states using combined sets of seventy synthetic coupled link-failure system states and the remaining four empirical link-failure system states; and

(16) the LINKOD PLUS model was applied to predict changes in the Los Angeles O-D trip matrix due to the opening of the Glen Anderson Freeway and the closure of seven links caused by the Northridge earthquake.

Conclusions from this research include the following:

(1) the usefulness of two TNA procedures was demonstrated with results from various link-failure applications. Associative memory models provide rapid and reliable estimates of network flows. . In the case of synthetic flows, AM models provide very good estimates. Flow estimates in the case of multiple link failres are very good. . AM models trained on synthetic system states provide very close flow estimates of the five empirical system states summarized here. Flow estimates provided by the best associative memory matrix results were closer to empirical link volumes than simulated traffic flows provided by the static user equilibrium.

(2) Flow estimates improve with the number of training cases. Increasing the number of training system states improved the estimations provided by power of associative memory models. Results from combined data sets demonstrated the possibility of combining empirical data sets with syntheticdata sets.

(3) The aggregated Los Angeles freeway network developed in this research was sufficient to capture relevant details of the actual Los Angeles freewa network.

(4) The decomposition method successfully captured seasonal and trend patterns from observed link volumes provided by Caltrans District 7.

(5) We did not use AM models to directly estimate Origin-Destination trip changes. Rather, we used the equilibrium assignment method to predict O-D trip changes from link volume changes associated with the opening of I-105 freeway and the Northridge earthquake. The LINKOD PLUS model

successfully extracted the peak-hour weekday O-D trip matrix from link volumes.

(6) The results from the application of the LINKOD PLUS model to of travel demand changes demonstrated a way of predicting travel demand changes due to the opening and/or closure of highway links.

(7) The procedure is fast, and speed is one of its principal advantages. The bigger the network, the more system states that must be accounted for, and the more time can that can be saved.

Consider modeling traffic flows for 1,000 post-earthquake system states for a network of the size described here. The best conventional implementation of the network equilibrium model may take one minute to simulate traffic flows for each system state. This results in a total requirement of 1,000 minutes of computing time. However, the associative memory approach requires only sufficient training information to understand the generalized pair association between network configurations and their traffic flows. Use the network configurations and traffic flows for the first 100 system states to train an associative memory matrix. Using an associative memory to estimate a set of 100 system states simultaneously would also require around one minute. Thus the associative memory approach requires 100 minutes for the first 100 applications of the conventional network equilibrium model, and 9 minutes for the remaining 900 system states to be estimated. The total computation time for the associative memory appraoch is 109 minutes. This is a substantial reduction in computational requirements.

If a transportation network has 1,000 traffic analysis zones and 10,000 links, conventional models will require considerably more time to model each link-failure system state. Worse, there are about 50,000,000 system states involving failures in exactly two of the 10,000 links. The speeds associated with an AM approach is the only way to simulate traffic flows for a representative set of system states.

(8) This research was completed in a distributed Unix mainframe computing environment, but parallel work shows that micro-computing resources would be adequate to support applications of this scale. The primary requirement is a reliable computer code for computing generalized matrix inverses. This work was done with Speakeasy, and Matlab, but other readily available products such as SAS/IML also Mathematica also compute generalized inverses. FORTRAN or C codes are available for computing the generalized inverses in any environment.

The following research directions are recommended to evaluate and improve the TNA procedure:

(1) other transportation problems such as congestion pricing, infrastructure investments, or temporary road closures can be used to evaluate the applicability of the TNA procedure, and

(2) the TNA procedure can be further improved by incorporating dynamic network equilibrium, trip change prediction methods, and other artificial intelligence approaches.

References

Beagan, D. and Bromage, J. (1987) "Trip Table Estimate from Observed Traffic Volumes," *Proceedings of the North American Conference on Microcomputers in Transportation*, ASCE, Boston, pp. 275-283.

Beckmann, M., C. McGuire and C. Winsten. (1956) *Studies in Economics of Transportation,* New Haven; Yale University Press.

Ben-Akiva, Moshe. (1985) "Dynamic Network Equilibrium research," *Transportation Research*, 19A, No.5/6, pp.429-431.

Benjamin, Julian. (1986). "A Time-Series Forecast of Average Daily Traffic Volume," *Transportation Research A.,* Vol. 20A, No. 1, pp. 51-60.

Boyce, D. E. (1984) "Urban transportation network-equilibrium and design models: recent achievements and future prospects," *Environment and Planning A,* vol. 16, pp. 1445-1474.

Boyce, D. E., B. N. Janson, and R. W. Eash. (1981) "The Effect on equilibrium trip assignment of different link congestion functions," *Transportation Research A*., Vol. 15A, No. 3, pp. 223-232.

California Depatment of Transportation. (1994a) *Interstate 10 Recovery Report: Northridge Earthquake Recovery*, Caltrans District 7.

California Depatment of Transportation. (1994b) *Northridge Earthquake Recovery: Interim Transportation Report #1,* Caltrans District 7.

California Depatment of Transportation. (1994c) *Northridge Earthquake Recovery: Interim Transportation Report #2*, Caltrans District 7.

California Depatment of Transportation. (1993) *The California State Highway Log*, Caltrans.

California Department of Transportation (CALTRANS). (1992) *CALTRANS: Transportation Vision for California*, Caltrans.

California Department of Transportation (CALTRANS). (1990) *Report to the Governor on Seismic Safety*, Caltrans.

California Depatment of Transportation. (_) *An Introduction to the California*

Department of Transportation, Caltrans District 7.

Carey, M. (1986) “A Constraint Qualification fir a Dynamic Traffic Assignment Model,” *Transportation Science*, v. 20, pp. 55-58.

Carey, Malachy. (1992) “Nonconvexity of the Dynamic Traffic Assignment Problem,” *Transportation Research B*, vol. 26B, No. 2, pp. 127-133.

Chatfield, C. (1989) *The Analysis of Time Series: An Introduction*, London; Chapman and Hall.

Dafermos, S. C. (1968) *Traffic Assignment and Resource Allocation in Transportation Networks,* Baltimore; Johns Hopkins University.

Dafermos, S. C. (1972) "The traffic assignment problem for multiclass-user transportation networks," *Transportation Science* 6, pp. 73-87.

Dafermos, S. (1982) "The General Multimodal Network Equilibrium Problem with Elastic Demand," *Networks*, v. 12, n. 1, pp. 52-72.

Dafermos, S. and Nagurney, A. (1983) "Sensitivity Analysis for the Asymmetric Network Equilibrium Problem," *Math Program*, v., 28, n. 2, pp. 174-184.

Dafermos, S. C. and F. T. Sparrow (1969) "The traffic assignment problem for a general network," *Journal of Research of the National Bureau of Standards B* 73, pp. 91-113.

Dafermos, S. C. and F. T. Sparrow (1971) “Optimal resource allocation and toll patterns in user-optimized transport networks,” *Journal of Transport Economics and Policy* 5, pp. 1-17.

Daganzo, C. and Sheffi, Y. (1977) "On Stochastic Models of Traffic Assignment," *Transportation Science*, v. 11, pp. 253-274.

Davis, G. (1994) "Exact Local Solution of the Continuous Network Design Problem via Stochastic User Equilibrium Assignment," *Transportation Research*, v. 28B, n. 1, pp. 61-75.

Davis, Gary A. and Nancy L. Nihan (1993) “Large Population Approximations of a General Stochastic Traffic Assignment Model,” *Operations Research*, vol. 41, no. 1, pp. 169-178.

Dial, R. B. (1971) “Probabilistic Multipath Traffic Assignment Model Which Obviates

Path Enumeration," *Transportation Research*, 5, pp. 83-111.

Dowling, R. G. and A. D. May. (1984) "Comparison of Small Area O-D Estimation Techniques," Unpublished.

Drissi-Kaitouni, Omar. (1993) "A variational inequality formulation of the Dynamic Traffic Assignment Problem," *European Journal of Operational Research* 71, pp. 188-204.

Easa, S. M. and D. McColl. (1987) "Assessing traffic and emergency benefits of railroad grade separations," Journal of Transportation Engineering, Vol. 113, pp. 593-608.

Eash, R. W., B. N. Janson, and D. E. Boyce. (1979) "Equilibrium trip assignment: advantages and implications for practice," *Transportation Research Record*, no. 728, pp. 1-8.

Faghri, Ardeshir and Partha Chakroborty. (1994) "Development and Evaluation of a Statistically Reliable Traffic Counting Program," *Transportation Planning and Technology*, Vol. 18, pp. 223-237.

Florian, M. (1984) "An Introduction to Network Models Used in Transportation Planing," *In Transportation Planing Models*, Florian, M. (ed.), Elsever Service Publisher, New York, New York.

Florian, M. and Los, M. (1982) "A New Look at Static Spatial Price Equilibrium Models," *Regional Science and Urban Economics*, v. 12, pp. 579-597.

Florian, M. and S. Nguyen (1976) "An application and validation of equilibrium trip assignment models," *Transportation Science* 10, pp. 374-390.

Florian, M and H. Spiess (1982) "The convergence of diagonalization algorithms for asymmetric network equilibrium problems," *Transportation Research B* 16, pp. 447-483.

Frank, M. and P. Wolfe (1956) "An Algorithm for Quadratic Programming," *Naval Research Logistics Quarterly*, v. 3, pp. 95-110.

Friesz, Terry L. (1985) "Transportation Network Equilibrium, Design and Aggregation: Key Developments and Research Opportunities," *Transportation Research A*, Vol. 19A, No 5/6, pp.413-427.

Friesz, T., Luque, F., Tobin, R. and Wie, B. (1989) "Dynamic Network Traffic Assignment Considered as a Continuous Time Optimal Control Problem," *Operations Research*, v. 37, pp. 893-901.

Friesz, Terry L., David Bernstein, Tony E. Smith, Roger L. Tobin, and B. W. Wie. (1993) "A Variational Inequality Formulation of the Dynamic Network User Equilibrium Problem," *Operations Research*, vol. 41, no. 1, pp. 179-191.

Fuller, Wayne A. (1976) *Introduction to Statistical Time Series,* New York; John Wiley & Sons.

Gilbert, A. (1993) "*Developments in Seismic Prioritization of Bridges in California*," Proceedings: Ninth Annual US/Japan Workshop on Earthquake and Wind Design of Bridges, Tsukuba Science City, Japan, May 1993.

Giuliano, Genevieve and Kenneth A. Small. (1994) *The Determinants of Growth of Employment Subcenters*, Berkeley; The University of California Transportation Center.

Gordon, Peter and James E. Moore, II. (1989) "Endogenizing the Rise and Fall of Urban Subcenters via Discrete Programming Models," *Environment and Planning A*, Vol. 21, pp. 1195-1203.

Granger, C.W.J. (1989) *Forecasting in Business and Economics*, Boston; Academic Press, Inc.

Gur, Y. (1983) "Estimating Trip Table from Traffic Counts: Comparative Evaluation of Available Techniques." *Transportation Research Record*, 944.

Gur, Y. J., M. Turnquist, M. Schneider, L. LeBlanc, and D. Kurth. (1980a) *Estimation of An Origin-Destination Trip Table Based on Observed Link volumes and Turning Movements: Vol. 1. Technical Report*, Federal Highway Administration.

Gur, Y. J., P. Hutsebaut, D. Kurth, M. Clark, and J. Castilia. (1980b) *Estimation of An Origin-Destination Trip Table Based on Observed Link volumes and Turning Movements: Vol. 2. User's Manual*, Federal Highway Administration.

Gur, Y. J., P. Hutsebaut, D. Kurth, M. Clark, and J. Castilia. (1980c) *Estimation of An Origin-Destination Trip Table Based on Observed Link volumes and Turning Movements: Vol. 3. Program Manual*, Federal Highway Administration.

Hall, M., Van Vliet, D. and Willumsen, L. (1980) "SATURN - A Simulation - Assignment Model for the Evaluation of Traffic management Schemes," *Traffic Engineering and Control*, v. 21, n. 4, pp. 168-176.

Han, A. F., R. G. Dowling, E. C. Sullivan, and A. D. May. (1981) "Deriving Origin-

Destination Information from Routinely Collected Traffic Counts," *Volume II: Trip Table Synthesis for Multipath Networks*, RR81-9, Institute for Transportation Studies, University of California, Berkeley.

Han, A. F. and E. C. Sullivan. (1983) "Trip Table Synthesis for CBD-Networks: Evaluation of the LINKOD Model," *Transportation Research Record 944*, pp. 106-112.

Housner, George W. (1990) *Competing against Time: Report to Governor George Deukmejian from The Governor's Board of Inquiry on the 1989 Loma Prieta Earthquake*, the State of California.

Janson, Bruce N. (1995) "Network Design Effects of Dynamic Traffic Assignment," *Journal of Transportation Engineering*, vol. 121, no. 1.

Johnson, Aaron C. Jr., Johnson, Marvin B, and Buse, Rueben C. (1987) *Econometrics: Basic and Applied*, New York; MacMillan Publishing Company.

Johnston, J. (1984) *Econometric Methods*, New York; McGraw-Hill, Inc.

Kalaba, R., Lichtenstein, Z., Simchnoy, T., and Tesfatsion, L. (1990) "Linear and Nonlinear Associative Memories for Parameter Estimation," *Information Sciences, v.* 61, pp. 177-194.

Kalaba, R., Kim, M., and Moore II, J. (1991) " Linear Programming and Associative Memories," *Applied Mathematics and Computation*, v. 40, pp. 203-214.

Kalaba, R., Kim, M., and Moore II, J. (1992) " Linear Programming and Recurrent Associative Memories," *International Journal of General Systems,* v. 20, pp. 177- 194.

Kalaba, R., Moore II, J., Xu, R., and Chen, G. (1994) "A New Perspective on Calibrating Spatial Interaction Models" to be submitted to *Location Science*.

Kalaba, R., and Rasakhoo, N. (1986) "Algorithms for Generalized Inverses," *Journal of Optimization Theory and Applications*, v. 48, pp. 427-435.

Kalaba, R., and Tesfatsion, L. (1991) "Obtaining Initial Parameter Estimates for Nonlinear Systems Using Multicriteria Associative Memories," *Computer Science in Economics and Management*, v. 4, pp. 237-259.

Kalaba, R., and Udwadia, F. (1991) " An Adaptive Learning Approach to the Identification of Structural and Mechanical Systems," *Computers and Mathematics with Applications,* v. 22, pp. 67-75.

Kennedy, Peter. (1992) *A Guide to Econometrics,* Cambridge; The MIT Press.

Knight, F. (1924) "Some Fallacies in the Interpretations of Social Costs," *Quarterly Journal of Economics,* v. 38, pp. 582-606

Kohonen, T. (1989) *Self-Organization and Associative Memory*, Third edition, New York: Springer-Verlag.

Kurth, D., M. Schneider, and Y. Gur. (1979) "Small-Area Trip Distribution Model," *Transportation Research Record 728*, pp. 35-40.

Lam, W. and Lo, H. (1991) "Estimation of Origin-Destination Matrix from Traffic Counts: A Comparison of Entropy Maximizing and Information Minimizing Models," Transportation Planning and Technology, v. 16, pp. 85-104.

Lardaro, Leonard. (1993) *Applied Econometrics*, New York; Harper Collins College Publishers.

Larsson, T. and Patriksson, M. (1992) "Simplicial Decomposition with Disaggregated Representation for the Traffic Assignment Problem," *Transportation Science*, v. 26, n. 1, pp. 4-17.

LeBlanc, L. J. (1973) *Mathematical Programming Algorithms for Large Scale Network Equilibrium and Network Design Problems*, Northwestern University.

LeBlanc, Larry J., Edward E. Morlock, and William P. Pierskalla. (1975) "An Efficient Approaches to Solving Road Network Equilibrium Traffic Assignment Problems," *Transportation Research* 9, pp. 309-318.

Low, D. (1972) "A new Approach to Transportation Systems Modeling," *Traffic Quarterly*, v. 26, pp. 391-404.

Matsu, H. (1987) "A Model of Dynamic Traffic assignment," In text of Infrastructure Planning Lectures, *Japan Soc. Civil Eng.*, v. 18, pp. 84-96.

Merchant, D. K. and G. L. Nemhauser. (1978) "A Model and an Algorithm for the Dynamic Traffic Assignment Problems," *Transportation Science*, 12, pp. 183-199.

Mills, Edwin S. and Bruce W. Hamilton. (1989) *Urban Economics,* Glenview; Scott,

Foresman and Company.

Moehle, Jack P. (Editor) (1994) *Preliminary Report on the Seismological and Engineering Aspects on the January 17, 1994 Northridge Earthquake*, University of California at Berkeley.

Moore II, J., Kalaba, R., Kim, M., and Park, H. (1993) "Time Series and Turning Point Forecasts: A Comparison of Associative Memories and Bayesian Econometric Techniques Applied to LeSage's Data," *Journal of Regional Science*, v. 34, pp. 1-26.

Moore II, J., Kalaba, R., Kim, M., Seo, J. and Kim, G. (1994) "Time Series and Turning Point Forecasts: A Comparison of Artificial Neural Networks and Bayesian Econometric Techniques," forthcoming in *Mathematical Modeling and Scientific Computing*.

Moore II, J., Kim, M., Seo, J., and Kalaba, R. (1994) "Obtaining Initial Parameter Estimates for Nonlinear Systems: Comparing Associative Memory and Neural Network Approaches," *Mathematical Modelling and Scientific Computing*, v. 1, pp. 89-115.

Moore II, J., Kim, M., Seo, J., Wu, Y., and Kalaba, R. (1991) "Linear Programming, Recurrent Associative Memories, and Feed-Forward Neural Networks," *Computers and Mathematics with Applications*, v. 22, pp. 71-90 .

Moore, James E. II and Geun-Young Kim (1994) "Rapid Estimation of Equilibrium Transportation Flows in Networks Subject to Congestion Tolls," A Paper presented at the Spring 1995 Los Angeles Conference of the Institute for Operations Research and Management Science (INFORMS).

Nagurney, A. (1993) *Network Economics: A Variational Inequality Approach*, Kluwer Academic Publishers, London, England.

Nguyen, S. (1977a) "Estimating an O-D Matrix from Network Data: A Network Equilibrium Approach," *Publication No. 87*, Centre de Recherche sur les Transports, Universite de Montreal.

Nguyen, S. (1977b) "On the estimation of an O-D Trip Matrix by the Equilibrium Methods Using Pseudo Delay Functions," *Publication 81*, Centre de Recherche sur les Transports, Universite de Montreal.

Pang, J. and Chen, D. (1982) "Iterative Methods for Variational and Complementary Problems," *Math Program*, v. 24, n. 3, pp. 284-313.

Patriksson, M. (1993) "A Unified Description of Iterative Algorithms for Traffic Equilibrium," *European Journal of Operational Research*, v. 71, pp. 154-176.

Pignataro, Louis J. (1973) *Traffic Engineering*, Englewood Cliffs; Prentice-Hall, Inc.

Pindyck, Robert S. and Rubinfeld, Daniel L. (1991) *Econometric Models & Economic Forecasts*, New York; McGraw-Hill, Inc.

Ramanathan, Ramu. (1992) *Introductory Econometrics with Applications,* Fort Worth; Harcourt Brace Jovanovich College Publishers.

Ran, Bin and David E. Boyce. (1994) *Dynamic Urban Transportation Network Models*, Berlin; Springer-Verlag.

Ran, Bin, David E. Boyce, and Larry J. LeBlanc. (1993) "A New Class of Instantaneous Dynamic User-Optimal Traffic Assignment Models," *Operations Research*, vol. 41, No. 1, pp. 192-202.

Robillard, P. (1973) "Estimating the O-D matrix and Network Characteristics from Observed Link Volumes." *Proceedings of the International Conference on Transportation Research.* First Conference.

Robillard, P. (1975) Estimating an O-D Matrix from Observed Link Volumes," *Transportation Research*, v. 9, pp. 123-128.

Sever, Vital. (1993) "Dynamic equilibria in transport systems," *European Journal of Operational Research* 71, pp. 419-438.

Sherwood, Arnold (1993) *1991 Southern California Origin-Destination Survey: Summary Findings*, Southern California Association of Government.

Smith, R. and McFarlane, W. (1978) "Examination of A simplified Travel Demand Model," *Transportation Engineering Journal of ASCE*, v. 104, n. TE1, pp. 31-42.

Soumis, F. and Nagurney, A. (1993) "A Stochastic Multiclass Airline Network Equilibrium Model," *Operations Research*, v. 41, n. 4, pp. 721-730.

Southern California Association of Governments (SCAG). (1994) *Regional Mobility Element*, SCAG.

Stecher, Cheryl. (_) *1991 Southern California Origin-Destination Survey: Project Documentation,* Applied Management & Planning Group.

Symons, J., Wilson, R. and Patterson, J. (1976) "A Model of Inter-City Motor Travel Estimated by Link Volumes," *ARRB Proceedings*, v. 8, n. 20, pp. 53-65.

Transportation Research Board (TRB). (1985) *Highway Capacity Manual*, Washington, D.C.; Transportation Research Board.

Turnquist, M. and Gur, Y. (1979) "Estimation of Trip Tables from Observed Link Volumes," *Transportation Research Record 730*, pp. 1-6.

U.S. Bureau of Public Records. (1964) *Traffic Assignment Manual*, U.S. Department of Commerce, Washington, D.C.

Van Vliet, Dirck (1987) "The Frank-Wolfe Algorithm for Equilibrium Traffic Assignment Viewed as a Variational Inequality," *Transportation Research B*, Vol. 21, No. 1, pp. 87-89.

Wardrop, J. (1952) "Some Theoretical Aspects of Road Traffic Research," *Proceedings of the Institute of Civil Engineers*, v. 1, n. 2, pp. 325-378.

Wie, B-W., Friesz, T. and Tobin, R. (1990) "Dynamic User Optimal Traffic Assignment on Congested Multi-destination Networks," *Transportation Research*, v. 24B, pp. 431-442.

Willumsen, L. (1981) "Simplified Transport Models Based on Traffic Counts," *Transportation 10*, pp. 257-278.

Wilson, A. (1970a) *Entropy in Regional Modelling*, Pion Press, London.

Wilson, A. (1970b) "The Use of the Concept of Entropy in System Modeling," *Operational Research Quarterly*, v. 21, pp. 247-265.

Wilson, A. and Senior, M. (1974) "Some Relationships between Entropy maximizing Models, Mathematical Programming Models, and Their Duals," *Journal of Regional Science*, v. 14, pp. 207-214.

Wonnacott, Ronald J. and Wonnacott, Thomas H. (1979) *Econometrics,* New York; John Wiley & Sons.

Xu, R., Udwadia, F., Moore II, J., and Kalaba, R. (1994) "Lagrange's Problem Without Lagrange Multipliers I: The Holonomic Case." *Nonlinear World,* v. 1, n. 2, pp. 229-243